A novel role for the chromatin remodeling ATPase Brg1 during zygotic genome activation in *Xenopus*

Dissertation

Zur Erlangung des akademischen Grades Doctor rerum naturalis (Dr. rer.nat.)

Vorgelegt der Fakultät für Biologie der Ludwigs-Maximilians-Universität zu München

Gabriele Maria Wagner

aus Heidelberg

München 2014

Tag der Einreichung: 20. Mai 2014

Tag der mündlichen Prüfung: 31. Juli 2014

Erstgutachter: Prof. Dr. Peter Becker

Zweitgutachter: Prof. Dr. Hans Straka

Drittgutachter: Prof. Dr. Angelika Böttger

Viertgutachter: Prof. Dr. John Parsch

Eidesstattliche Erklärung

Ich versichere hiermit an Eides statt, dass die vorgelegte Dissertation von mir

selbständig und ohne unerlaubte Hilfe angefertigt ist.

München, den ....

                                                            -Unterschrift-

Table of contents

Zusammenfassung

Die vorliegende Arbeit beschreibt mittels Protein-Überexpression und -Knockdown Analysen eine essentielle Rolle für den Chromatin remodelierenden Faktor Brg1 in der embryonalen Musterbildung von *Xenopus*. Während eine ubiquitäre Depletion von Brg1 Protein zu einem Absterben der Embryonen führt, überleben dorsal bzw. ventral Brg1 depletierte Embryonen bis zum Kaulquappenstadium und erlauben damit eine phänotypische Analyse. Bereits ab der späten Blastula sind die Folgen einer lokalen Verminderung des Brg1 Proteinspiegels zu erkennen. Insbesondere zwei dorsal liegende Signalzentren - die BCNE und das Nieuwkoop Center - sind in ihrer transkriptionellen Signatur stark beeinträchtigt. Diese Defekte setzen sich in der Gastrulation weiter fort und führen zu einem funktionell abgeschwächten Organizer. Homotope Transplantationen von Brg1-depletiertem Gewebe in Wildtyp Embryonen belegen, dass das Brg1 Protein in der BCNE Region benötigt wird, um eine normale Kopfentwicklung zu ermöglichen. Jedoch zeigt die zielgerichtete Depletion von Brg1 in der vegetalen Hemisphäre auch, dass Brg1 eine über die BCNE hinausgehende Funktion besitzt. Insgesamt belegen die embryologischen Analysen von Brg1-defizienter Embryonen ein gestörtes Gleichgewicht zwischen dorsalisierenden und ventralisierenden Faktoren, welches zu erheblichen Entwicklungsschäden innerhalb des Körperbauplans führt.

Um mehr Informationen über die Zielgene von Brg1 zu erfahren, wurde eine genomweite Transktiptomanalyse von Brg1-depletierten Embryonen im späten Blastulastadium durchgeführt. Hier zeigte sich, dass hauptsächlich Gene, die mit Embryonalentwicklung und Musterbildung assoziiert sind, in ihrer Transktiption beeinträchtigt sind. Zu den Brg1-benötigenden Genen zählen sowohl dosalisierende als auch ventralisierende Loci. Dies widerspricht der Zuordnung von Brg1 zu einem bestimmten Differenzierungsprogramm und deutet auf eine generelle Funktion hin. Da die transktiptionelle Veränderungen im Blastulastadium einen Zusammenhang mit der zygotischen Genomaktivierung vermuten ließen, wurde eine weitere Transkriptomanalyse durchgeführt, in welcher das Expressionslevel von Embryonen unmittelbar vor und nach der MBT verglichen wurde. Dabei zeigte sich, dass insbesonders Gene, die eine massive Transktriptionsteigerung erfahren, von Brg1 abhängig sind. Brg1 ist also ein essentieller Amplifikator der transkriptionellen Genomaktivierung. Die von ihm ausgelöste Aktivierungswelle wird benötigt um eine embryonale Induktion der frühen Signalzentren auszubalancieren, so dass eine intakte Musterbildung und Embryonalentwicklung gewährleistet werden kann. Damit ist Brg1 ein essentieller Bestandteil der embryonalen Musterbildung im Wirbeltier.

Summary

This study establishes by gain- and loss-of function analysis an essential role for the chromatin remodeling factor Brg1 during embryonic patterning in *Xenopus*. While embryos depleted ubiquitously for Brg1 protein die from gastrulation onwards, embryos locally depleted on either dorsal or ventral sides survive until tadpole stage and display specific phenotypes. Already at late blastula, antisense knockdown of Brg1 protein levels reduced critical gene expression in two dorsal signaling centers, i.e. the BCNE and the Nieuwkoop center. This impairment is sustained during gastrulation and results in a functionally impaired Spemann organizer. Homotopic transplantations of Brg1-depleted tissue into wild typ embryos indicate a requirement for Brg1 in the BCNE for the differentiation of normal eye and brain structures. The local knockdown of Brg1 protein in the vegetal hemisphere, however, reveals the existence of additional functions for Brg1 outside the BCNE. Taken together, the embryological results indicate a disequilibrium between dorsalizing and ventralizing pathways in Brg1-depleted embryos, which leads to detrimental malformations of the embryonic body plan, in particular in dorso-anterior structures.

To obtain more information about Brg1 target genes a genome-wide transcriptome analysis at the late blastula stage was performed. Strikingly, developmental and pattern specific genes were preferentially altered in their transcription. The Brg1-dependent genes include both dorsalizing and ventralizing factors, consistent with my embryological results. This result denies a link between Brg1 and a single developmental program, but suggests more general functions. Since the earliest transcriptional changes observed in Brg1 morphant embryos occur at late blastula stage, a connection between Brg1 and global zygotic genome activation was suspected. This hypothesis was investigated with a second microarray experiment, in which the transcriptomes of wild type *Xenopus* embryos were compared immediately before and after the onset of zygotic transcription. This data set revealed that preferentially those genes depend on Brg1, which become strongly activated at the MBT. Therefore, Brg1 serves an essential function as a dose-dependent transcriptional amplifier of the zygotic genome activation. The full amplitude of transcriptional response, which Brg1 generates, is needed to counterbalance the activities of the early signaling centers to achieve a proper embryonic patterning and development. This identifies Brg1 as an essential component of embryonic patterning in vertebrates.

1   Introduction

1.1   *Xenopus* as a model organism

The African claw frog is a long standing model organism in developmental research. Due to its extrauterine development, easy handling and its big egg size, researchers studied and characterized the development of *Xenopus* already beginning of last century. The detailed experiments that were performed reached from labeled cell tracking within the developing embryo up to cell or tissue transplantation. This opened up fundamental knowledge about e.g. the gastrulation processes and cell specification and commitment. Given that *Xenopus* and human evolutionary are only 344 million years apart, segregates *Xenopus* among other model organisms like worm, fly and fish as the closest relative to humans (Schmitt et al, 2014). This indicates high homolog rates in humans, chromosomal symmetry, a similar organ blueprint and makes biochemical analyses between *Xenopus* and humans valid. The just mentioned similarities paired with the diploid genome of *Xenopus tropicalis* and the big knowledge about cell biology highlights *Xenopus* in a leading position for biomedical research in the post-genomic era.

1.1.1   Life cycle of *Xenopus*

The *Xenopus* egg can be distinguished into two entities. The upper pigmented animal pole and the lower non-pigmented vegetal pole. After fertilization, the embryo undergoes 13 holoblastic cell divisions that consist of alternating S and M phases only. G-phases are excluded from the cell cycle in order to rapidly increase embryonic cell numbers. At the end of this period of cleavage divisions, the embryo reaches the blastula stage. Its spherical shape is not changed, but inside the embryo a fluid-filled cavity, called blastocoel, has formed underneath the animal pole. If animal pole cells are cultured individually they form epidermal tissue. The floor is lined with bigger yolk-rich cells that later will form mesendodermal cells. At this particular developmental stage, approximately 6 hours after fertilization the "midblastula-transition" (MBT) takes place. The embryo undergoes major rearrangements on both cellular and genomic level. The gap-phases are included into the cell cycle, tissues show asynchronous cell division and cells become motile (Newport & Kirschner, 1982a). Also on genomic level major changes are happening. The zygotic genome is activated and maternal protein is successively degraded. With this burst of transcription also pluripotency is established, which is needed for the specification process during development. In summary, major rearrangements happen to prepare the embryo for the upcoming gastrulation, in which cells start to migrate and the three germ layers and body axes are specified. The first visible morphological feature

of gastrulation is the appearance of the dorsal lip. Cells in the dorsal marginal zone, called "bottle cells", undergo apical constriction, start to elongate and initiate the involution process, which defines gastrulation (Hardin & Keller, 1988). The leading cells actively migrate into the embryo, while the cell-cell contacts results in an involution process which spreads from dorsal to ventral. During gastrulation the three germ layers and the body axes are specified. Furthermore, convergent extension movements lead to an elongation of the embryo along the antero-posterior axis. Within 12 hours post fertilization this crucial developmental period is accomplished. After gastrulation, the neural plate forms and at the boarders the neural folds rise and fuse from posterior to anterior. The underlying mesoderm thereby forms the notochord which then secretes factors that specify somites and the neural crest cells. Meanwhile, the neural plate forms the CNS and brain structures. After neurulation the main body axes are established and brain structures are specified. Following the neurulation, the organogenesis takes place. At the same time the embryo has elongated much further and the tail is formed. After approximately three days the embryo hatches and embryogenesis is completed. Now the tadpole has to be fed in order to grow and go through metamorphosis in which the limbs are formed and the tail again gets reduced. After additional 12 month the frogs are sexually mature (after (Nieuwkoop & Faber, 1994)).

1.1.2 The zygotic genome activation

In higher eukaryotes the first developmental processes are dependent solely on maternal information, whereas the zygotic genome has to be activated. In mice and humans the zygotic activation is one of the earliest steps after fertilization, namely at the 2 or 4 cell stage, respectively (Baroux et al, 2008). However in other species like *Drosophila*, zebrafish and *Xenopus* this event happens much later after the 10th or 13th cell division and is one feature of the midblastula transition (Kane & Kimmel, 1993; Newport & Kirschner, 1982b). This process can be subdivided in two major steps. First the maternal transcript destabilization and second the transcriptional activation of the zygotic genome. In *Drosophila*, it has been shown that 35% of the maternal transcripts are destabilized and successively degraded over the time of the "zygotic genome activation" (ZGA) (De Renzis et al, 2007). There are several mechanisms how the destabilization is achieved in *Drosophila*. Already with egg activation a major cascade is started, in which the transcription of Smaug, an RNA-binding protein which recognizes cis-regulatory elements in maternal transcripts, is induced. Smaug-binding recruits a deadenylase complex which removes the poly-A tail and thereby destabilizes the maternal transcripts (Semotok et al, 2005; Smibert et al, 1996; Tadros & Lipshitz, 2009). In *Xenopus* it was shown that maternal transcripts are destabilized via an AU-rich cis element (ARE)-mediated pathway. Maternal transcripts with such a cis-element are recognized and bound by

the Embryo Deadenylation Element Binding Protein (EDEN-BP). Upon fertilization a phosphatase is activated, which dephosporylates EDEN-BP and thereby promotes deadenylation, which leads successively to destabilizing of the maternal transcripts. However, no deadenylation is observed until the onset of the zygotic transcription, which indicates that an additional zygotic factor is required to initiate the destabilization process (Detivaud et al, 2003; Tadros & Lipshitz, 2009). In both, *Drosophila* and in zebrafish, it was shown that microRNAs are also involved in the destabilization process. This suggests a *de novo* synthesized transcript at MBT as a possible candidate also for *Xenopus* to initiate the degradation of maternal protein.
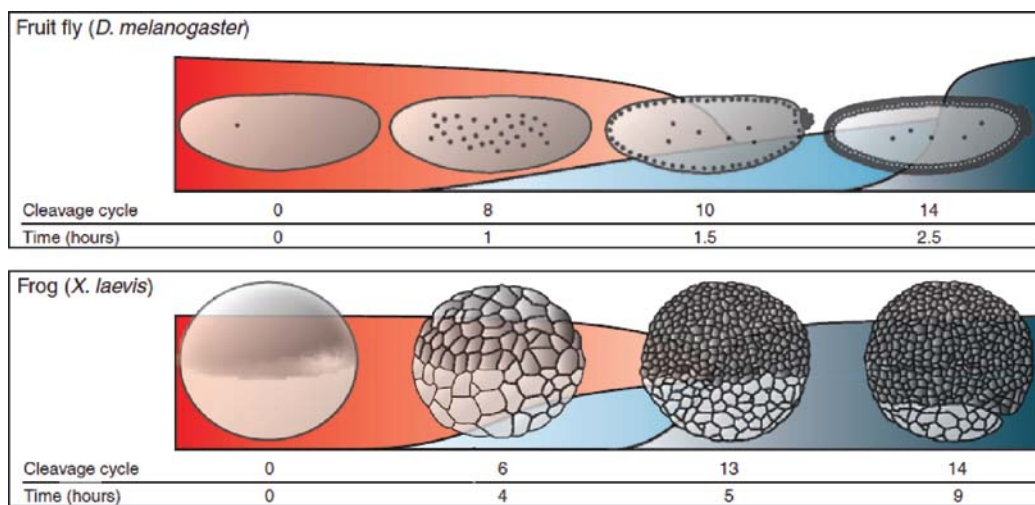
Figure 1.1: Overview of zygotic genome activation in *Drosophila* and *Xenopus*. Depicted are early developmental stages of *Drosophila* and *Xenopus* embryos. In the background the changes in gene expression is displayed schematically. The red curve represents the maternal RNA and its successive degradation with onset of ZGA. The two blue curves indicate minor (light blue) or major (dark blue) waves of zygotic genome activation (modified from (Tadros & Lipshitz, 2009)).

The second step is the transcriptional activation of the zygotic genome. The timing of the activation was long time under debate. Besides the hypothesis of an intrinsic maternal clock, which gets activated by the time of fertilization and "counts" the numbers of cell divisions, there are strong evidences that argue for the model of a critical "nucleocytoplasmic ratio" (Howe & Newport, 1996; Newport & Kirschner, 1982b; Tadros & Lipshitz, 2009). This model hypothesizes that distinct maternal repressive factors are diluted out through the earliest cell division. Over 30 years later four factors were characterized in *Xenopus*, which support this hypothesis (Collart et al, 2013). It was shown that overexpression of maternal DNA replication factors Cut5, RecQ4, Treslin and Drf1 lead to a prolonged synchronous cell cycle, beyond the 13th cell division, which results *in vivo* in a delay of transcriptional activation of several genes at the MBT. With the activation of the zygotic genome,

3

hundreds of genes are either *de novo* synthesized or undergo a rapid transcriptional upregulation. This phase of extensive changes in the transcriptome needs a very tight and efficient regulation. Unfortunately in *Xenopus*, very little is known about the mechanism and the regulation behind this burst of transcription. In *Drosophila*, in contrast, over the last years the research and knowledge about this critical phase of early development has grown. It was shown that a majority of early transcribed genes in the *Drosophila* embryo share a cis-regulatory hepta repeat. Shortly after finding this common motif, the transcription factor Zelda was characterized, which binds to this element and initiates the transcription of early zygotic genes (Harrison et al, 2011; Liang et al, 2008). Regarding the synchrony of transcription, a mechanism through paused RNA polymerase II is suggested (Lagha et al, 2013). This is very likely as promoter regions are preinitiated and only need a start signal which could be either another protein or microRNA.

1.1.3 Axial patterning during *Xenopus* development

1.1.3.1 Phase I: Fertilization to MBT

The body of Bilateria contains three body axes. The dorso-ventral, the antero-posterior and the left-right body axes. This body plan is determined very early during embryogenesis. In the amphibian embryo already the fertilization determines the dorso-ventral body plan. In the oocyte ventral Bmp2 is distributed ubiquitously and during oocyte maturation specific mesendodermal-fate promoting factors, like VegT, and a dorsalizing activity are transported to the vegetal pole (Houston, 2012; King et al, 2005). After sperm entry, the egg undergoes the cortical rotation and the dorsalizing activity is shifted and thereby activated (Gerhart et al, 1989; Houston, 2012; Larabell et al, 1997). A schematic overview of this period is depicted in Figure 1.2. Although well studied, the process of the cortical rotation is still not completely resolved. Approximately 45 min after fertilization, vegetal microtubules polymerize thereby causing a 30° rotation of the cortex, usually in the opposite direction to the sperm entry point. The rotation of the cortex accordingly induces also a translocation of the underlying subcortical cytoplasm (Houston, 2012). With this cytoplasmic translocation the dorsalizing activity is activated and accumulates on the prospective dorsal side that later on establishes the first patterning centers in blastula embryos. So far, it is known that the dorsalization is mediated by nuclear ß-catenin, but whether ß-catenin is activated by cytoplasmic factors or via an extracellular wnt-signal, is not solved yet. Since Wnt11 mRNA is maternally expressed, accumulates in the vegetal cortical cytoplasm during oogenesis and is translocated with cortical rotation, it is very likely that the dorsalizing activity is induced by maternal Wnt11 and mediated by maternal ß-catenin (Houston, 2012).
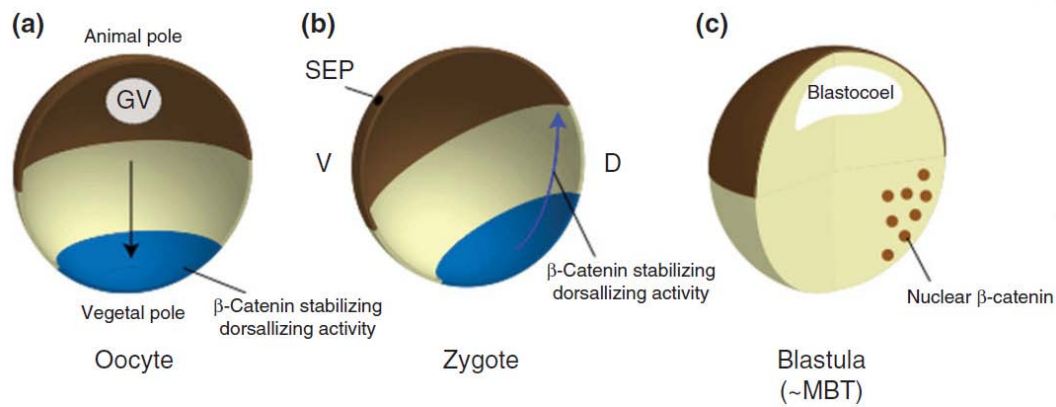
Figure 1.2: Schematic events of cortical rotation and its consequences. (a) During oogenesis VegT and dorsalizing factors are translocated to the vegetal pole. **(b)** Sperm entry triggers polymerization of microtubules in the egg and lead to a ~30° shift of the egg cortex relative to the inner cytoplasm. Cortical and subcortical cytoplasmic factors are thereby translocated, amongst them the dorsalizing activity. **(c)** ß-catenin is stabilized in the nuclei of prospective dorsal cells and induces a specific gene regulatory network. GV, germ vesicle; SEP, sperm entry point; V, ventral; D, dorsal (adapted from (Houston, 2012).

1.1.3.2   Phase II: MBT to gastrulation

Given that preMBT cells are immobile, the expression pattern of maternal mRNAs and proteins are similar at the time of fertilization and at blastula stage. The vegetally located maternal T-Box transcription factor VegT and dorsally localized ß-catenin in combination with the burst of transcription lead to distinct protein gradients and signaling centers, which pattern the embryo. At blastula stage two signaling center arise, the "blastula Chordin- and Noggin-expression center" (BCNE) and the "Nieuwkoop center". In the dorsal-vegetal quadrant of a blastula embryo, *vegT* and *ß-catenin* are coexpressed. The cooperation of the two transcription factors first induces a high expression of nodal-like signaling (Agius et al, 2000). The combination of VegT, ß-catenin and high nodal-like signaling successively leads to the expressions of genes which are associated with the "Nieuwkoop center" and have important roles during axial patterning (Agius et al, 2000; Robertis & Kuroda, 2004). One of these genes is *cerberus*, which is required for head formation in later stages (Kuroda et al, 2004). For *cerberus*, at least four inductive transcriptions factors are known which underlines the needed interplay of various signaling pathways (Heasman, 2006; Yamamoto et al, 2003). One is Xlim1, which is a target gene of maternal VegT and another is Siamois, which is a target of the ß-catenin signaling. *Cerberus* is expressed in involuting mesendodermal cells and acts as an inhibitor for BMP-, wnt- and nodal signaling (Bouwmeester et al, 1996; Piccolo et al, 1999a).

The second signaling center is located in the dorso-animal quadrant and is characterized by an excess of maternal nuclear ß-catenin protein. As the name already implies, the BCNE is defined by expression of BMP-inhibitors Chordin and Noggin (Kuroda et al, 2004). Recently it was discovered

that Noggin proteins under physiological conditions, besides BMP, also inhibit Nodal and Wnt factors, albeit to less extent, and thereby help to develop forebrain structures (Bayramov et al, 2011). BCNE cells later on give rise to the central nervous system and notochord cells and are essential for proper dorso-anterior development (Robertis & Kuroda, 2004). Although both genes are coexpressed and have similar functions, a hierarchy of the two factors was observed. Whereas Chordin is required and sufficient for dorso-anterior development, Noggin is dispensable and a loss can be compensated (Kuroda et al, 2004).

In the ventro-vegetal quadrant of blastula embryos solely maternal VegT and TGF-ß factor Vg1 inductive signals are present. Since ß-catenin is not nuclear, the nodal concentration is low and endodermal signals are induced. One of the first targets of VegT and Xnr proteins is the gene *mixer*, which then induces endodermal genes like the *gata* factors and *sox17α* (Heasman, 2006; Xanthos et al, 2001) .
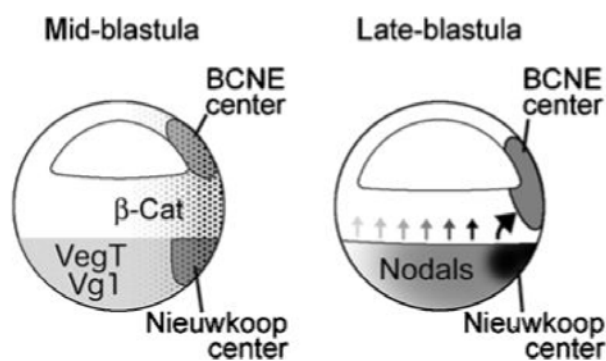
Figure 1.3: Scheme of inductive signals in the blastula. At Mid-blastula the Nieuwkoop center forms in dorso-vegetal compartments, when vegetal VegT expression overlaps with dorsalizing nuclear ß-catenin stabilization. The BCNE forms in the dorso-animal part in which mainly maternal ß-catenin is active. In late-blastula embryos the nodal factors specify the overlying cells as mesoderm (adapted from (Robertis & Kuroda, 2004).

1.1.3.3 Phase III: Gastrulation

At the MBT, cells start to divide asynchronously and some cells become mobile, which is an essential feature for the upcoming gastrulation. Cells in the dorsal marginal zone (DMZ) involute into the embryo and by this process inductive signals specify the three germ layers. Furthermore, the dorso-ventral and antero-posterior body axes are determined (Newport & Kirschner, 1982a). With the beginning of gastrulation, *bmp4* is ventrally expressed and induces genes like v*ent1* and *vent2* (Heasman, 2006; Onichtchouk et al, 1998). The *vent* genes are important for keeping the identity of ventral mesoderm. In ventral marginal zone (VMZ) antisense knockdown studies it was shown that a loss of Vent function induces muscle containing secondary body axes, indicating dorsalization of ventral mesoderm. (Onichtchouk et al, 1998). Simultaneously on the dorsal side, cells that belong to

the Nieuwkoop center initiate the involution process and form the Spemann organizer. These organizer cells secrete BMP, Nodal-like and Wnt inhibitors in order to counteract ventralizing signaling. Noteworthy, many of the secreted proteins are already present at blastula stage, like Chordin, Noggin (De Robertis et al, 2000). Both, dorsal and ventral factors, spread into the equatorial zones and thereby refine the gradients to balance fate determination in the embryo (De Robertis et al, 2000; Lee et al, 2006). This basal principal of antagonistic signals is further refined by feedback mechanisms. For example Sizzled has an important function in DV-patterning. It is under transcriptional control of BMP-signaling and is expressed on the ventral side. It was shown that Sizzled protein acts as a proteolytic inhibitor of Xolloid-related, a metalloproteinase, which is expressed ventrally and clips Chordin protein, resulting in a release of the bound BMP protein. The inhibitory effect of Sizzled against Xolloid-related then leads to stabilization of Chordin protein on the ventral side and therefore to a negative feedback loop of BMP-signaling (Lee et al, 2006). Such a mechanism indicates that DV-tissue can only form if both counteracting signals are present and interact with each other.
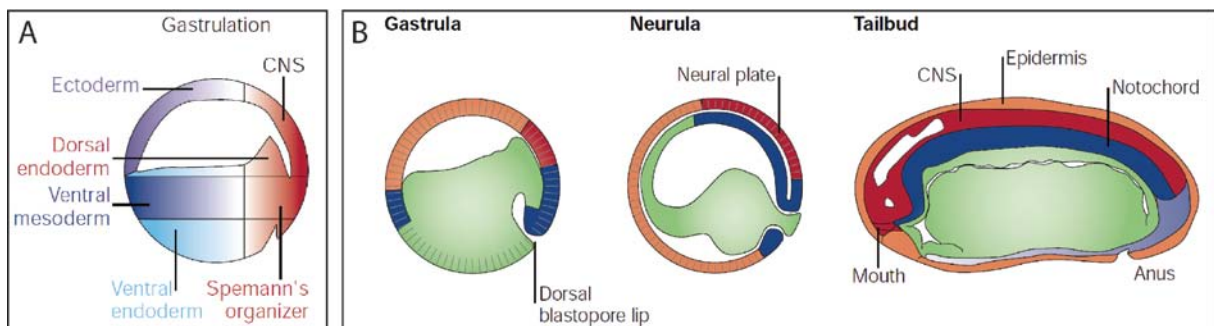
Figure 1.4: Schematic illustration of all movements and signaling centers during gastrulation. A shows a scheme of an early gastrula embryo with the organizer territory and specified germ layers. **B** shows an overview of cellular movement during gastrulation and neurulation. The Organizer involutes into the embryo and specifies head and CNS structures into the overlying ectoderm. Cells arising from the BCNE do not involute and form the neural plate and CNS during neurulation. In the tailbud scheme the final body plan is set and organogenesis starts. CNS, central nervous system (Modified from (De Robertis et al, 2000).

During gastrulation, the antero-posterior axis (AP-axis) is established. As mentioned above, cells of the Nieuwkoop center are the first ones that involute. This migration is guided by proteins such as Fibronectin (Rozario et al, 2009). The first involuting cells, defined as prechordal mesoderm, will become the most anterior part of the embryo while still secreting BMP-, Wnt- and Nodal- inhibitors. The secreted proteins spread into the overlying ectoderm and induce head structures (Durston et al, 2010). They are followed by the prospective chordamesoderm, which undergoes convergent

extension movements while migrating (Heasman, 2006; Ninomiya et al, 2004). This leads to an elongation of the embryo along the antero-posterior axis. Furthermore, the lateral non-organizer mesoderm establishes the transient expression of the Hox cluster genes, which then become stabilized by the organizer mesoderm cells. The refinement of the Hox gene expression continues through the neurulation process until the AP-axis is set (Durston et al, 2010).

1.2   Chromatin dynamics

Chromatin is defined as the association between DNA and its binding proteins. It has the ability of constantly rearranging, which is the key feature for cell survival and differentiation. Every cell contains the same DNA amount, the same genomic sequence. However during DNA-replication, mitosis and differentiation, specific genomic loci have to be opened, silenced, enhanced or repressed. These different needs results in unique chromatin states for each cell subtype. The regulation above the genetic level is named "Epigenetics". One definition of Epigenetics was formulated in 1994: "Nuclear inheritance which is not based on differences in DNA sequence" (Holliday, 1994).

1.2.1   Chromatin structure

Nucleosomes are the repeating unit of chromatin and consist of an histone octamer with ~ 147 bp of DNA wrapped around it (Luger et al, 1997). The histone octamer consists of four dimers of H2A, H2B, H3 and H4. Nucleosome assembly starts with the deposition of an H3-H4 tetramer onto the DNA followed by the H2A-H2B tetramer. Histones are composed of a globular domain, which lies in the core of the nucleosome. Besides the globular domain, histones also carry flexible N-terminal histone tails, which protrude from the nucleosome and are favorable targets of post-translational modifications (PTM) (Allis et al, 2007). This highly organized composition ensures a multitude of protein-protein interactions, which regulate the octamer stability. Several electrostatic and hydrogen bonds additionally strengthen the connections within the octamer but also the connection to the DNA. (Luger et al, 2012). The DNA between adjacent nucleosomes is called "linker DNA", and makes chromatin more flexible. Accordingly, chromatin forms nucleosomal arrays and short-range interconnection between the nucleosomes, which results in so called "fibers" (see Figure 1.5). It is thought that the chromatin fibers are organized in further "secondary" structures. One example is the 30 nm fiber, which was postulated as the chromatin structure, in which chromosomes are compacted in mitotic cells. However, some studies could not support this hypothesis *in vivo* (Nishino

et al, 2012; Robinson et al, 2006). Besides the highly controversial predictions of the chromatin organization there are aspects of common agreement. Firstly, the composition of the histone octamer affects the overall stability of the nucleosome and thereby also the overlying chromatin organization. For all histones, isoforms are known which contribute to the nucleosomal composition and change the nucleosomal stability. Secondly, the modified N-terminal tails of histones play a crucial role in chromatin organization. Thirdly, incorporation of linker histone H1 leads to a higher compacted and dense chromatin fiber. Fourthly, higher ordered chromatin is dynamic and interconnected with its environment, e.g. the nuclear envelope and lamina (Allis et al, 2007; Dambacher et al, 2013).
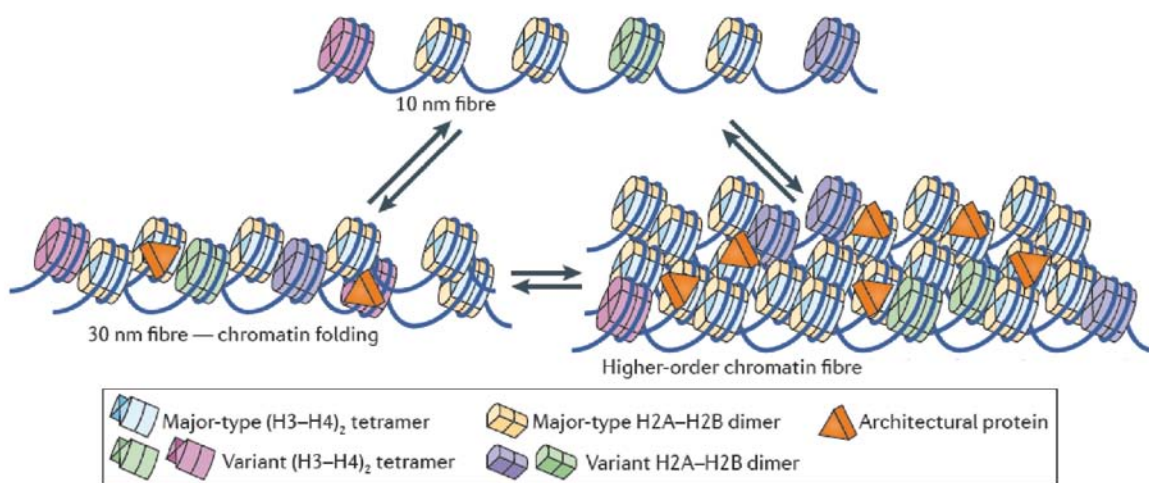
Figure 1.5: Chromatin dynamics and higher order structure. DNA is wrapped around nucleosomes and the linker DNA connects the nuclesomal subunits. This evenly spaced nucleosomal array displays a 10 nm fiber, like beads on a string. The fibers can interconnect and thereby create a more compacted chromatin structure, often referred to 30 nm fiber. To keep the architectural integrity chromatin structural proteins like Histone H1 (here: architectural proteins) have to be incorporated. A higher order structure of chromatin is necessary in order to organize and compact the DNA. Histone variants and histone modifications help to form, organize and change chromatin structure (modified after (Luger et al, 2012)).

A long-standing agreement was the division of chromatin in euchromatin and heterochromatin. Euchromatin is characterized by permissive, open, decondensed chromatin, which is highly accessible for transcription factors and RNA polymerases. Heterochromatin, in contrast, is defined as a highly condensed, repressive, closed chromatin structure, which is associated with repressed genes and pericentric or telomeric chromosomal regions. Interestingly, several recent studies have suggested that the accessibility of heterochromatin for DNA-binding-proteins, like transcription factors, does not differ significantly (Chen & Widom, 2005; Filion et al, 2010). However, some chromatin conformation and post-translational modification are clearly associated with either permissive, open chromatin or condensed, repressive chromatin.

As embryogenesis proceeds, it is obvious that chromatin rearranges throughout the development. Pluripotent genes get restricted and tissue specific gene expression is stabilized. A study performed in *Xenopus* showed, that repressive histone marks increase during development in contrast to active histone modification which show a peak of enrichment before the onset of gastrulation (Schneider et al, 2011). In accordance to this, Heterochromatin Protein 1 stabilization on DNA is strengthened over differentiation (Meshorer et al, 2006). Additionally, DNA-dense regions, indicating a condensed state of chromatin, accumulate in differentiating cells (Xie et al, 2013; Zhu et al, 2013). Thus, the overall agreement is that ES cells are very permissive and display hyperdynamic plasticity. But during differentiation this plasticity is restricted, resulting in distinct cell type with a distinct gene expression profile. In 2011, the group around Bas van Steensel used genome-wide DamID mapping in *Drosophila* Kc167 cells and classified five different chromatin types, defined by the presence of distinct proteins and/ or histone modifications (Filion et al, 2010; van Steensel, 2011).

1.2.2 Posttranslational modifications

The flexible histone tails that protrude from nucleosomes are, as mentioned above, a favored target for posttranslational modifications, which affect chromatin dynamics, structure and gene expression. A large set of chromatin-modifying enzymes were discovered over the last decade. The combinatorial possibilities of various histone modification paired with enrichments of distinct modifications at particular loci have led to the proposition of the "histone code" (Jenuwein & Allis, 2001). This code should give information about chromatin features depending on their marks and the binding of chromatin-modifying enzymes.

One of the best studied histone modification is methylation. Two amino acids can be methylated: arginine and lysine. Protein arginine methltransferases (PRMTs) methylate the two amino groups in the side chain of an arginin. This is possible either in a symmetric way: one CH_3 on each nitrogen atom, or in an asymmetrical way: two CH_3 on one nitrogen (Bedford & Clarke, 2009). In 2010, a distinct function for Prmt2 during *Xenopus* development was revealed. In preMBT embryos, maternal ß-catenin recruits Prmt2 to specific loci of dorsalizing genes and marks the promoter region with asymmetrical H3R8me2. This mark was sufficient to establish the dorsalizing program *in vivo* (Blythe et al, 2010).

Besides arginine, also lysine residues can be methylated. Up to three methyl groups can be attached to the lysine side chain amino group. Some methyltransferases are very specific for one particular reaction. One example is PrSet7, which sets the monomethylation on H4K20, whereas the Suv4-20 proteins catalyze the conversion of monomethyl to the di- or tri methylated state (Pannetier

et al, 2008; Schotta et al, 2004). Presumably, the best studied methylation marks are on lysine 4 and 27 of histone H3. The marks are thought to be mostly counteracting, as promoters of actively transcribed genes are decorated with H3K4me3 and silenced genes are marked with H3K27me3 (Cao & Zhang, 2004; Guenther et al, 2007; Schuettengruber et al, 2009). Notably, one exception to this rule can be found in ES cells. In this special cell state particular genes are decorated with both marks, referred to as bivalent state (Azuara et al, 2006).

Figure 1.6: Posttranslational modifications on histone N-tails. Shown are the N-terminal histone tails of the four core histones, H2A, H2B, H3 and H4 and the various modifications, which can be found on specific positions. A histone tail can be decorated with several modifications simultaneously. ph, phosphorylation; ac, acetlyation; ub1, ubiquitinilaytion; me, methylation (Bhaumik et al, 2007).

Another important histone modification is the acetlyation of lysine residues. Specific histone acetylases catalyze the transfer of an acetyl group on to the amine group in the lysine side chain. A hallmark for open chromatin and active transcription is the acetlyation of H4K16. Also, this modification is reversible and histone deacetlyases (HDAC) specifically remove the acetyl group.

Other histone modification, which were shown to contribute to the network of the "histone code" are phosphorylation, ubiquitination, sumoylation, adenylation and biotinylation.

1.2.3 Chromatin remodeling complexes

Besides the chromatin modifying enzymes that write, read or erase histone modifications, chromatin remodeling complexes display another class of chromatin modifying enzymes. These multi-protein complexes rearrange nucleosomes by using the energy of ATP-hydrolysis. In doing so, they alter histone-DNA contacts and move nucleosomes along the DNA, evict or exchange nucleosomes or histones (Becker & Horz, 2002; de la Serna et al, 2006; Hargreaves & Crabtree, 2011). Three different subclasses of chromatin remodeling complexes are described, depending on their ATPase subunit: SWI/SNF, ISWI and CHD. Common to all ATPase subunits is the origin of superfamily 2 (SF2) DNA helicases (Mueller-Planitz et al, 2013a).

The remodeling SWI/SNF family is characterized by the presence of a bromodomain containing ATPase subunit. The bromodomain mediates binding to acetylated histones (Hassan et al, 2002). The ATPase subunits are highly conserved through evolution and can be found from yeast (Swi2/Snf2), over *Drosophila* (Brahma) to man (Brahma/SMARCA2 and Brg1/SMARCA4) (Hargreaves & Crabtree, 2011). Besides the catalytic subunit, the mammalian SWI/SNF complex consists of several "Brahma-associated factors", the BAF proteins. Some of the BAF proteins, like Baf250/ARID1A and BAF155/SMACD1, are always present in the complex. Other BAF proteins, like BAF60/SMARCD or BAF53, contribute to complex formation in a tissue or cell signal specific fashion (Lessard & Crabtree, 2010; Simone, 2006; Yoo & Crabtree, 2009). Additionally, tissue- or signal-specific binding partners are known which also contribute to complex composition. Initially, Brahma was identified and isolated in a screen for dominant suppressors of Polycomb mutations (Tamkun et al, 1992). Similar to the findings in yeast, this suggests a role as transcriptional activator (Laurent et al, 1991). Meanwhile several studies have shown that the mammalian SWI/SNF complex is present in both, gene activation and repression, depending on the tissue and gene (Murphy et al, 1999; Wang et al, 2010). Besides a crucial function in development, which is described in detail in chapter 1.3 below, the SWI/SNF complex is also required for cell cycle progression. Mutations in Brg1 alleles were broadly characterized in malignant tumor tissue, indicating a role for SWI/SNF complex in cell cycle check points (Wong et al, 2000).

The second big chromatin remodeling family is characterized by the ATPase "Imitation SWI", ISWI. ISWI is defined by a C-terminal HAND-SANT-SLIDE (HSS) domain. However, recently it has been shown that the ATPase domain of ISWI exclusively is involved in its chromatin remodeling activity (Mueller-Planitz et al, 2013b). As for Brahma and Brg1, various complexes are described in which only ISWI is incorporated. For example in *Drosophila*, three different complexes are described. The ACF and CHRAC complexes contain, aside from ISWI, the bromodomain containing protein Acf1. The NuRF complex is characterized by the NURF31 subunit, which mediates interaction with nuclear

hormone receptors and increases nuclesomal sliding activity of the complex. Also for ISWI containing complexes, numerous functions within the cell or during differentiation were described (Becker & Horz, 2002; Hargreaves & Crabtree, 2011).

The third class of ATPase remodelers is the CHD family. These ATPase enzymes are characterized by two N-terminal chromodomains. Several CHD ATPase enzymes were classified and depending on functionality further subdivided. The NuRD complex, a well studied complex containing CHD3/Mi-2α or CHD4/Mi-2β, was shown to bind histone deactelyases HDAC1/2, suggesting that NuRD represses transcription by removing acetlyation marks from histones (Hargreaves & Crabtree, 2011). For Chd7, a direct interconnection with Brg1 in neural crest formation was described in *Xenopus* and humans (Bajpai et al, 2010).

1.3   The SWI/SNF complex in development

In *Drosophila*, the SWI/SNF ATPase Brahma was described as a positive regulator of homeotic genes, which counteracts their repression by Polycomb group genes (Tamkun et al, 1992). Flies deficient for Brahma function, die as unhatched larvae and both maternal as well as zygotic Brahma is required for *Drosophila* embryogenesis (Brizuela et al, 1994; Tamkun et al, 1992). In mammals, a second ATPase subunit of the SWI/SNF complex evolved, namely Brahma related gene 1 (Brg1). Notably, the two ATPase subunits are mutually exclusive and display different functions during development. Mice deficient for Brahma, develop normal but adult mice were 15% heavier than control siblings, which is explained with an increase of cell proliferation (Reyes et al, 1998). In contrast to the mild phenotype of Brm$^{-/-}$, a loss of Brg1 causes early embryonic lethality during implantation. Noteworthy, Brg1 heterozygotes survive but are predisposed to exencephaly and tumors (Bultman et al, 2000). This striking difference between Brahma and Brg1 is also displayed on the transcriptional level. The gene expression of both ATPase subunits were monitored during mouse development and *brg1* expression is clearly more abundant than *brahma* gene expression (Bultman et al, 2000). Oocytes depleted for Brg1 complete meiosis, but exhibit a developmental arrest at the 2 cell stage. At this stage of mouse development the zygotic genome activation takes place. One third of α-amanitin sensitive genes showed a reduction in gene expression, which indicates a requirement of Brg1 during the onset of zygotic transcripts (Bultman et al, 2006). Since Brg1-deficient primary mouse embryonic fibroblasts (PMEFs) proliferate normally, Brg1 containing SWI/SNF chromatin remodeling complexes are essential for embryogenesis, but not for cell vitality (Bultman et al, 2000). Further proof for the requirement of Brg1 in ZGA comes from the fact that mouse wild type zygotes depleted for *brg1* by RNAi, also arrest at the 2 or 4 cell stage (Bultman et al, 2006).

Little is known whether Brg1 is required during *Xenopus* development. One study suggested that it is necessary during neurogenesis. Kirsten Kroll's laboratory investigated the expression pattern of Brg1 and stated an excess of *brg1* transcripts in neural tissue. By knocking down Brg1 protein level with a translation-blocking antisense morpholino oligonucleotide, they showed that Brg1 is crucial for progression of neuronal cell differentiation. Neural tissue, positive for neural progenitor *sox2*, was expanded from midneurula stage 15 on, whereas terminally differentiated neural marker *n-tubulin* was diminished. Furthermore, Brg1 morphant embryos display truncated anterior structures and reduced eye size (Seo et al, 2005). These defects correlate well with the apparent exencephalic phenotype seen in heterozygote mice. Another study dealing with Brg1 function during *Xenopus* development was performed by a former PhD student in our lab, Nishant Singhal. The morphological phenotype he generated with a different morpholino oligonucleotide also displayed dorso-anterior defects. In addition, he could observe an earlier requirement for Brg1 than neurogenesis. The discrepancy between the two studies in *Xenopus* and the differences of Brg1 function between the species is still unraveled and needs further detailed investigation.

Primarily, the research of SWI/SNF during development focused on Brg1. However, over the recent years the interest in the associated BAF increased. The protein Baf60 is a very good example. Three isoforms are characterized, named Baf60 a-c. Baf60a was shown to be part of various SWI/SNF complexes. In mouse ES cells Baf60a is incorporated in the so called esBAF complex. This complex was shown to be important for ES-cell renewal and pluripotency (Ho et al, 2009). Furthermore, Baf60a was described in the nBAF complex, which is present in postmitotic neurons (Yoo & Crabtree, 2009). The Baf60c isoform in contrast contributes to the SWI/SNF complex present in heart and skeletal muscle differentiation. Mice deficient for Baf60c show malformations in both muscle tissues and insufficient expansion of the anterior, secondary heart field. This study revealed that Baf60c mediates the physical interconnection between cardiac transcription factors and SWI/SNF chromatin remodeling ATPase Brg1 (Lickert et al, 2004). Recently, a detailed study about the mechanism of this interconnection was published. In proliferating mouse myoblasts, direct binding of Baf60c to MyoD on myogenic gene loci was observed. During differentiation a kinase is activated, which phosphorylates Baf60c and thereby induces the recruitment of Brg1-containing SWI/SNF remodeling complex supporting the activation of the myogenic loci (Forcales et al, 2012).

These examples define Brg1 as a transcriptional coregulator. The interplay with ß-catenin is probably one of the most interesting ones, as there are various roles and requirement for ß-catenin signaling during embryogenesis. A physical and genetic interaction of ß-catenin and Brg1 was firstly described in HEK293T cells and within this study it was suggested that Brg1 and ß-catenin interact in order to positively regulate Tcf-responsive reporter genes (Barker et al, 2001). Besides this, a role for

Brg1 was also suggested in TGF-ß signaling, as Brg1 interacts with Smad2 and Smad3 (Xi et al, 2008). Furthermore, a dual role of Brg1 in Sonic hedgehog signaling was shown (Zhan et al, 2011). With an involvement in such various cell signaling pathways, it is not surprising that Brg1 plays multiple roles in differentiation. Additional functions of Brg1 were described during ES-cell renewal, reprogramming and cancerogenesis (Bultman et al, 2000; Ho et al, 2009; Singhal et al, 2014; Singhal et al, 2010). Together, this data underlines Brg1 as a multifaceted regulator within development, differentiation and chromatin dynamics.

1.4 Objectives

The focus of this thesis is to clarify the functional role of Brg1 during early development in *Xenopus*. Unpublished data from Nishant Singhal, a former lab member, had suggested a functional link between Brg1 and canonical Wnt signaling, but had not provided conclusive evidence for this hypothesis. Therefore, the following goals were set in order to approach detailed informations:

• Characterize the morphological and molecular consequences of ubiquitous and region-specific perturbation of Brg1 activity by gain- and loss-of-function approaches *in vivo*

• Distinguish autonomous functions from paracrine functions of Brg1

• Determine the Brg1-dependent transcriptome

Ideally, the results from these approaches should allow to formulate a unifying hypothesis, which describes accurately the developmental regulatory impact of Brg1 in a vertebrate model organism.

2 Materials and Methods

2.1 Materials

2.1.1 Animals

In this work pigmented African claw frog *Xenopus laevis* and *Xenopus tropicalis* were used. Frogs were purchased from Nasco (Ft, Atkinson, USA). Frog husbandry was performed after the guidelines of the Deutsches Tierschutzgesetzt. The developmental stages were defined after P.D. Nieuwkoop and J. Faber (Nieuwkoop & Faber, 1994)

2.1.2 Bacteria

For DNA cloning and plasmid preparation DH5α *E.coli* from NEB were used.

DH5α	F´proA+B+ lacIqΔ(lacZ)M15 zzf::Tn10 (TetR) / fhuA2Δ (argF-lacZ)U169 phoA glnV44 f80 D(lacZ)M15 gyrA96 recA1 relA1 endA1 thi-1 hsdR17	NEB

2.1.3 Enzymes

The following enzymes were used:

enzyme	company
Advantage®2 Polymerase Mix	BD Biosciences
Alexa Fluor® 488, 594	Invitrogen
Alkaline phosphatase	Roche
BSA fraction V	Roth
Dig-NTPs	Roche
DTT	Promega
G (5')pppGcap analog	NEB
NTP-mix	Roche
Restriction endonucleases	NEB
RNase A	Sigma-Aldrich
RNAsin	Promega
Transcription buffer 5x	Promega
T3, T7, Sp6 RNA polymerase	Promega

enzyme	company
Proteinase K	Sigma-Aldrich
RNAse-free DNAse I	Promega
PeqGOLD protein marker V	Peqlab
Taq DNA polymerase	NEB

2.1.4 Chemicals

The chemicals used on a regular basis for solutions and buffers are ordered from Fluka, Merck, Sigma or USB.

Special chemicals are listed in the following table.

chemical	company	chemical	company
Agarose	Gibco/BRL	Lamb Serum	Gibco/BRL
Ampicillin	Difco	Levamisol	Vectro Lab
ß-glycerol phosphate	Sigma-Aldrich	Nitro blue tetrazolium, NBT	Biomol
5-Bromo-4-Chloro-3-indoyl-phosphate, BCIP	Biomol	Phenylmethanesulfonylfluoride, PMSF	Sigma-Aldrich
Calf serum	Gibco/BRL	Sodium orthovanadate	Sigma-Aldrich
Gentamycin	PAA labor. GmbH	Sodiumfluorid	Sigma-Aldrich
Glycogen	Fermentas	TRIzol® Reagent	Ambion
Human choriongonadotropin, Gonasi 500	ISBA, Farmac.	Xgal	Roth

2.1.5 Antibodies

The following antibodies were used in this thesis for the respective methods:

	dilution	method	company
primary antibodies			
rat α-Brg1, monoclonal	1:3	Western Blot	Dr. Elisabeth Kremmer
mouse α-alpha tubulin, monoclonal	1:8000	Western Blot	Sigma
rabbit α-ACTIVE®Caspase3 pAB, polyclonal	1:20000	ICC	Promega

		dilution	method	company
secondary antibodies				
goat α-mouse 700		1:10000	Western Blot	Biomol
donky α-rat IR800CW		1:10000	Western Blot	Biomol
α-rabbit IgG AP-Conjugate		1:1000	ICC	Promega
sheep α-Digoxigenin-AP Fab fragment		1:2000	WMISH	Roche

2.1.6   Oligonucleotides

2.1.6.1   Oligonucleotides for cloning

Oligonucleotides (primers) for cloning were designed and purchased from Sigma-Aldrich:

plasmid		vector	5'-sequence-3'
XhoI_Luciferase	for	pCS2+ GW	-CA CTCGAG_GAAGACGCCAAAAACATAAA-
Luciferase_XbaI	rev	pCS2+ GW	-CG TCTAGA_CACGGCGATCTTTCC-
attB1_BISH	for	pCS2+ GW	-GGGACAAGTTTGTACAAAAAAGCAGGCTTAACT_ GATAGTTGGTGGAAAACGTCAGAAGGA-
BISH_attB2	rev	pCS2+ GW	-GGGGACCACTTTGTACAAGAAAGCTGGGTC_ TCCCATCATGCTATGTGCGG-
ClaI-Siamois	for	pCS2+	-CAG ATCGAT_ATGACCTATGAGGCTGAAATGG-
Siamois_XhoI	rev	pCS2+	-CAG CTCGAG_TCAGTTTGGGTAGGGC-
ClaI_chordin	for	pCS2+	-CA ATCGAT_ATGCAGTGTCCCC-
Chordin_XhoI	rev	pCS2+	-CA CTCGAG_CTAAAAACTCCATGGA-

2.1.6.2   Oligonucleotides for quantitative RT-PCR

The following primers were designed using the online software Primer3 (http://biotools.umassmed.edu/bioapps/primer3_www.cgi), purchased from Sigma-Aldrich and quantitative RT-PCR was performed with the Roche Light Cycler 480 System. The following primer sequences target *X. laevis* gene sequences:

gene		5'-sequence-3'
foxa4	*for*	-GGAAACAAGCCAGGAGATGA-
foxa4	*rev*	-GAGTCCCTACCCCCATCATT-
gs17	*for*	-CTGGGGCTTGAGTCCTACAG-
gs17	*rev*	-AGCTTCCTGGCTGGTGATTA-
gsc	*for*	-GCTGGCAAGGAGAGTTCATC-
gsc	*rev*	-TTCCACTTTTGGGCATTTTC-
h4	*for*	-GACCGCGGTCACCTACACC-
h4	*rev*	-CTGGCGCTTCAGAACATACA-
siamois	*for*	-GAGCCTCAGGTCAGCAAAAC-
siamois	*rev*	-GGTACTGGTGGCTGGAGAAA-
xnr3	*for*	-AAGGTGAATGGATTTCGGAGACT-
xnr3	*rev*	-GCTGCCCCATCCGATCT-
xnr5	*for*	-GCTGCACCGCTACCTCTATC-
xnr5	*rev*	-TCAGCTAGGAGACCATTGCAT-
xnr6	*for*	-GGGAATGCTACAGACCTTTCAGT-
xnr6	*rev*	-ACATGTCAAAAGATAATGCCCAG-

Quantitative RT-PCR primers targeting *X. tropicalis* gene sequences:

gene		5'-sequence-3'
bmp4	*for*	-AGCCCAGTAAGGATGTGGTG-
bmp4	*rev*	-GGTCTCTCCGGGTACTCCAT-
cerberus	*for*	-TCCATGTTCCAAATCAGCAA-
cerberus	*rev*	-AATTCAGTGCCAGGTGGTTC-
chordin	*for*	-TCTGCTATACAGCGGCCTTT-
chordin	*rev*	-TACCCAGACCAGTCACCACA-
crbp	*for*	-CTGGCAAGTCCTCCAATGATA-
crbp	*rev*	-CTCTGTCTCCACCACCACCT-
crx	*for*	-CCCACGGAAACAAAGAAGAG-
crx	*rev*	-TTTAGCAAAGAGGGCTTCCA-
egr1	*for*	-CTCTCACACCCCTGTCTACCA-
egr1	*rev*	-CATTCTGCTTGGCTTGATGA-
follistatin	*for*	-TACCCAACAGCACCCTCTTC-

follistatin	*rev*	-GGGCCACAGTCTACGTTCTC-
foxc1	*for*	-GACCCGGACTCGTACAACAT-
foxc1	*rev*	-CTTTCAGGAGCCGATCTTTG-
foxd3	*for*	-CCCAGGCAAGGGAAACTACT-
foxd3	*rev*	-AATGAGTCCGGCTGTTGTCT-
foxd4l1	*for*	-ACCATGCCAACTCACCTTTC-
foxd4l1	*rev*	-TTATCAGCATCCAGGGCTTC-
foxi1	*for*	-TCCTCAGCGACCTTCAAACT-
foxi1	*rev*	-CATGAAATGGCTTGTGTTGG-
foxi4.2	*for*	-CTCCTACTCTGCCCTCATCG-
foxi4.2	*rev*	-AGCCTGCTTTGCTCTTTTTG-
gapdh	*for*	-ACCCAGAAGACTGTGGATGG-
gapdh	*rev*	-GTTGAGGCAGGGATGATGTT-
gata4	*for*	-ACGAAAGCGCAAACCTAAGA-
gata4	*rev*	-GAGCTGGTGGAAGGAGTGAG-
gata6	*for*	-GCTCGGCTACGATCACTCTC-
gata6	*rev*	-GGAGCCAACTCTGCTAGTGG-
gs17	*for*	-AGGGGGCATAAAGAGTGGTC-
gs17	*rev*	-CGAGGAGCAAACTGTGGAGT-
hes4	*for*	-AAGTCACCCGATTCCTCTCC-
hes4	*rev*	-GGGTTGCTGGTAATTCATGG-
jhdm1	*for*	-TTAAAGCATGGGGTGAAAGC-
jhdm1	*rev*	-GAGATGCCCAGGTCTGATGT-
kiaa1279	*for*	-GGCTGCAAAAGAGAATGAGG-
kiaa1279	*rev*	-TTTTACCCAACATCGTGCAA-
lrx2	*for*	-AATCACCAACAGGACGGAAG-
lrx2	*rev*	-GATCCGAGGTGGCTATTTCA-
meis3	*for*	-TTATGGGCACCCTCTGTTTC-
meis3	*rev*	-TGGGAATGACCCTGAATTGT-
noggin	*for*	-CGGAGGAGAGACTTGGAGTG-
noggin	*rev*	-CTGTGCTTTTTGCCCTGAA-
nr6a1	*for*	-CAGAAAGCAATCAGCCTTCC-
nr6a1	*rev*	-AGTGAGCCGAATCCATTGAG-
odc	*for*	-CCCTGGTTCAGAGGACGTTA-

odc	*rev*	-AGTATCTCCCAGGCTCAGCA-
otx2	*for*	-CAGCACCTCAGTTCCAGTCA-
otx2	*rev*	-TCATGGGGTAAGACCTCTGC-
prdm1	*for*	-TGTCATAAGCGGTTCAGCAG-
prdm1	*rev*	-TGCACTGGTAGGGCTTCTCT-
siamois	*for*	-GAACGGAGGGAATGTAAGAGG-
siamois	*rev*	-TCTGAAGGAAGTGGGTTTGC-
sizzled	*for*	-CCTGATGGGACACACTAGCA-
sizzled	*rev*	-CCGGTCTGTAGGAGGTTCTG-
sox1	*for*	-AGAACCCCAAGATGCACAAC-
sox1	*rev*	-GCCTCCGACATAACTTTCCA-
sox2	*for*	-AGATGGCTCAGGAGAACCC-
sox2	*rev*	-TCGTCGATGAATGGTCTTTTC-
sox11	*for*	-CAAGAAATGCCCCAAGCTAA-
sox11	*rev*	-GGACTTGATGGTGAGCGACT-
sox21	*for*	-GAGGAAGCCCAAGACCCTAC-
sox21	*rev*	-CCATGTAACCCAGCAACCTT-
tgif	*for*	-CTCGCCCTTCTGTGATCTGT-
tgif	*rev*	-TAAGTTGCTCGCTTCGGTCT-
twin	*for*	-ACACAGCACTGACCCTACAAGA-
twin	*rev*	-GATCAGGAATCAGGCCAAAA-
xnr3	*for*	-ACGTATTTGCCTCCCTTCCT-
xnr3	*rev*	-TCCTTTGTGTCCTTGGTATGG-
xnr5	*for*	-TCAGGCTCCTCATGGAAAGT-
xnr5	*rev*	-TGCTTGTGAAGTTGCCTTTG-
xnr6	*for*	-AAACCGTCTGCCAATCTGAC-
xnr6	*rev*	-TGGTTCCTTCCTCGATCTTG-
zic1	*for*	-GACACTACGGGCCACTTGAT-
zic1	*rev*	-AGCCTCATCTGTCCGTTCAC-
zic2	*for*	-TACTTTTCCCCGGCATACAC-
zic2	*rev*	-TCCGTCCTACCGAACATCTC-
zic3	*for*	-TGAACCGTCCTCAGAAAACC-
zic3	*rev*	-GGACATTCCTCCCAGTAGCA-

2.1.6.3 Morpholino oligonucleotide

Three different morpholino oliogonucleotides were tested for inhibiting *Xenopus* Brg1 mRNA translation. BMO1 and BMO2 target both *Xenopus laevis* and *Xenopus tropicalis* Brg1 gene sequences. BMO3 binds only the *Xenopus laevis* Brg1 gene sequence. The Control morpholino is directed against the human ß-globin mRNA. All morpholinos were purchased via GeneTools, LLC, USA.

morpholino	5'-sequence-3'
BMO1	-CCATTGGAGGGTCTGGGGTGGACAT-
BMO2	-GACATCACTGCAGGGAGAAGATCCA-
BMO3	-CAGGGAGAAGATCCAGTCACTGCTA-
CoMO	-CCTCTTACCTCAGTTACAATTTATA-

2.1.7 Plasmids

2.1.7.1 Synthetic mRNA templates

For microinjections, *in vitro* transcription of the following plasmids was performed:

plasmid	linearization	polymerase
xBrg1 WT	NotI	SP6
hBrg1 WT	HpaI	SP6
Chordin	XbaI	SP6
Siamois	NotI	SP6
Wnt8	NotI	SP6
Xnr5	XbaI	T7
Activin	SmaI	SP6
Nuclear lacZ	NotI	SP6
BISH_luciferase	NotI	SP6

2.1.7.2 Synthetic RNA *in situ* probes

The following plasmids were used for *in vitro* transcription to generate dig-labeled antisense RNA for *in situ* RNA hybridization:

plasmid	linearization	polymerase
Cerberus	BamHI	T7
Chordin	EcoRI	T7
Foxa4	EcoRI	T7
foxD5	XbaI	T7
Goosecoid	EcoRI	T7
Hhex	NotI	T7
Hoxb9	BamHI	T7
Krox20	EcoRI	T7
Myf5	BamHI	T7
MyoD	EcoRI	T7
Noggin	EcoRI	T7
Otx2	EcoRI	T3
Siamois	HindIII	T7
Vent1	SalI	T7
Vent2	BamHI	T7
Xbra	HindIII	T7
Xnr3	EcoRI	T7
Xnr5	NotI	T7

2.1.8 Equipment

product	company	product	company
Centrifuge 5417C	Eppendorf	Minitherm 2	Dinkelberg
G:BOX	Syngene	Nanodrop ND-1000	PeqLab
Glass 1BBL W/FIL 1.0 mm	WPI	PCR Express	Hybaid
Leica DFC 310FX	Leica	Stereomicroscope Stemi SV6	Zeiss
Li-Cor	Odyseey	Stereo-fluorescence System M205FA	Leica
Light Cycler 480 System	Roche	Optical microscope DM	Leica
Microneedle puller P-87	Sutter Instrument	Microinjector Pli-100	Digitimer Ltd.
Micromanipulator Mm-33	Science Products	Lumat LB9501	Berthold

2.1.9   Software

product	company	product	company
CLC Sequence Viewer 6	CLCbio	Leica Application Suite V3 3.0	Leica
Endnote X7	Thomson		
Gene Snap Image Acquisition Software	Syngene	Light Cycler 480 Software Release 1.5.0 SP1	Roche
Illustrator CS5	Adobe	Photoshop CS5	Adobe
ImageJ	Wayne Rasband	Odysee Application Software Version 3.0	Odyseey

2.2   Methods

2.2.1   DNA standard methods

2.2.1.1   Gel electrophoresis

To visualize nucleic acid fragments with different sizes agarose gel electrophoresis was performed. Therefore 0.6 g agarose was dissolved in 60 ml 1x TBE buffer, resulting in a 1% agarose solution. To the DNA containing samples 6x Gel loading dye (NEB) was added and loaded onto the gel. After running and separating the fragments, the result was documented using the Gel documentation System G:BOX.

stock solution:

10x TBE pH 8,6

100 mM Tris/HCL

83mM borate

0,1 mM EDTA

2.2.1.2   Isolation of DNA fragments from agarose gel

In order to isolate and extract a particular DNA fragment, a 1% TAE agarose gel was prepared. After running the gel, the appropriate DNA fragment was cut out under UV light and DNA was extracted by using the QIAquick® Gel extraction Kit (Quiagen) after the manufacturer's protocol.

stock solution:

20x TAE

2 M Tris

1 M glacial acetic acid

0,05 M EDTA

2.2.1.3   DNA digestion

For standard cloning procedures and *in vitro* transcription the above mentioned plasmid templates had to be enzymatically digested or linearized. The following protocol was used:

reagents	volume/concentration
template plasmid	2-10 µg
10 x buffer	4 µl
10 x BSA	4 µl
Enzyme 20/U	3 µl
H$_2$O	add 40 µl

The reaction was incubated for 2 hours at 37°C followed by a clean-up step using the QIAquick® PCR purification Kit (Quiagen) after manufacturer's instruction.

2.2.1.4   Ligation

For cloning DNA, fragments had to be ligated into the pCS2+ or pCS2+GW vector backbone. The DNA fragments and the linearized vector were incubated with 1 µl of 10x T4 Ligation buffer and 1 µl Ligase T4 in a total volume of 10 µl. The reaction took place over night at 16°C.

2.2.1.5   Chemical transformation

For standard cloning procedures 3-5 µl of the plasmid was incubated in 100 µl DH5α bacteria for 30 min on ice. After a 90 sec heatshock on 42°C, 1 ml LB-Media was added and the reaction was incubated on 37°C for 1 hour shaking. After the incubation step the bacteria were centrifuged 2 min with 5000 rpm. 1 ml of the supernatant was discarded and the bacteria were resuspended in the left

over liquid. 100 µl of the bacteria were plated on a LB/agarose dish with the appropriate antibiotics for selection. The plate was incubated over night at 37°C.

2.2.1.6 Plasmid preparation

To amplify a single clone grown on the LB/agarose plate this particular clone was inoculated in 100 ml LB-Media with the appropriate antibiotics added and incubated over night shaking at 37°C. The next day the plasmid was extracted using the QIAGEN® Plasmid Midi Kit after manufacturer's instructions.

2.2.1.7 Gateway® cloning

The Gateway® cloning technology was established by the company "life technologies". The technology is based on recombinant events that circumvent the classical cloning technique via enzyme digestions and ligation steps. Firstly, the desired fragment has to be amplified in a PCR with oligonucleotides that contain distinct recombinant sequences, the attB-sides, flanking the gene sequence. The fragment had to be recombined into the "donor-vector", which contains a cassette that has the recombinant complementary sequence. The protocol is the following:

BP-reaction

attB-containing PCR fragment	30-150 ng
donor vector	150 ng
TE buffer	add 4 µl
BP-clonase II	1 µl

The reaction was incubated 1-2 hours at 25 °C. Afterwards DH5α bacteria get transformed and plated onto a LB/zeocin agar plate as the donor vector contains a zeocin resistance. Clones have to be inoculated and the "entry clone", donor vector backbone with desired DNA-fragment, had to be extracted via the QUIAGEN® Plasmid Midi Kit after manufacturer's instruction.

In another step the desired DNA fragment is recombined from the entry vector into the "destination vector". Therefore the gateway cassette A was introduced into a variant pCS2+ expression vector, called pCS2+GW. The following protocol was used to recombine the DNA fragment into the pCS2+GW:

LR-reaction

entry clon	150 ng
destination vector	150 ng
TE buffer	Add 4 µl
LR-clonase	1 µl

The reaction was incubated 1-2 hours at 25°C, followed by transformation of DH5α cells and plating on to a LB/agarose plate with ampicillin. To extract the vector a clone was picked, inoculated and a plasmid preparation was performed with the QUIAGEN® Plasmid Midi Kit after the manufacturer's instruction.

2.2.1.8 Polymerase Chain Reaction, PCR

In this thesis the BD Biosciences Clontech PCR Systems with the Advantage DNA Polymerase was used according to manufacturer's protocol. A typical thermocyclin program was:

	temperature	time	cycles
Denaturation	95°C	2 min	1x
Denaturation	95°C	45 sec	
Annealing	52-67°C	45 sec	28x
Elongation	68°C	90 sec- 5 min	
Elongation	68°C	10 min	1x
Cooling	4°C	∞	

* The annealing temperature depends on the GC content of the primers
** Elongation time depends on the size of the amplified DNA fragment

2.2.1.9 Quantitive Reverse Transcription Polymerase Chain Reaction, qRT-PCR

A method to quantify the amount of amplified template for each single PCR cycle is the qRT-PCR. This method is more precise and more informative than the standard PCR. In this study, all gene expression analyses were done via the relative quantitative RT-PCR. As reference genes the housekeeping genes H4, ODC and GAPDH were used.

The Roche LightCycler® system with 384 well plates was used. A volume of 10 µl/well was prepared with the following protocol:

reagent	volume
cDNA template	2 µl
Fast SYBR Green Master Mix	5 µl
For and *rev* primer (each 3 µM)	1 µl
H_2O	2 µl

All used oligonucleotides were designed with a common annealing temperature between 59,7°C and 60,3°C with the Primer3 online software. The thermocyclin program was performed as follows:

	temperature	time	cycles
Denaturation	95°C	5 min	1x
Denaturation	95°C	10 sec	
Annealing	60°C	20 sec	45x
Elongation	72°C	10 sec	
Melting	95°C	5 sec	
	65-97°C	1 min	1x
Cooling	40°C	30 sec	1x

For each condition and every primer pair, technical triplicates were performed and the mean of the triplicates was used for further data analysis.

2.2.2 RNA standard methods

2.2.2.1 *In vitro* transcription of sense RNA

For embryonic microinjections, artificial mRNA has to be generated. For this purpose the linearized DNA plasmid of the requested construct is used as template. In order to obtain a stable and functional mRNA the following protocol was used:

reagent	volume
Linearized template	2 μg
5x transcription buffer	10 μl
25 mM G (5')pppGcap analog	5 μl
100 mM NTPs-mix	10 μl
100 mM DTT	5 μl
RNAsin 40U/μl	0,5 μl
RNA polymerase	2 μl
RNAse-free H_2O	Add to 50 μl

The reaction was incubated 2 hours at 37°C then another 1 μl RNA polymerase was added and the reaction was incubated at 37°C over night. To remove the template, 2U of DNAse was added following another 15 min of incubation at 37°C. Afterwards the RNA was purified with the RNeasy® mini kit (Quiagen) after manufacturer's instruction and stored at -80°C.

2.2.2.2   *In vitro* transcription of antisense RNA

For whole-mount *in situ* hybridization a digoxygenin-labeled complementary antisense RNA was generated. Again a linearized DNA plasmid of the requested gene is used as template. The reaction protocol is the following:

reagent	volume
Linearized template	2 μg
5x transcription buffer	10 μl
10 mM DIG-NTPs-mix	5 μl
100 mM DTT	5 μl
RNAsin 40U/μl	0,5 μl
RNA polymerase	2 μl
RNAse-free H_2O	Add to 50 μl

The reaction was incubated for 2 hours at 37°C. Afterwards another 1 μl of RNA-Polymerase was added and the reaction was incubated over night at 37°C. To digest the template, 1 μl of DNAse was added, followed by 15 min incubation at 37°C. The dig-labeled *in vitro* synthesized antisense RNA was purified with the RNeasy® mini kit (Quiagen). For stabilization formamide was added in a 1:1 ratio and the Dig-labeled RNA was stored at -20°C.

2.2.2.3 RNA isolation

10 *X. tropicalis* embryos or 10 dissected *X. laevis* explants were collected, lysed in 300 µl TRIzol, shock frozen in liquid N_2 and stored at -80°C. After thawing the samples for 5 min at RT, the cell debris was separated by a 10 min centrifugation step at 14000 rpm at 4°C. The supernatant was transferred into a new low-binding 1.5 ml eppendorf tube, mixed with 60 µl of Chloroform and kept for 2 min at RT. The solution was then centrifuged at 14000 rpm at 4°C for 15 min. The upper colourless organic phase was transferred to a new low-binding tube and the Chloroform extraction was repeated. After transferring the colourless phase to another low-binding tube, 1 µl of a 2 mg/ml Glycogen solution was added as a carrier for the precipitated RNA nucleotides. To precipitate the RNA, 150 µl Isopropanol was added, mixed for 30 sec and incubated at RT for 10 min. The solution was centrifuged again for 10 min at 14000 rpm at 4°C. Now the precipitated RNA accumulates as a pellet. The supernatant was discarded and the RNA pellet was washed with 70% Ethanol and successively centrifuged for 5 min with 10000 rpm at 4°C. Again the supernatant was discarded. To remove the remaining Ethanol the tube was put into a 50°C heating block with open lid. Afterwards the RNA pellet was resuspended in 30 µl of RNAse-free water and a clean-up step with the RNeasy® mini kit including the DNAse on-column digestion was performed. The isolated RNA was measured using the Nanodrop ND-1000 from PeqLab and stored at -80°C.

2.2.2.4 cDNA synthesis

To analyze distinct gene expression in whole embryos or explants tissue the isolated RNA was reversed to complementary DNA. The cDNA was then used as template for quantitative RT-PCR. For this purpose the DyNAmo cDNA Synthesis Kit was used after the manufacturer's instructions.

2.2.2.5 Whole mount RNA *in situ* hybridization

To prepare embyros used for whole mount *in situ* hybridization, they were fixed at the desired stage for 2 hours at RT or over night at 4°C in MEMFA and stored at -20°C in 100% Ethanol for at least 2 hours.
To rehydrate, embryos were washed 1x in 75% EtOH/PBSw, 50% EtOH/PBSw, 25% EtOH/PBSw and 3x PBSw, each step 5 min at RT. In order to permeablize the cells and increase the RNA accessibility, the embryos were incubated in 10 µg/ml proteinaseK/PBSw for 20 min without agitation followed by two washing steps with PBSw. Embryos were refixed afterwards in 4% paraformaldehyd for 20 min and washed again 5 times for 5 min in PBSw. For the hybridization step, embryos were equilibrated 3

min in 50% hybridization solution/50% PBSw, followed by a 3 min wash in 100% hybridization solution. The hybridization solution was refreshed and the embryos were incubated in a waterbath for 1 hour at 65°C. In order to prehybridize, embryos were incubated for a minimum of 4 hours in a waterbath at 60°C. 3-5 µl of the dig-labeled desired antisense RNA was added to 100 µl of hybridizing solution and heated up for 2 min to 95°C. The probe was cooled down and then added to the embryos and the hybridization solution. Embryos were incubated with the antisense probe over night at 60°C. The next day, the unhybridized antisense RNA probe was removed and stored at -20°C. The probes can be reused several times. To wash out the remaining antisense RNA, the embryos were washed again for 10 min in fresh hybridizing solution at 60°C followed by three times 2x SSC, each step 20 min and twice 0,2x SSC, each for 30 min at 60°C in a waterbath. Afterwards the embryos were washed twice in 1x MAB for 15 min at RT and then exchanged with 1x MAB containing 2% BMB Blocking solution for 1 hour in order to block unspecific binding sites. After this preincubation, the specimen were incubated for 4 hours at RT with 1x MAB/2% BMB blocking solution supplemented with an 1:2000 dilution of the affinity-purified α-digoxigenin antibody coupled to an alkaline phosphatase. After the incubation with the antibody, the embryos were washed over night in 1x MAB. The next day, the embryos were washed again additional 4-6 times in 1x MAB 30 min per wash at RT. To prepare the embryos to the upcoming colour staining reaction, they were washed twice in AP-buffer followed by incubation in alkaline phosphatase substrates 4,5 µl/ml NBT and 3,5 µl/ml BCIP in AP buffer. The colour reaction took place at RT in the dark. When the desired staining intensity was reached, the colour reaction was stopped by rinsing the embryos with PBS, followed by MEMFA fixation over night at 4°C.

To improve visibility of the colour precipitate, the pigment of the embryos had to be removed by bleaching. Therefore, the embryos were incubated for minimum 20 min in 75%EtOH/PBS at RT and then incubated in bleaching solution containing formamide and H_2O_2 (Mayor et al, 1995). The process of bleaching was performed on a light box for at least 4 hours. After bleaching of the pigmented cells, the embryos were put in MEMFA and stored at 4°C until pictures were documented.

stock solutions:

Alkaline Phosphatase (AP)	**Bleaching solution**	**Hybridization solution**
100 mM Trichlorethane	1% H_2O_2	5 x SSC
100 mM NaCl	5% Formamide	50% Formamide
50 mM $MgCl_2$	0.5 x SSC	1% Boehringer blocking
0,1% Tween-20		0,1 % Torula RNA
		0.01% Heparin
		0,1% Tween-20
		0,1% CHAPS
		5 mM EDTA

Maleic Acid Buffer (MAB)	**MEMFA**	**PBS pH7,2**
100 mM maleic acid	0,1M 3-(N-Morpholino)-	137 mM NaCl
150 mM NaCl, pH7,5	propanesulfonic acid	2,7 mM KCL
	2 mM EGTA	8 mM Na_2HPO_4
	1 mM $MgSO_4$	1,7 mM KH_2PO_4
	3,7% formaldehyde pH7,4	

PBSw	**20x SSC pH 7**
1x PBS	3 M NaCl
0,1% Tween-20	0,3 M sodium citrate

2.2.2.6 Microarray analysis

Genome-wide transcriptome analyses were performed with the Affymetrix GeneChip®*Xenopus* Tropicalis Genome Array. These arrays carry over 58000 probe sets, representing 51000 transcripts. The RNA for the analysis was isolated, the quality was controlled on the Bioanalyzer and samples with a RIN-value ≥7 were used for genome-wide analysis. The RIN is composed of the purity of the RNA and the ratio between 18S and 28S RNA-the better the RNA quality, the higher the RIN-value (between 0-10). The "Facility for functional genomics" at the Gene Center performed the sample hybridization and the microarray readout. The raw data was forwarded to Dr. Tobias Straub, Head of the Bioinformatics Core Unit at the Adolf-Butenandt-Institut and subjected to bioinformatic analysis.

2.2.3   Protein analysis

2.2.3.1   SDS- polyacrylamid gelelectrophoresis, SDS-PAGE

15 *Xenopus* embryos at NF 9 were lysed in 75 µl cold lysis buffer supplemented with protease inhibitors and homogenized with a 45G needle. To remove the cell debris the cell lysate were centrifuged for 20 min at 14000 rpm at 4°C. 50 µl of the liquid supernatant was transferred into a new 1.5 ml eppendorf tube and 12 µl of Rotiphoresis loading dye was added. To shear the remaining DNA, the sample was frozen in liquid N_2 and immediately thawn to 37 °C. This procedure was repeated 3-5 times. Before loading 2 "embyro equivalent" onto an 8% SDS gel, the samples were heated up for 2 min to 92°C in order to denature the proteins.

stock solutions:

Lysis buffer	Protease inhibitors	10x SDS-PAGE buffer pH 8,3
10 mM Tris-HCl pH 7,5	1 mM NaF	250 mM Tris
100 mM NaCl	20 mM beta-glycerol	2 M gylcerine
0,5 % NP-40	0,1 mM NaV	35 mM SDS
	1 mM PMSF	

2.2.3.2   Western Blot analysis

After size-separation, proteins were transferred onto a nitrocellulose membrane using the Bio-Rad Wet/Tank Blotting Systems. Blotting was performed with a voltage of 120 V for 2 hours at 4 °C. Afterwards the membrane was washed in PBSw, the 1st antibody was applied and incubated over night at 4°C. After removing the 1st antibody, the membrane was washed 3 times in 5% milk/PBSw for 15 min. The secondary antibody was diluted and the membrane was incubated for 90 min at RT in the dark, followed by 3 washing steps for 15 min in 5% milk in PBSw. To detect the protein signals on the membrane, the Odyseey LiCOR system was used. The Odysee Application Software Version 3.0, was used for quantification.

stock solution:

Blotting puffer
25 mM Tris
200 mM glycerine
0,7 mM SDS
20% Methanol

2.2.3.3   Immunocytochemistry

The vitelline membrane of NF9 embryos was manually removed using two forcipes, followed by fixation in MEMFA over night at 4°C. After fixation, the embryos were stored in 100% Methanol at -20°C. To rehydrate the embryos, successive washing steps with 75% Methanol/PBSw, 50% Methanol/PBSw and 25% methanol/PBSw, each step for 5 min, were performed. Afterwards the embryos were washed in PBT for 15 min. To block protein binding sides, the embryos were incubated 1 hour with PBT supplemented with 10% heat inactivated lamb serum. After the blocking step, the primary antibody specific for the protein of interest, was added and incubated over night at 4°C. The antibody was removed, stored at 4°C for reuse. In order to remove possible remaining primary antibody, the embryos were washed 6 times, each 30 min, with PBT. Afterwards the embryos were incubated with the AP-coupled secondary antibody over night at 4°C. To wash away the secondary antibody, the embryos were washed 5 times 1 hour with PBT. For the alkaline phosphatase staining reaction, the embryos were washed twice 15 min with AP-buffer supplemented with 2mM levimasol. To start the AP-reaction the substrates NBT and BCIP were added and the embryos were kept in the dark until the colour staining was visible. The colour reaction was stopped by rinsing the embryos in 1x PBS. To remove the pigmentation of the whole embryos a bleaching step was added. The embryos were incubated for minimum 20 min in 75% EtOH with PBS followed up by incubation with bleaching solution, containing formamide and H_2O_2, on a light source. Subsequently, the embryos were stored in MEMFA at 4°C until the experiment was documented.

stock solutions:

PBT	AP buffer
1x PBS	AP-Buffer (see WMISH)
2 mg/ml BSA	2 mM levamisol
0,1% TritonX-100	

2.2.3.4 Luciferase assay

To quantitate morpholino blocking efficiency, a luciferase assay was employed with a target-specific reporter plasmid. Therefore 5 times 5 embryos per condition were pooled and lysed with 10 µl/embryo 1x PBL-lysis buffer from the Dual-Luciferase® Reporter Assay System (Promega). To remove the cell debris the samples were centrifuged for 10 min at 13000 rpm at 4°C. 50 µl of the clear supernatant was transferred into a new eppendorf-tube and followed by another centrifugation step for 10 min at 10000 rpm at 4°C. 20 µl of the suspension was then added to 100 µl LARII from the Dual-Luciferase® Reporter Assay Kit and the luciferase activity was measured with the luminometer.

2.2.3.5 ß-galactosidase staining

The injected blastomeres were lineage-traced by coinjection of nuclear ß-gal mRNA. The embryos were collected in the desired developmental stage, fixed with MEMFA for 30 min at RT and subsequently washed with PBS 3 times each for 10 min. To start the color reaction, the Xgal-solution was added and the embryos were incubated in the dark until the staining was visible. To stop the reaction the embryos were washed again 3 times, each 10 min, in PBS. The lacZ stained embryos were stored in 100% Ethanol at -20°C until documentary or proceeding with a WMISH.

solutions:

Xgal solution, freshly made

1x PBS

5 mM $K_3Fe(CN)_6$

5 mM $K_4Fe(CN)_6$

2 mM $MgCl_2$

1 mg/ml Xgal

2.2.4 Embryological methods

2.2.4.1 Superovultion of *Xenopus* females

Xenopus laevis female were stimulated by an injection of 800 units of human Choriongonadotropin (hCG) into the dorsal lymph sac. Egg laying started 12-14 hours later.

To stimulate *Xenopus tropicalis* females, the frogs were primed with 10U of hCG into the dorsal lymph sac 12-20 hours before usage is necessary. The next day 200U of hCG were injected. 4-5 hours later the females started laying eggs. *Xenopus tropicalis* females were kept at 23 °C.

2.2.4.2 Testes preparation

Xenopus males were anaesthetized in 5 g/l 3-Aminobenzoeacid-ethyl-ester (MS222). After a minimum of 30 min and no further signs of consciousness, the males were killed by decaptitation. The testes are located in the abdominal cavity, attached to fat tissue. With two incision of the skin, fat tissue and the testes can be pulled out and isolated. Testes were cleaned in 1x MBS and stored at 4°C in 1x MBS/CS. *X. laevis* testes can be stored up to 10 days, *X. tropicalis* testes only two days.

2.2.4.3 *In vitro* fertilization and culturing

When female *Xenopus* started laying eggs, they were carefully squeezed and the freshly laid eggs were collected in a petri dish. A slice of one testis was cut off and minced in 1x MBS and the suspension was applied to the eggs. Immediately 0,1x MBS was added, mixed with the eggs and incubated at RT for 20 min. The eggs then were covered with 0.1x MBS and cultivated at 18-23°C.

For *Xenopus tropicalis* a piece of one testis was minced in 300 µl 1x Ringer solution, mixed with the freshly laid eggs, after 3 minutes covered with 0,1x Barth's solution and incubated at 23°C.

stock solutions:

5x Barth's solution pH 7,6	10 x MBS pH 7,8	1x Ringer solution
440 mM NaCl	880 mM NaCl	116 mM NaCl
5 mM KCL	10 mM KCL	2,9 mM KCL
12 mM NaHCO$_3$	10 mM MgSO$_4$	1,8 mM CaCl$_2$
4,1 mM MgSO$_4$	50 mM HEPES	5 mM HEPES pH 7,2
1,65 mM Ca(NO)$_2$	25 mM NaHCO$_3$	
2,05 mM CaCl$_2$		
50 mM HEPES		

2.2.4.4 Dejellying *Xenopus* embryos

The spawn of water-living amphibian animals have a very robust multi-protein network, the jelly coat. In order to perform microinjections this coat has to be removed by a 2% Cystein solution.

For *X. laevis* embryos approximately 60 min after fertilization the embryos are transferred in a 2% cysteine/0.1x MBS solution. By constant mild agitation it takes 2-3 minutes to remove the jelly coat. The eggs have to be washed 3 times in 0.1x MBS and then are cultivated in 0,1x MBS.

X. tropicalis eggs have to be separated from the jelly coat 25 min after fertilization by a 2% cysteine solution in 1/9th Modified Ringer (MR). The embryos of *X. tropicalis* are more sensible to mechanical agitation and therefore sustain only mild agitation and approximately 10 min in the cysteine solution to remove the jelly coat. The embryos are washed 2 times in 0,1x Barth's solution and additional 3 times with 0,1x 1/9th MR. Dejellied embryos were cultivated in 1/9th MR at 23°C until they reached the desired developmental stage. To avoid exogastrulation embryos had to be replaced after several hours to 1/18th MR.

stock solution:

1x Modified Ringer, MR

100 mM NaCl

1,8 M KCL

2 mM $CaCl_2$

1 mM $MgCl_2$

5 mM HEPES pH 7,6

2.2.4.5   Microinjections

To manipulate *Xenopus* embryos or single blastomeres, an injection needle from capillaries was made with the Microneedle Puller (Sutter instruments, settings: heat: 800; pull: 35; vel: 140; time:139). The microinjection needle was put into either a fixed needle holder or a free-hand needle holder. The needle had to be calibrated by stepwise clipping with a forceps to allow injections of a 5 nl drop in 30 msec and with a pressure of 30 psi. The injection volume in this thesis ranged from 1.25 nl/blastomere - 5 nl/blastomere. Embryos were injected from 2 cell stage up to the 16 cell stage. The total volume injected was limited to 10 nl/ embryo for *X. laevis* and 5 nl/ embryo for *X. tropicalis*.

After injection, *X. laevis* embryos were cultivated in 0,1x MBS/Gentamycin and buffer was refreshed on a daily basis. To avoid attaching of the embryos to the petri dish surface, it was coated with 1% Agarose/ 0,1xMBS.

Prior to (15 min) and after (1hour) injections, the *X. tropicalis* embryos were transferred to 1/9th MR with 2% Ficoll, then transferred in 1/9th MR/Gentamycin for several hours and finally transferred to 1/18th MR/Gentamycin until the desired developmental stage was reached. Petri

dishes were covered with 1% agarose in 1/18th MR. *X. tropicalis* embryos were only cultivated at 20°C (RT) or 23°C.

2.2.5 Embryological explantations

2.2.5.1 Ectodermal explantation

To target microinjections to the animal cap region, the mRNAs were injected radially into the animal pole between the 2 - 8 cell stage and cultivated in 0,1x MBS until the blastula stage. The embryos were then transferred into 1x Steinberg Solution and the vitelline membrane was carefully removed with two forcipes. Next the Blastocoel roof was cut out with two forcipes and the ectodermal explants were transferred separately into one well of a 96 well plate. The wells were covered with 1% agarose in 1x Steinberg solution and filled with 1x Steinberg solution. The animal caps were cultivated until uninjected control embryos reached the midgastrula stage.

stock solution:

10 x Steinberg Solution

580 mM NaCl

6,7 mM KCL

3,4 mM CaNO3

8,3 mM MgSO4

50 mM Tris

0,1 g Kanamycin

2.2.5.2 Transplantation

In this thesis homotopic BCNE transplants were examined. A morphant BCNE was transplanted into a wild type host embryo. At the 2 cell stage embryos were injected in both blastomeres with BMO1. At the 16 cell stage the two dorso-animally located blastomeres were injected with Alexa 488 or Alexa 594 in morphant or wild type embryos, respectively. At blastula stage the embryos were transferred into 0.8x MBS/gentamycin and the vitelline membrane was removed. The area of the BCNE was identified by fluorescence of the lineage tracer. The red BCNE in the host embryo was removed and exchanged with the green morphant or WT BCNE. To stabilize the transplant, it was covered with a cover slip. After 1 hour the cover slip was removed and the transplanted embryo was transferred into 0,1x MBS/gentamycin and cultivated at RT in a 1% agarose-coated petri dish.

3 Results

3.1 Comparison of morpholino oligonucleotides

In order to perform knockdown analysis in *Xenopus*, morpholino oligonucleotides, which block the protein translation, were designed. Three Brg1 morpholinos with different targeting sides were tested, which all target the homeologs in *Xenopus laevis* mRNA. In Figure 3.1 the alignment of both homeologs is shown. Whereas brg1.a (NCBI: AY762376) implies the whole coding sequence, the second allele brg1.b (NCBI: BG554361) contains only a partial coding sequence and the 5'UTR. The two sequences are 96% identical on nucleotide level.
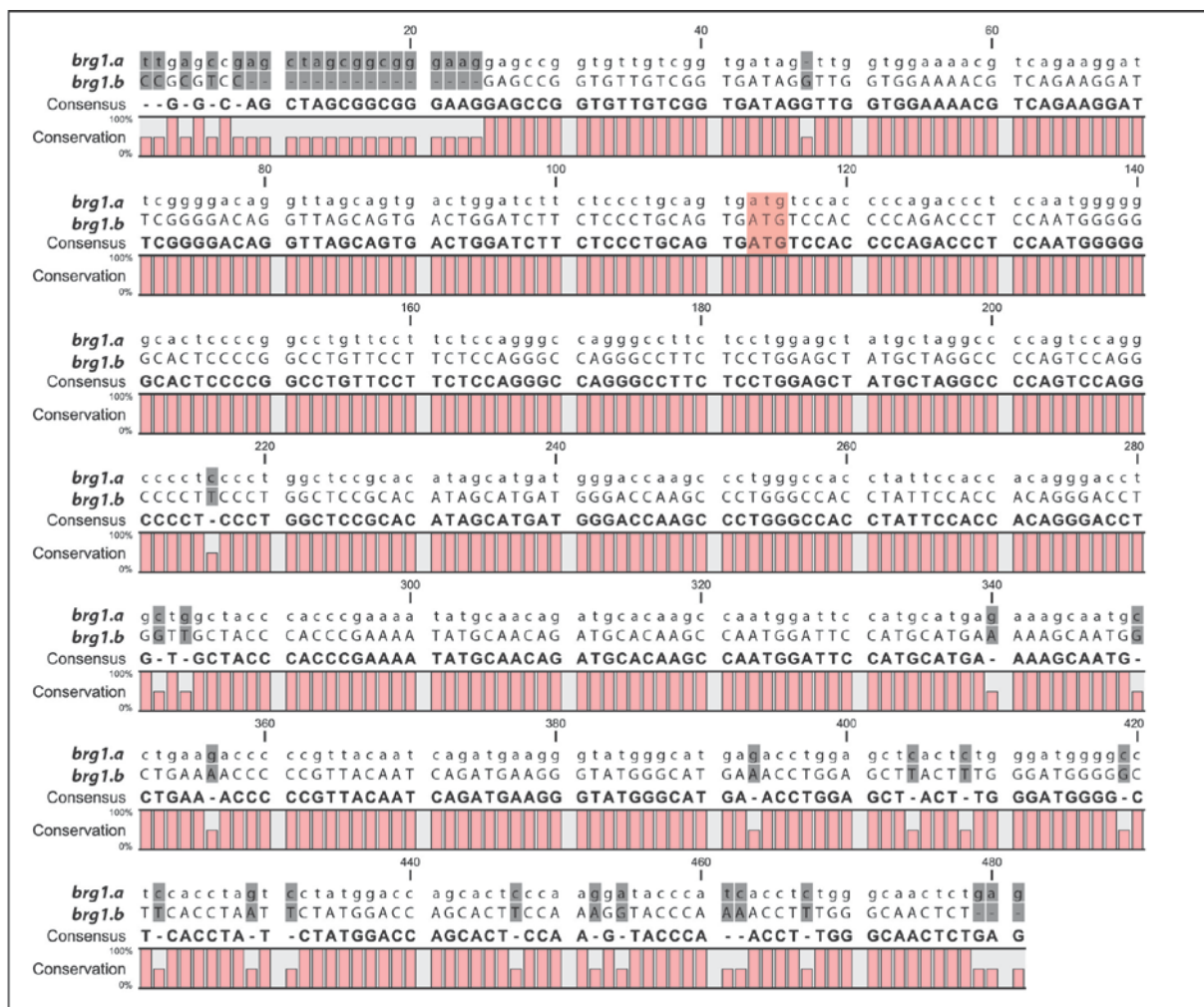
Figure 3.1: Partial cDNA sequence alignment of *Xenopus* homeologs *brg1.a* and *brg1.b*. Sequences of *brg1.a* (AY762376) and *brg1.b* (BG554361) are provided from NCBI. Shown are the 5'UTR and the first nucleotides of the coding region of both homeologs. In red the starting codon ATG is depicted. Differences in the two gene sequences are highlighted in gray. The alignment was generated by CLC workbench viewer.

The morpholino targeting sites of all three morpholinos are shown in Figure 3.2 A. To compare their individual efficiency, a luciferase reporter gene assay was established. A ~ 700 bp fragment, reaching

from -77 bp - +617 bp of the Brg1 sequence, called BISH, was cloned into the pCS2+GW vector with a C-terminal luciferase tag. *Xenopus laevis* embryos were injected in the 2 cell stage with the indicated morpholino radially and in the 8 cell stage the 4 animal blastomeres were injected with synthetic BISH-luciferase mRNA. The embryos were cultivated until NF12 and luciferase activity was measured. The efficiency of translation blocking is displayed in Figure 3.2 B. All three morpholinos showed an inhibition efficiency of more than 50%. However a clear ranking can be made. BMO3 was the less efficient, with an inhibition up to 0.35%, BMO2 reduces the luciferase luminescence to 0.22% and BMO1 showed the best blocking efficiency with a reduction to 0.14%. Given that BMO1 inhibits the translation best, any further analysis in *Xenopus laevis* was executed with this morpholino.
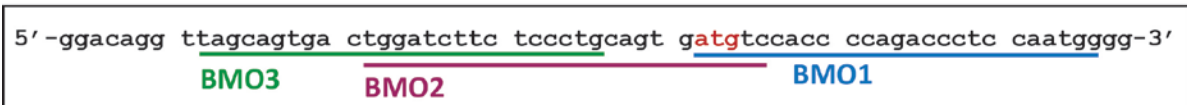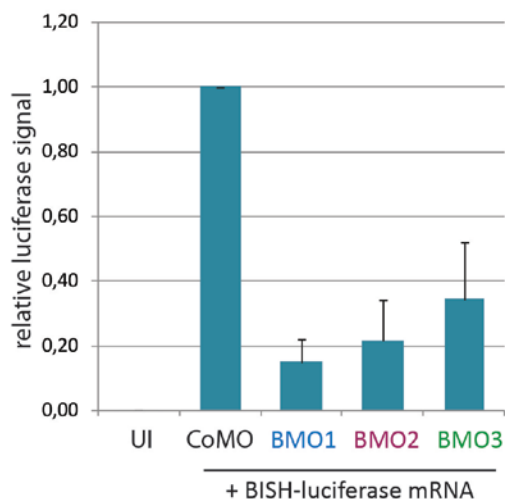
Figure 3.2: Different morpholino targeting sites result in different translation blocking efficiencies. In **A** the ATG-region of brg1.a and brg1.b is shown and the three different morpholino targeting sites are depicted. **B** shows the result of the luciferase assay, in order to quantify the translation blocking. In each condition 25 pg of BISH-luciferase mRNA was coinjected with either CoMO or BMO1, BMO2 or BMO3, each 60 ng. The luciferase signal of all tested conditions was normalized to CoMO signal intensity. The mean of 3 independent experiments is shown.

3.2 BMO1 reduces Brg1 protein level from MBT on

As described in the introduction, the development up to midblastula in *Xenopus* is entirely regulated by maternal mRNA and protein. Furthermore transcription is blocked during this period. With the midblastula transition (MBT) this transcription blocking is abrogated and the zygotic gene transcription begins. To examine the time point when BMO1 is acting and Brg1 protein level is decreased, the protein level before MBT (NF7) and after MBT (NF9) was monitored. In Figure 3.3 A a Western Blot is depicted, showing that at preMBT the Brg1 protein level is not changed after BMO1 injections. At late blastula stage (NF9), 3 hours later, the protein level of Brg1 is reduced under these conditions.
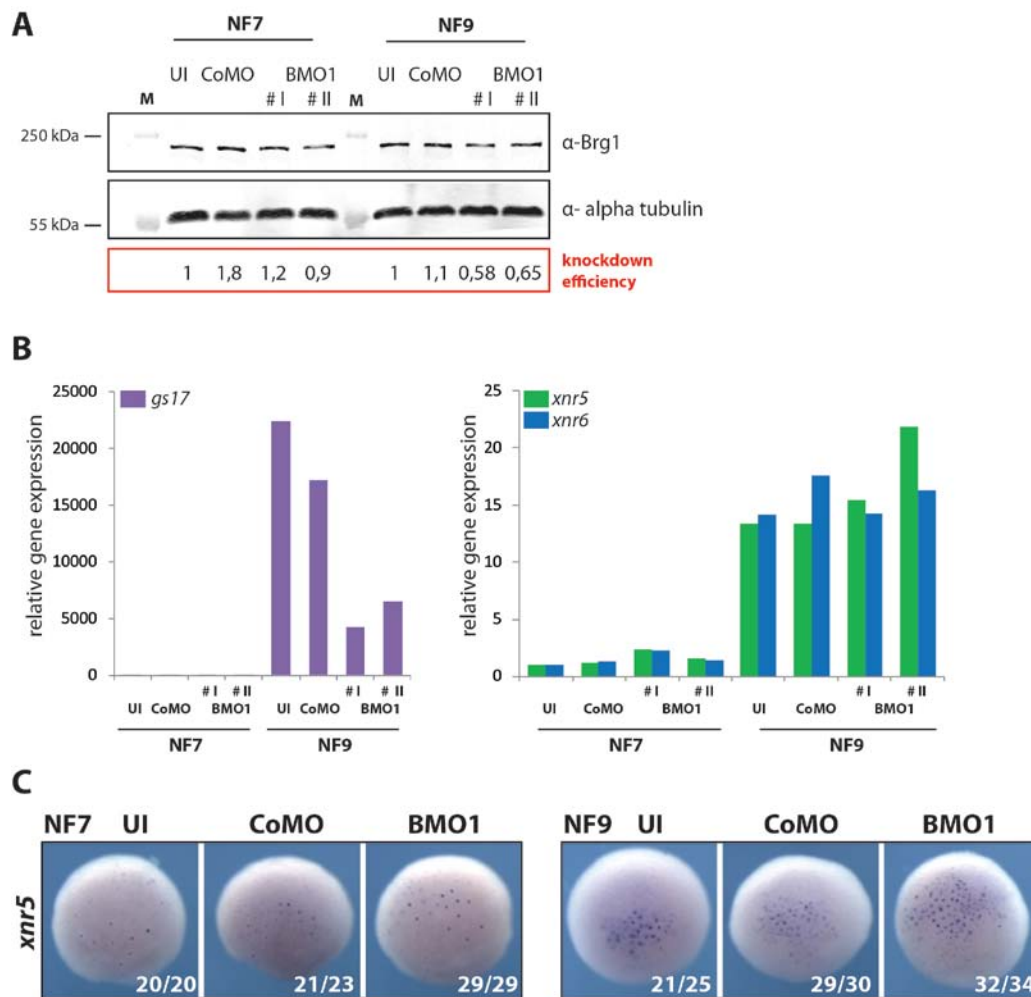
Figure 3.3: BMO1 inhibits only newly synthesized Brg1 protein. In **A** one representative Western Blot out of three independent experiments is shown. Brg1 protein level was analyzed preMBT (NF7) and postMBT (NF9). As a reference α-tubulin protein level was measured and the knockdown efficiency was calculated. The protein level ratio was normalized to UI samples. Two different samples (#) of BMO1 were examined within one biological repeat. **B** shows one representative qRT-PCR analysis out of three independent experiments for MBT marker *gs17*, *xnr5* and *xnr6*. In panel **C** a WMISH against *xnr5* is shown under UI, CoMO and BMO1 conditions at NF7 and NF9. Shown is the vegetal pole. Numbers display the sum of 3 independent experiments. UI , uninjected.

The pre- and postMBT correlation of the two conditions was confirmed by measuring mRNA levels of *gs17*, a gene known to become activated at the MBT Figure 3.3 B (Krieg & Melton, 1985). Interestingly, BMO1 injected embryos consistently express lower amounts of Gs17 mRNA than control embryos. In addition, the gene expression levels of *xnr5* and *xnr6* were monitored by qRT-PCR. These two genes are expressed at low levels already at preMBT (Blythe et al, 2010). Also these two genes show an upregulation after MBT but none of them showed a downregulation like *gs17*. This indicates that not all genes require Brg1 function for their activation at MBT. Furthermore it proves that morphant embryos are not delayed in development.

The *xnr5* expression pattern was also analyzed in a WMISH analysis (see Figure 3.3 C). In more than 90% of the postMBT morphant embryos a slightly broader expression domain paired with stronger expression signal is observed. This slight upregulation of gene expression was not detected in preMBT embryos. In total these results show, that BMO1 blocks translation of Brg1 mRNA only from the time of MBT on. An explanation to this is that preMBT Brg1 protein is of maternal origin and therefore insensitive to morpholino inhibition.

3.3 Morphological gain- and loss-of-function studies

To obtain first information on Brg1 function during the development of *Xenopus laevis,* knockdown studies with BMO1 or overexpression with ectopic Brg1WT mRNA were performed. In *Xenopus* it is possible to distinguish the prospective dorsal from the prospective ventral side already at the 4 cell stage. This allows targeted injections and the independent investigation of Brg1 function in both entities of the developing embryo.

3.3.1 Targeted loss-of-function analysis

For the knockdown analysis, BMO1 was injected either in the dorsal-marginal zone (DMZ) or in the ventral-marginal zone (VMZ). 5 ng/blastomere CoMO or BMO1 were injected together with 25 pg/blastomere lacZ mRNA for lineage tracing. Embryos injected with CoMO developed normal in 93% (DMZ) or 87% (VMZ), respectively (Figure 3.4 A, E, D, G). However, a knockdown of Brg1 in the DMZ led in 80% of the embryos to severe perturbations of dorso-anterior structures (Figure 3.4 D) and only 20% developed normally. These morphant embryos displayed various phenotypes, ranging from a reduced eye size up to a complete loss of anterior structures. An example of a strong phenotype is shown in Figure 3.4 B. Besides the dorso-anterior impairments, also the antero-posterior body axis is shortened compared to controls. To ensure that this phenotype is specific and not the result of off-target effects, coinjections with human WT Brg1 mRNA were performed. Due to the Brg1 gene sequence divergence between human and *Xenopus*, the translation of the human Brg1 mRNA is not inhibited by BMO1. Indeed, under rescue conditions the phenotype of morphant embryos can be reduced to less than 18% (Figure 3.4 D). In Figure 3.4 C a rescued embryo is shown.
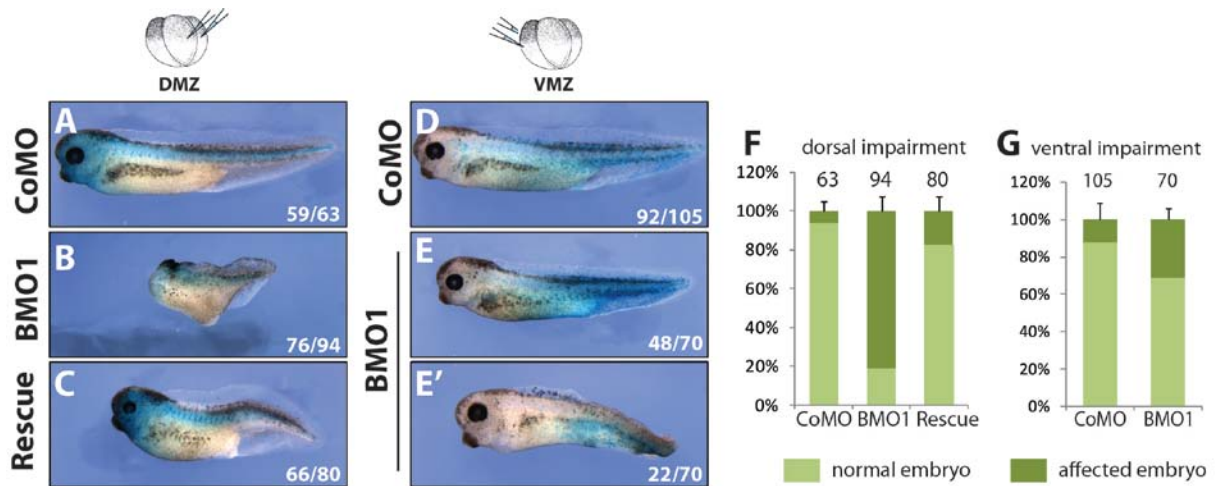
Figure 3.4: Embryonic morphology after targeted Brg1 knockdown. Panels **A-C** show lateral views of NF35 embryos injected in the DMZ with either CoMO (5 ng/blastomere) (**A**), BMO1 (5 ng/blastomere) **(B)** or BMO1 coinjected with 1 ng hBrg1WT mRNA **(C)**. **D-E'** show lateral views of NF35 embryos injected in the VMZ with either CoMO (5 ng/blastomere) **(D)** or BMO1 (5 ng/blastomere) **(E, E')**. In **F** and **G** the quantification of either DMZ- (**F**) or VMZ- (**G**) injections are shown. DMZ, dorsal marginal zone; VMZ, ventral marginal zone.

VMZ-injected embryos displayed a different morphology. 68% of Brg1 morphant embryos developed wild type morphology (Figure 3.4 E and G). The remaining 32% developed normal heads and dorsal structures, but they failed to form a fin and their tails were bent and reduced (Figure 3.4 E'). Furthermore they apparently lost ventral cell mass. If this is due to apoptosis or reduced cell proliferation is not clear. From this result it can be concluded that Brg1 has an important role in axial patterning, which mainly occurs on the dorsal side of the embryo but to a less extent Brg1 is also required for proper ventral development.

3.3.2   Targeted gain-of-function analysis

The above described loss-of-function analysis uncovered a strong requirement for Brg1 in dorsal development. To complete the analysis of Brg1 impact on morphogenesis, similar targeted microinjections with exogenous xBrg1WT mRNA were performed, to test a possible effect under overexpression conditions. DMZ-overexpression of 500 pg xBrg1WT mRNA did not lead to a phenotype, the embryos developed normally (data not shown). Strikingly, an excess of Brg1 mRNA in one ventral blastomere produced partial secondary axis in 50% of the cases (Figure 3.5). The second body axes were anteriorly truncated and showed trunk tissue. This phenotype is reminiscent of axis induction by components of the wnt pathway, like Siamois or Chordin.

To validate the trunk character of the xBrg1WT mRNA induced axial structure, a WMISH with *cardiac actin*, a muscle-specific marker, was performed. All embryos tested in the WMISH, which exhibited a secondary axis also showed staining for skeletal muscle in the truncated body axis. Figure 3.5 G-I display such an embryo from lateral and dorsal view. The secondary axis typically branch off from the primary body axis, as shown in Figure 3.5 I'. This result indicates that an excess of Brg1 on the ventral side leads to a conversion of ventral mesoderm to dorsal mesoderm. Additionally it suggests a potential role of Brg1 in wnt signaling.
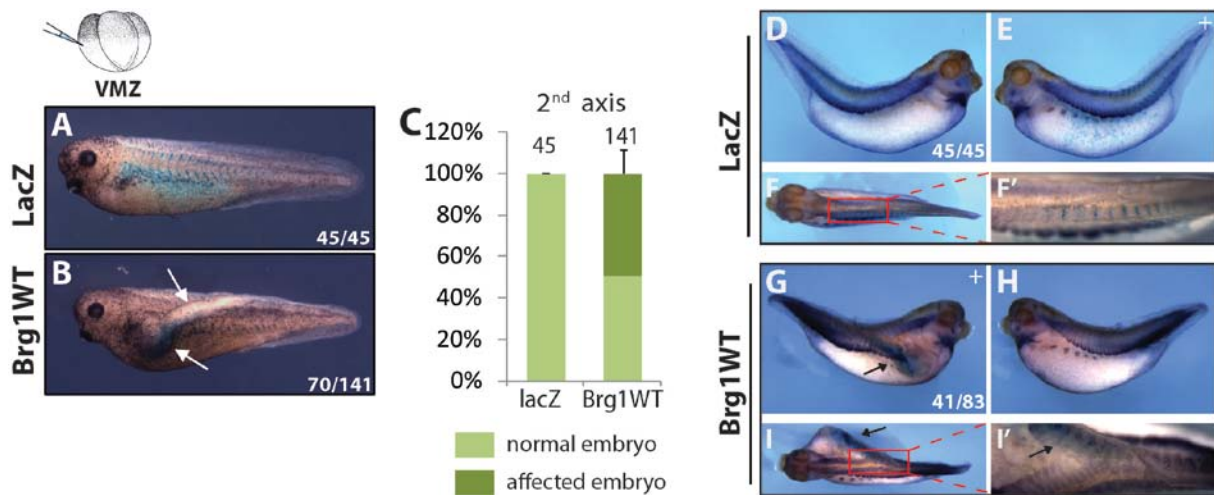
Figure 3.5: Gain of function on the ventral side causes truncated secondary axes. A shows a VMZ lacZ (100 pg/blastomere) injected embryo in lateral view with normal shape. An overexpression of xBrg1WT mRNA (500 pg/blastomere) induced formation of a truncated secondary axis in 50% of the embryos (**B**). In **C** the quantification of 3 independent experiments is shown. **D-I'** show WMISH embryos stained with *cardiac actin*. In **D-F'** the lacZ injected embryos are displayed in lateral (**D, E**) and dorsal view (**F**). In **F'** a higher magnification of **F** is shown. In **G-I'** WMISH of xBrg1WT overexpressed embryos are shown in lateral (**G; H**) or dorsal (**I**) view. In **I'** a close-up of the branching secondary axis is depicted.

3.4 Wnt signaling is not affected in Brg1 morphants

The results so far point to an involvement of Brg1 in axis formation and vertebrate embryogenesis, even though the mechanism Brg1 employs is not known. Whereas the ventral program is considered to be the ground state of the fertilized egg, the dorsal gene expression program has to be established *de novo* in the developing embryo (Robertis & Kuroda, 2004). One very important signaling pathway that induces dorsal genes is the canonical Wnt pathway. The findings raise the question, whether Brg1 acts directly on the pathway and its target genes. To resolve this issue an epistatis experiment was performed.
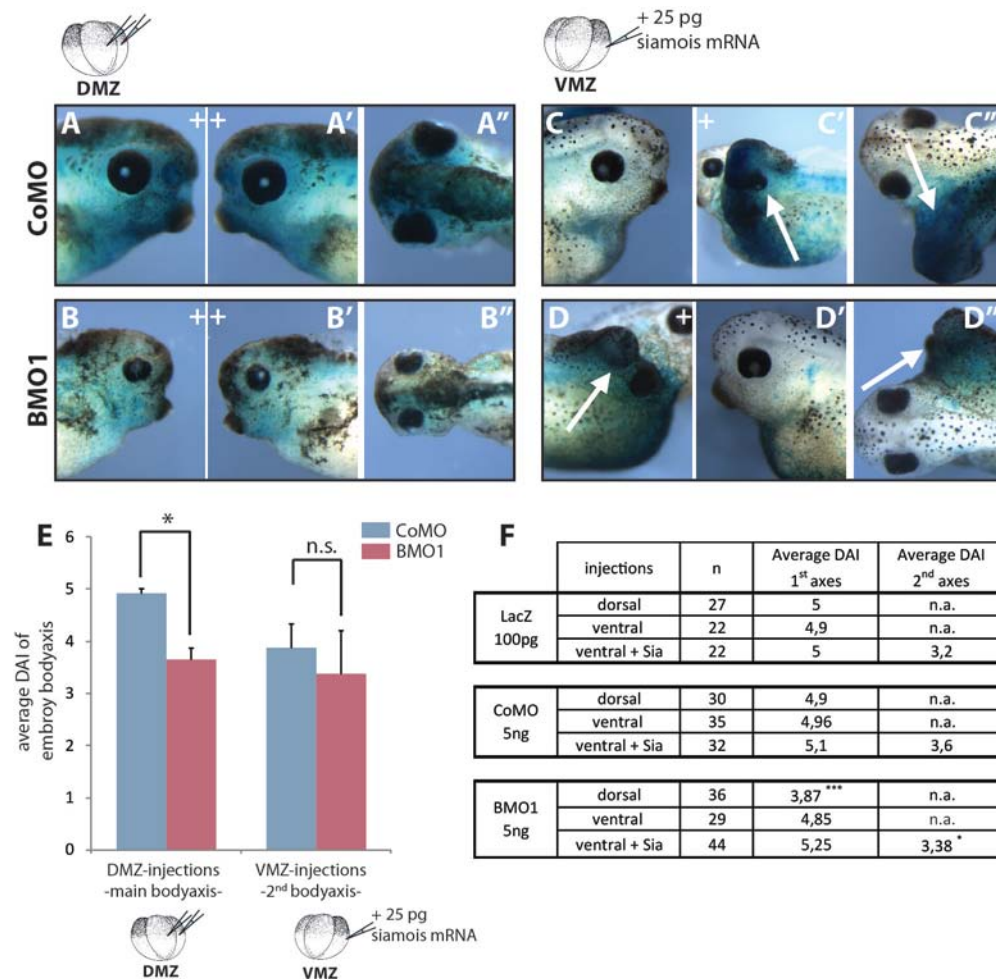
Figure 3.6: Loss of Brg1 on the ventral side does not inhibit axis induction by Siamois. A-D, A'-D' and **A''-D''** show the head of embryos either DMZ-injected (**A-A''; B-B''**) or VMZ-injected (**C-C''; D-D''**) under CoMO (**A-A''; C-C''**) or BMO1 (**B-B''; D-D''**) conditions in lateral or dorsal views. For both morpholinos a total of 5 ng/embryo was injected. In VMZ-injections 25 pg of Siamois mRNA was coinjected in order to create a secondary axis. In **E** the result of the displayed embryos is visualized in a graph. In **F** all tested conditions are listed. DMZ, dorsal marginal zone; VMZ, ventral marginal zone; + indicates injection site; n.a, not applicable; n.s., not specific; ***, $p \le 0.005$; *, $p = 0.52$.

Induction of a complete second embryonic axis by wnt signaling is achieved by injections of exogenous Siamois mRNA into one ventral blastomere (Lemaire et al, 1995). Coinjections of BMO1 (5 ng/blastomere) should reveal if the loss of Brg1 blocks the forming of the ectopically induced secondary axis. For quantification, the embryos were cultivated until NF38 and classified according to the Dorso-Anterior-Index (DAI) (Kao & Elinson, 1988). When CoMO was coinjected together with Siamois mRNA, the embryos developed a secondary axis with an average DAI of 3.8 (see Figure 3.6 C-C''). This dose of Siamois mRNA was chosen in order not to saturate the embryo's response, thus to provide a sensitive environment in which the BMO1 effect can be seen. This is the reason why some embryos did not develop a full secondary axis. In coinjections of BMO1 and Siamois mRNA the average DAI of the generated secondary axis was 3.38. A representative embryo is shown in Figure

3.6 D-D''. Although on average the secondary axes are reduced, this reduction is statistically not significant. To control the morpholino-mediated translation blocking, 5 ng/total of BMO1 were injected into the DMZ and the DAI was examined. As expected the BMO1 DMZ-injected embryos displayed a reduction of dorso-anterio structures with an significant average DAI of 3.87 in comparison to a DAI of 4.9 in control embryos (Figure 3.6 F). A morphant embryo with a corresponding DAI is shown in Figure 3.6 B-B''. This proves that BMO1 injections indeed were effective. This result is not in agreement to the results obtained from Nishant Singhal. Whereas his data indicated a positive coregulatory role for Brg1 within the wnt signaling pathway, the latter experiment rather suggests that Brg1 does not interfere in the dorsalizing program induced by Wnt signaling. This is demonstrates, at least, for the downstream events of Siamois. Nonetheless, it also does not exclude a broader role of Brg1 beyond or upstream of Siamois.

3.5   Axis patterning genes are downregulated in neurula stage

After completing the gross morphological analysis of Brg1 requirements, the underlying molecular causes of the morphant phenotype were investigated. Prominent candidates to analyze are genes that help to establish the vertebrate body plan. To investigate the antero-posterior patterning, control and morphant embryos were examined in a WMISH analysis at neurulation stage. Three markers were analyzed, which mark differing section along the AP body axis.

As an anterior marker *pax2* was chosen. It is a paired box transcription factor and is expressed in the eye primordium and anterior head structures during neurula. In later stages *pax2* marks and is essential for proper pancreas development (Heller & Brandli, 1997). In unilateral BMO1 injected embryos the expression pattern of *pax2* on the injected side is perturbed and the knockdown led to an unstructured expression pattern in more than 20% of the embryos (Figure 3.7.B and C). This effect is dose-dependent, since the percentage in 20 ng BMO1 injected embryos increased to almost 50%. The reduction of *pax2* expression was specific as the effect was less prominent if human Brg1 WT mRNA was coinjected.

As a more posterior marker, the gene early growth response 2, *egr2*, was chosen. This gene, formerly known as *krox20*, is expressed in rhombomeres r3 and r5 (Giudicelli et al, 2001). Already with 10 ng BMO1 unilateral injections, 80% of the embryos showed a clear reduction in *egr2* expression (Figure 3.7 A-D and F). Noteworthy rhombomere 5 was more affected than rhombomere 3. Again, a dose-dependency was seen as with 20 ng BMO1 almost 90% of the embryos responded with misexpression. Also this effect is specific for Brg1 because the penetrance could be reduced to 54% upon coinjection of 1 ng human Brg1WT mRNA.

As a posterior marker, homeobox B9, *hoxb9*, was analyzed. This gene belongs to the hox-cluster and marks the posterior part of the chordal plate (Godsave et al, 1994). In 43% of the 10 ng BMO1 injected embryos this gene is shifted posteriorly, meaning the expression area was not reaching as far anterior as its expression on the uninjected side (Figure 3.7 A'-C'). Upon 20 ng BMO1 injections, 62% of the embryos were affected. This percentage could again be reduced to 36% when hBrg1 mRNA was coinjected (Figure 3.7 G).
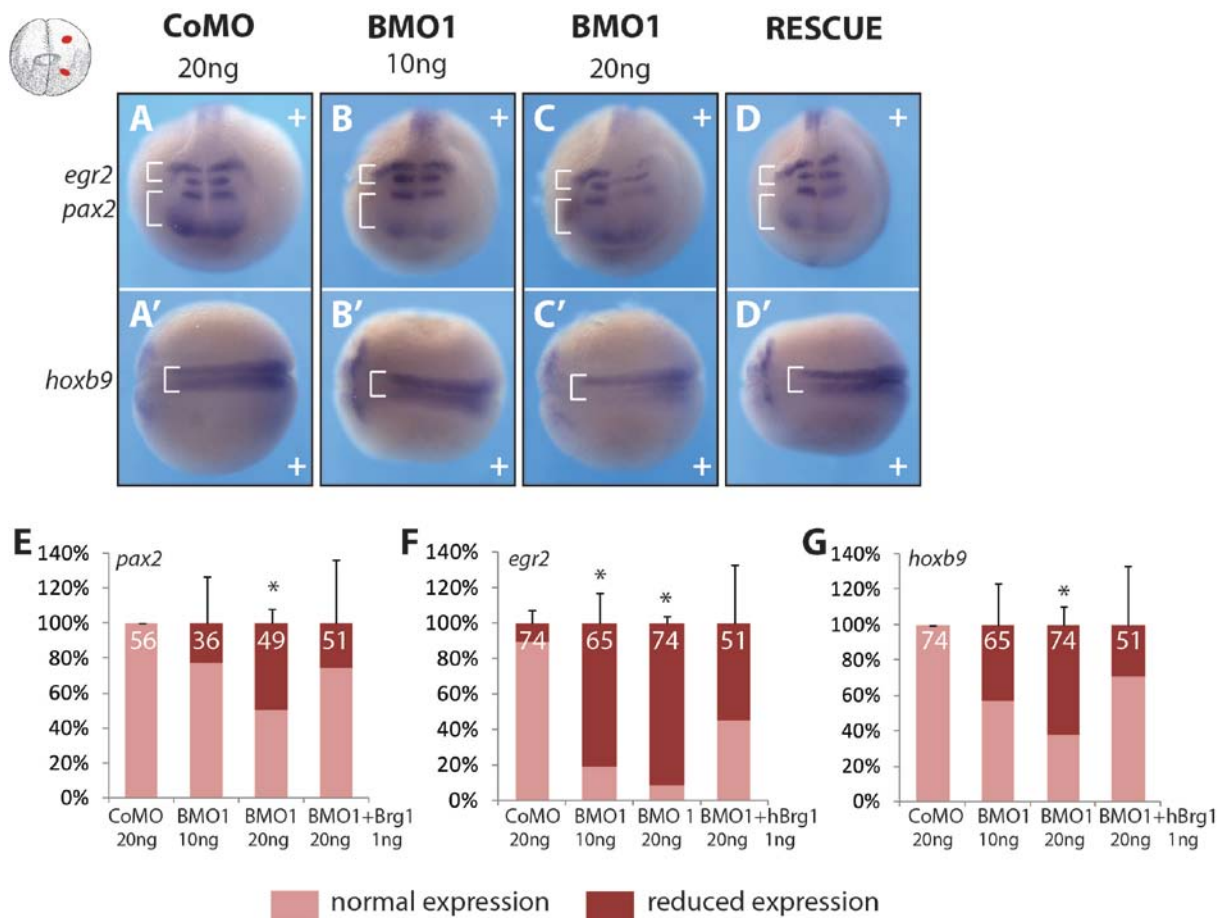
Figure 3.7: Antero-posterior axis markers are reduced in morphant embryos. A-A'; D-D' show neurula embryos, unilateral injected with either 20 ng/blastomere CoMO (**A, A'**), 10 ng/blastomere BMO1 (**B, B'**), 20 ng/blastomere BMO1 (**C, C'**) or 20 ng /blastomere BMO1 coinjected with 1 ng human Brg1WT (**D, D'**) in anterior **(A-D)** or dorsal **(A'-D')** views. Three axis markers were analyzed simultaneously by WMISH: *pax2*, *egr2* and *hoxb9*. The quantification for each marker is shown in **E-G** and represents the mean of 3 biological repeats. + indicates the injected site; *, $p \leq 0.05$.

In total, this experiment shows that embryos deficient for Brg1, have a general impairment of the antero-posterior patterning through all analyzed AP-tissues. Further, it suggests a defective gene expression pattern rather than a shift of AP-tissue, since the gene expression is reduced but the pattern localization is comparable to the uninjected body half.

3.6 Dorso-ventral patterning in gastrula embryos is perturbed

In neurula stages the gene expression domains of antero-posterior marker genes were clearly reduced upon loss of Brg1. Nevertheless this alone cannot explain the severe phenotype seen in the morphological studies. Morphant tadpoles mainly showed a loss of dorso-anterior structures. These defects may originate from early gastrula stage, when the organizer instructs the germ layer and axes patterning. At the beginning of gastrulation, mesoderm cells of the organizer initiate the involution process. During gastrulation, the involuting cells secret proteins that counteract and inhibit the ventralizing proteins. This interplay between dorsalizing and ventralizing factors patterns the embryo in a very precise manner. Several dorsalizing and ventralizing factors were analyzed at mid gastrula to further investigate axis patterning defects. As organizer genes *xnr3*, *otx2*, *foxa4*, *gsc* and *chordin* were analyzed.

Nodal-related 3 (*xnr3*) is an atypical member of the nodal family. In contrast to the other family members it is a direct wnt target gene and its expression domain locates in the animal hemisphere (Smith et al, 1995). During gastrulation it becomes expressed in the organizer territory and functions as a BMP-inhibitor (Hansen et al, 1997). Its expression at the blastoporus lip is reduced upon loss of Brg1 in 62% of the embryos, but only 3% of the CoMO injected embryos show reduced gene expression (Figure 3.8 A, A').

Another important organizer gene is orthodenticle homeobox2 (*otx2*). It starts to be expressed after MBT and marks the organizer field of early gastrula. At later stages it is expressed in anterior structures throughout all three germ layers (Pannese et al, 1995). Apart from superficial expression at the blastoporus lip also the involuted organizer can be visualized with *otx2* WMISH probe. In morphant embryos, a robust reduction of gene expression could be observed in 81% of the morphant embryos. Even more interestingly, the size of the organizer region was diminished (Figure 3.8 B, B'). This indicates a functional impairment of the organizer, which will promote ventralizing factors.

Foxa4, formerly known as XFD1', is also expressed in the organizer and its expression pattern was examined in gastrula embryos. This forkhead box gene is induced by Activin signaling and marks

the notochord in tadpole stages (Knochel et al, 1992). In 58% of the morphant embryos *foxa4* is reduced (Figure 3.8 C, C').

Notably, not all organizer genes were misregulated in Brg1 morphants. *Goosecoid* (*gsc*), is one example. 90% of the morphant embryos formed a normal *gsc* gene expression pattern (Figure 3.8 D, D'). The promoter region of *gsc* is well described and it contains a proximal binding site for the transcription factor Twin, which is regulated through wnt signaling and it contains a distal element for binding of Mixer, a nodal/TGF-ß transcription factor (Watabe et al, 1995).
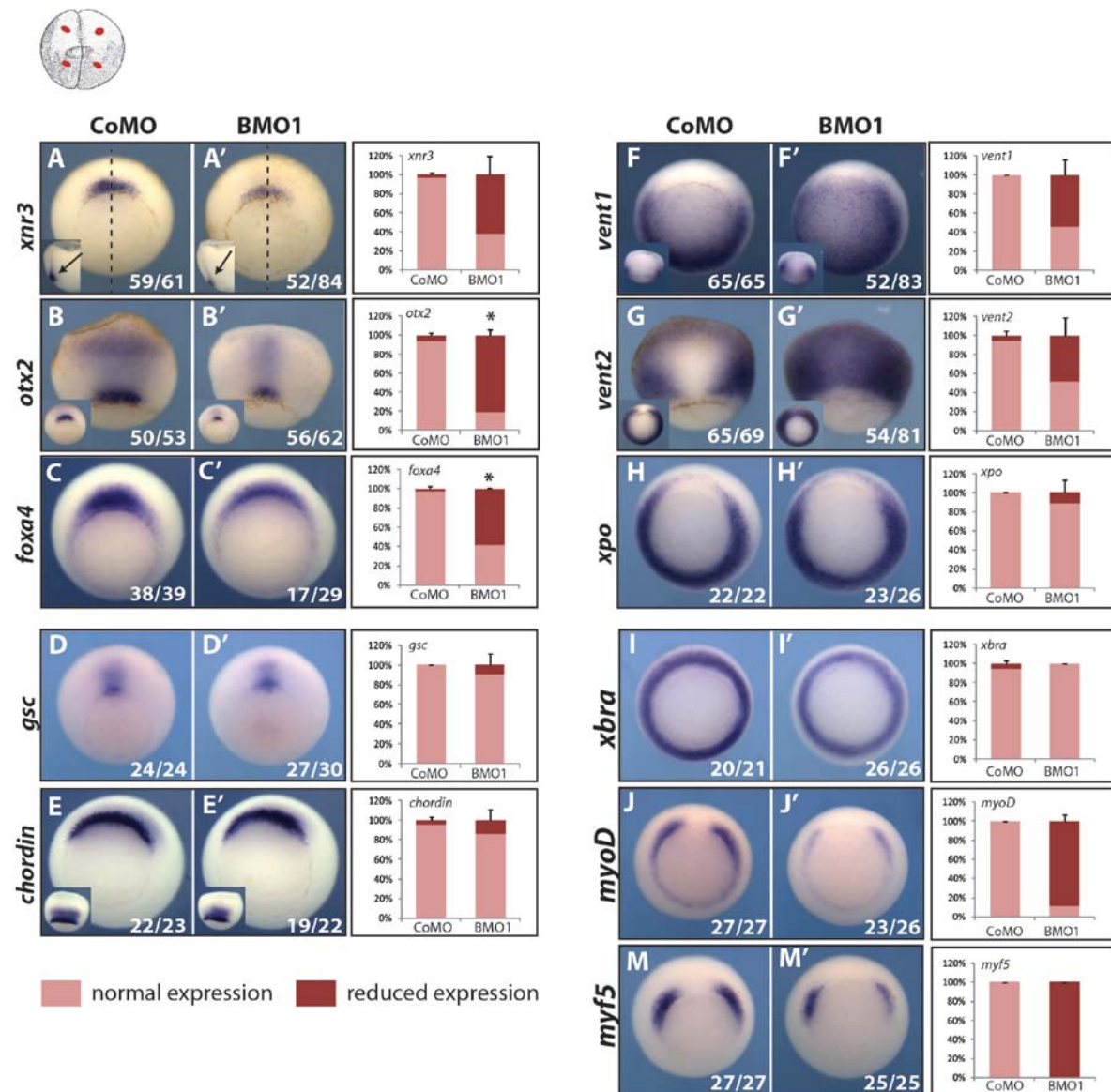
Figure 3.8: Loss of Brg1 disturbes the dorso-ventral patterning. Radially BMO1 (40 ng/embryo) injected embryos **(A'-M')** showed an impaired dorso-ventral patterning at gastrula stage compared to CoMO (40 ng/embryo) injected ones **(A-M)**. All embryos are shown from posterior with dorsal on the top and ventral on the bottom. Except for *otx2* **(B, B')** and *vent2* **(G, G'),** in which a dorsal view is shown with anterior on the top and posterior on the bottom. The inserts in **A**; **A'** show the lateral view of bisected embryos. The inserts in **B, B'** and **G, G'** show a posterior view of the embryo. In **E, E'** the insert shows a dorsal view of the embryos. Each marker was analyzed in 2-4 independent biological repeats. The numbers of each gene expression profile is depicted in the graph next to the pictures. *, *p* ≤ 0.05.

Another interesting candidate is BMP-inhibitor Chordin. This gene is also expressed in the organizer and it was not altered upon loss of Brg1 (Figure 3.8 E, E'). Like *goosecoid*, also *chordin* receives multiple inductive signals. While the first induction wave is triggered by wnt signaling in the ectoderm of late blastula, it becomes induced in the mesoderm by nodal signaling from early gastrula onwards (Wessely et al, 2001).

Taken together, these results indicate a weakening of the organizer in a selective manner, e.g. some but not all of its genes are expressed at lower level. The ventralizing genes are mainly under the control of BMP-signaling and *vent1* and *vent2* are direct target genes (Onichtchouk et al, 1998). In morphant embryos, both genes had a larger expression territory as in control embryos (Figure 3.8 F, F' and G, G'). In fact, their mRNAs were spreading into the organizer region. This is in particular seen for *vent2*. But among the ventralizing genes Brg1 specificity is seen as well. The expression of *xenopus-posterior* (*xpo*), another ventral-promoting gene, was not changed upon Brg1 knockdown (Figure 3.8 H, H').

As the majority of the tested markers are mesodermal genes, it was surprising that the pan-mesodermal marker *xbra* is unaffected (Figure 3.8 I, I'). Nevertheless, the skeletal muscle specific genes *myoD* (Figure 3.8 J, J') and *myf5* (Figure 3.8 K, K') were both reduced at high frequency.

In total, the selective reduction of gene expression at gastrula and neurula suggests that Brg1 is not functionally coupled to a particular signaling pathway or gene network. However, it clearly shows that dorso-ventral patterning in morphant embryos is impaired and the embryos are ventralized already at gastrula stages.

3.7   Brg1 knockdown affects gene expression already at blastula

So far, the molecular imbalance in Brg1 morphant embryos was already visible at early as gastrula. The organizer is one major signaling center, which helps to pattern the embryo during this crucial developmental phase. But the first axis patterning signals are expressed even earlier than gastrulation.

After the MBT, in which a burst of transcription is happening, two centers are established, which are important for later axis patterning. One is the dorso-animally located BCNE. In this tissue, the first wave of *chordin* gene expression is located. In addition, *noggin*, a gene induced by ß-catenin signaling, and *xnr3*, which was already shown to be downregulated in gastrula embryos, are coexpressed in this domain. In radially injected embryos all three genes were reduced in their gene expression pattern (Figure 3.9 A-C; A'-C'). Among these genes, *chordin* responds the most upon a loss

of Brg1 protein, as all morphant embryos were affected by the knockdown. This is a very interesting finding since it was shown in gastrula that *chordin* gene expression was not altered upon Brg1 knockdown (Figure 3.8 E and E'). As mentioned above, the expression wave in gastrula embryos is driven by nodal signaling, whereas the first wave in late blastula is induced by ß-catenin signaling. Nevertheless, this reduction is Brg1 specific, because the gene expression of all three genes can be rescued with coinjections of human Brg1WT mRNA (Figure 3.9 A''-C'').
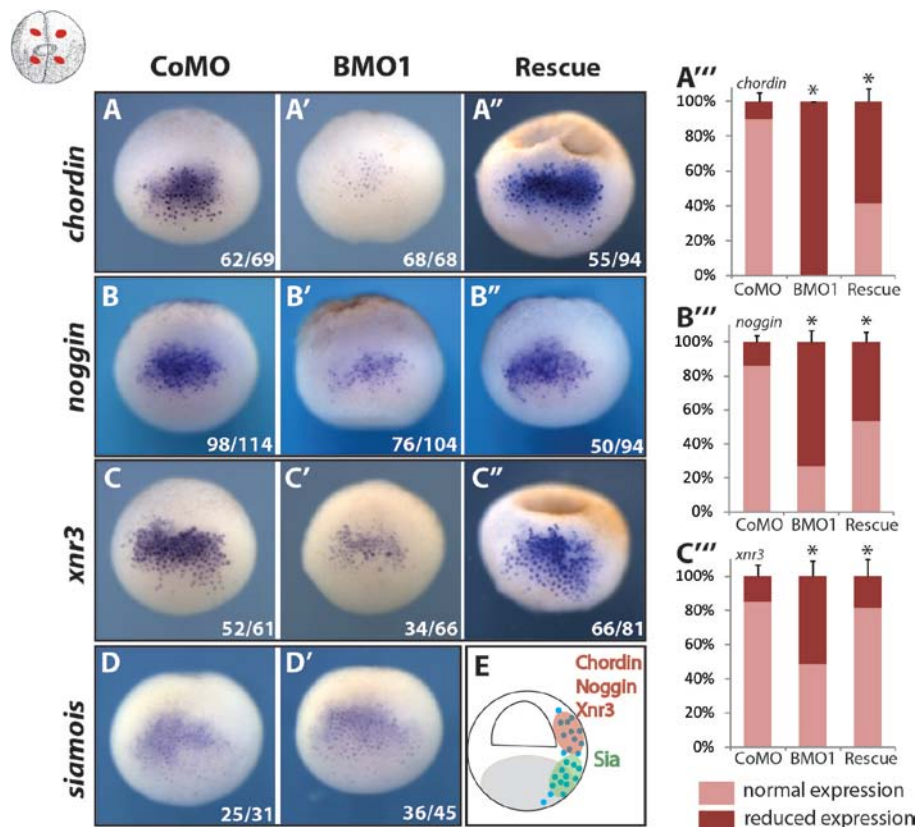
Figure 3.9: BCNE genes are downregulated upon Brg1 knockdown. Shown are late blastula embryos with animal pole on top and vegetal pole on bottom. The embryos were radially injected with either CoMO or BMO1 (both 60ng/total), followed by WMISH for BCNE genes. *Chordin* (**A, A'**), *noggin* (**B, B'**) and *xnr3* (**C, C'**) showed reduction in gene expression. The reduction was partially rescued by coinjections of 1 ng hBrg1WT mRNA (**A''; B''; C''**). S*iamois* (**D, D'**) was not altered in BMO1 injected embryos. **A'''-C'''** illustrate the quantification of 4-5 independent experiments of the indicated gene. **E** illustrates a scheme of blastula signaling centers and associated gene signature.*, $p \leq 0.05$.

Furthermore, *siamois* gene expression was investigated in late blastula embryos. Its gene expression is also dorsally located but more vegetally than the BCNE genes. Furthermore, *siamois*, as mentioned above, is a direct wnt/ß-catenin target gene. Interestingly, *siamois* gene expression was unaffected by the knockdown of Brg1 (Figure 3.9 D and D'). Because, the epistasis experiment suggested that Brg1 probably is upstream of *siamois*, this result was quite surprising. These findings refuse a general

requirement for Brg1 in canonical Wnt signaling but it has to have a gene specific role in and beyond wnt/ ß-catenin signaling.

3.8   ß-catenin target gene *siamois* is not changed upon loss of Brg1

The latter result revealed that *siamois* expression is not altered at late blastula stage after radial BMO1 injections. This result was unexpected and surprising for one particular reason. The reduction of dorso-anterior structures in the Brg1 knockdown embryos resembles a wnt defective morphological phenotype. Siamois is a very well described direct wnt target, which is known to mediate the hallmarks of wnt signaling during development: overrepresented on the ventral side it induces a complete secondary axis; reduced on the dorsal side, dorso-anterior structures and the AP-body axis are reduced (Bae et al, 2011; Lemaire et al, 1995). With the epistasis experiment, a Brg1 role downstream of Siamois signaling was be ruled out. With the last experiment, also an upstream role for Brg1 is unlikely. To exclude that Brg1 and *siamois* are interconnected, one additional experiment was performed. As the injection scheme between the morphological phenotype and the blastula analysis differ, *siamois* expression was also investigated in targeted DMZ injections. Therefore the two dorsal blastomeres were injected at the 4 cell stage with either 2.5 or 5 ng/blastomere BMO1. As lineage trace Alexa 488 was coinjected. Some embryos were collected at late blastula stage in order to perform a WMISH. At early gastrula, dorsal explants were isolated and RNA was extracted to perform a qRT-PCR. Additionally, some embryos were cultivated until tadpole stage in order to determine the strength of the morphant phenotype (see workflow Figure 3.10 A). Whereas the CoMO injected embryos developed normally, the ventralized phenotype of BMO1 injected embryos was apparent already with 2.5 ng/blastomere and more severely in 5 ng blastomere BMO1 injections (Figure 3.10 C, D). In the qRT-PCR analysis, *siamois* gene expression in dorsal explants is indeed slightly downregulated but not in a dose-dependent manner as one would expect from the morphological phenotype (Figure 3.10H).

The WMISH experiment underlines this result. Only 4% in the 2.5 pg/blastomere embryos showed a reduced *siamois* expression. In embryos injected with 5 ng/blastomere a minor fraction, namely 16% of the embryos, showed *siamois* reduction (Figure 3.10E-G). In total, this experiment testifies conclusively that morphant embryos display no severe alteration in *siamois* gene expression, independent of the mode of injections.
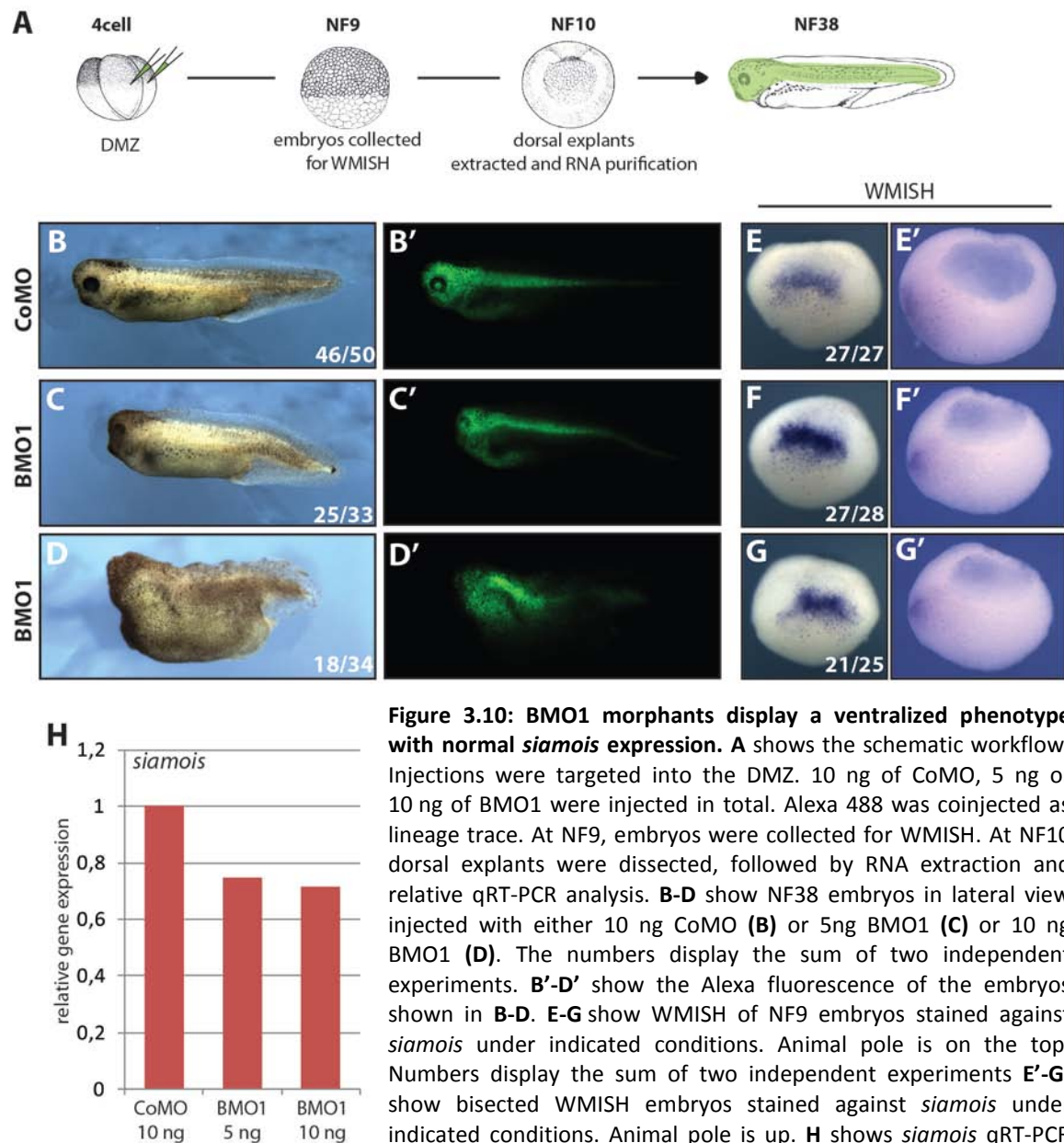
Figure 3.10: BMO1 morphants display a ventralized phenotype with normal *siamois* expression. A shows the schematic workflow. Injections were targeted into the DMZ. 10 ng of CoMO, 5 ng or 10 ng of BMO1 were injected in total. Alexa 488 was coinjected as lineage trace. At NF9, embryos were collected for WMISH. At NF10 dorsal explants were dissected, followed by RNA extraction and relative qRT-PCR analysis. **B-D** show NF38 embryos in lateral view injected with either 10 ng CoMO **(B)** or 5ng BMO1 **(C)** or 10 ng BMO1 **(D)**. The numbers display the sum of two independent experiments. **B'-D'** show the Alexa fluorescence of the embryos shown in **B-D**. **E-G** show WMISH of NF9 embryos stained against *siamois* under indicated conditions. Animal pole is on the top. Numbers display the sum of two independent experiments **E'-G'** show bisected WMISH embryos stained against *siamois* under indicated conditions. Animal pole is up. **H** shows *siamois* qRT-PCR result of dorsal explants under indicated conditions. Gene expression was correlated to *h4* gene expression and normalized to CoMO dorsal explants. Shown is one representative analysis out of two independent experiments.

3.9 Exogenous chordin mRNA can compensate for the loss of Brg1

From the last experiments a general interconnection between Brg1 and the ß-catenin signaling can be excluded. However, with the BCNE results it is obvious that the early wave of *chordin*, *noggin* and *xnr3* is dependent on Brg1 protein level. In order to analyze if Brg1 acts in the same gene network, the most sensitive gene was chosen for a rescue experiment. It was examined if exogenous chordin mRNA can compensate for a loss of Brg1. Therefore, at 4 cell stage the DMZ of one dorsal blastomere

was injected with 5 ng/blastomere BMO1, with or without chordin mRNA. As a control, chordin mRNA was injected alone. To characterize the phenotype, the injected embryos were cultivated until NF38. For quantification the "Eye-Size-Index" (ESI) was measured, as the ratio of the morphant eye size divided by the uninjected eye size. In Figure 3.11 A the workflow of this experiment is shown.
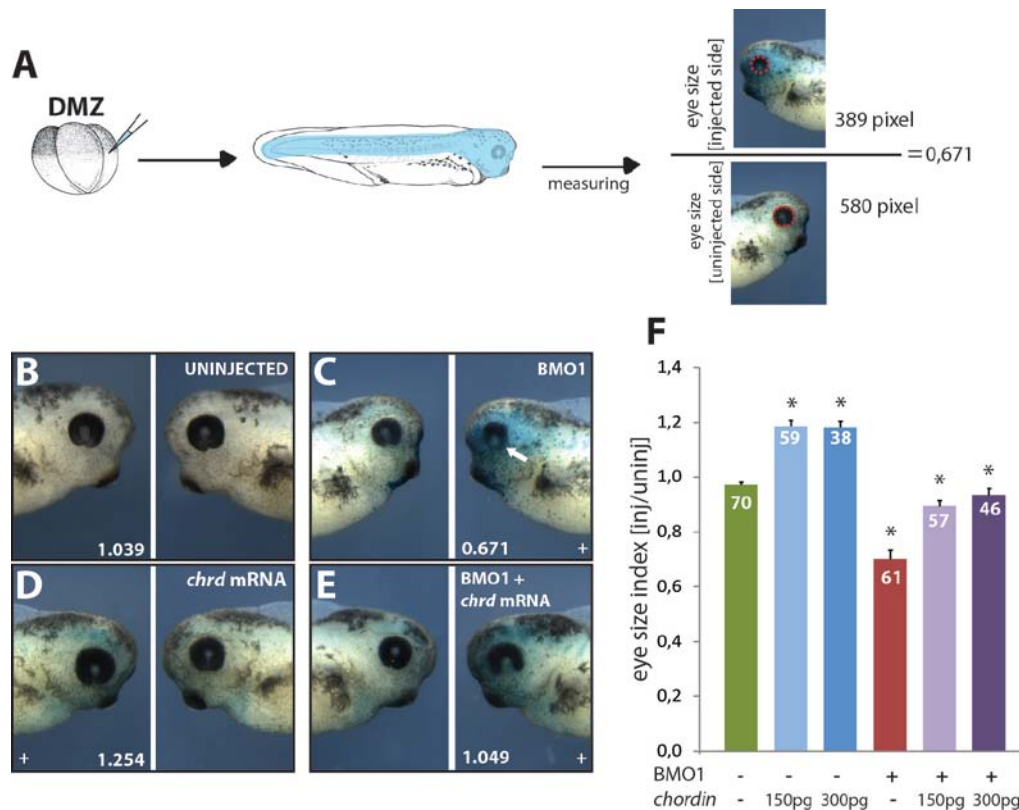
Figure 3.11: Exogenous chordin mRNA rescues the morphological BMO1 phenotype. A shows the workflow of the experiment. Embryos were injected in one DMZ at 4 cell stage. At NF38 the eye size (red dashed line) of the injected site and the uninjected site was measured and divided [injected/uninjected] in order to obtain the eye-size index (ESI). For uninjected embryos the ratio [left/right] was calculated. 5 ng of BMO1 was injected +/- exogenous chordin mRNA. 25 pg of lacZ mRNA was coinjected in every condition. In **B-E** lateral views of analyzed eyes are shown under indicated conditions. Numbers display the ESI of the shown embryos. In **F** the quantification of 3 biological replicates is shown. + marks the injected site; *, $p < 0.02^{-7}$.

As a control, the ESI of uninjected embryos was measured (Figure 3.11 B). In this case the left eye size was divided by the right eye size, leading to an expected average of almost 1, namely 0.973 (Figure 3.11 F). In morphant embryos the eye of the injected site was diminished significantly to an average size of 0.7 (Figure 3.11C and F). As a control two chordin mRNA doses were chosen, 150 pg and 300 pg. Both mRNA doses lead to an ESI higher than 1 (ESI: 1.18). Given that an overexpression of chordin mRNA led to dorsalization, this result was expected (Sasai et al, 1994). In order to investigate whether chordin mRNA can compensate for a loss of Brg1, the chordin mRNA was

coinjected with BMO1. Indeed, both doses normalize the eye size of the morphant embryos. In panel Figure 3.11 E a rescued embryo with 300 pg *chordin* mRNA is shown. On average this dose is sufficient to rescue the eye size to 0.939. In total, this result underlines the interconnection between Brg1 and the early chordin expression in the BCNE.

3.10 A Brg1 morphant BCNE causes loss of eye and brain structures

In 2004, it was shown that a functional BCNE is essential for proper brain and eye development (Kuroda et al, 2004). Since all examined BCNE genes were reduced in Brg1 morphants, the question arose, whether the defective BCNE could cause the observed ventralization of the body plan. To test this hypothesis a transplantation assay was performed. The workflow is shown in Figure 3.12 A.
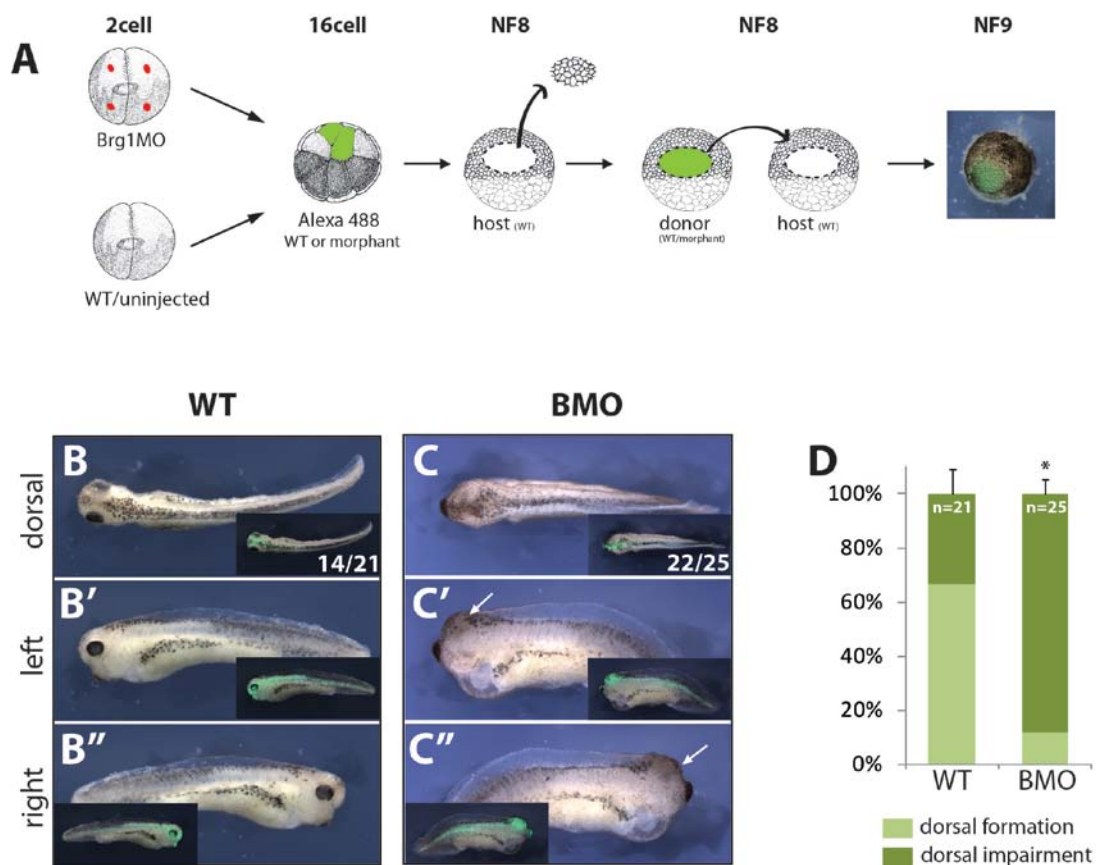
Figure 3.12: A Brg1 morphant BCNE fails to form proper eye and brain structures. A illustrates transplantation assay workflow. For details see text. **B-B''** lateral and dorsal view of an NF35 embryo are shown with a WT BCNE transplant. The insert (bright-field/fluorescence merge) shows that the transplants contributed to dorsal structures. In **C-C''** an embryo with a morphant BCNE transplant is shown in lateral and dorsal view. Note that the overall shape of the embryo is comparable to the WT transplant. However, eyes were not detectable (white arrow). The phenotype of transplanted embryos was classified in "dorsal formation", with normal eye and head structures or in "dorsal malformation", in which eyes and brain are missing. The quantification of five biological replicates is shown in **D**.

At 2 cell stage, 40 ng of BMO1 was radially injected. Morphant and wild type embryos were cultivated until the 16 cell stage and the BCNE region was marked by Alexa 488 injections into two dorso-animal blastomeres. At blastula stage the BCNE of a wild type host embryo was removed and homotopic grafting with either a morphant or a wild type BCNE was performed. The embryos were cultivated until NF38 and the phenotype was characterized and quantified.

Two-thirds of the transplanted WT BCNE formed a normal shaped embryo with eye and head structures (Figure 3.12 B-B''; D). In the case of a transplanted morphant BCNE only a minor fraction, namely 12%, of the embryos developed eye structures. The residual 88% showed clear impairment of eye tissue and head structures, see panel Figure 3.12 C-C''. This result indicates that the phenotype in morphant embryos results in part from the reduced gene expression within the BCNE region. Notably, the overall AP-axis of embryos transplanted with a morphant BCNE was less strong affected than the AP-axis of morphant embryos generated by DMZ injections (see Figure 3.4). This indicates that regions outside the BCNE contribute to axis formation such as anterior mesendoderm, which is formed by a combination of wnt and nodal signaling.

3.11 Molecular analysis of BCNE transplants

Already the morphological characterization of the transplanted embryos was very meaningful, but to gain a better understanding of the structural subdivisions of the brain, a WMISH with brain and eye marker was followed up. For this purpose *otx2* was chosen, which marks the retina and the three brain sections forebrain, midbrain and hindbrain. In panel Figure 3.13 A and B a WT BCNE transplant is shown. In B lateral and dorsal views of the *otx2* stain can be seen. In the lateral pictures the retina is nicely visible whereas in the dorsal view the forebrain with its olfactory patches, the midbrain between the eyes and the hindbrain is clearly structured. In panel Figure 3.13 D and E a partial morphant transplant is shown. As can be seen from the Alexa fluorescence, the BCNE was only partially removed in the host embryo. This is also displayed in the WMISH pattern of *otx2*. Whereas the right body site showed retina staining, the morphant left body site lacked this expression. More difficult to interpret was the brain expression of *otx2*. On the right body half *otx2* staining was visible but the brain was not well structured. In the case of a complete BCNE transplant only diffuse *otx2* staining was observed and no distinct brain structures could be defined (Figure 3.13 F and G). In those embryos, the anterior proportion of the brain appeared reduced in size and lacked *otx2* expression. Since the green Alexa signal proved the survival of the transplanted cells, the abnormal brain structure had to be due to the lack of Brg1 protein in the BCNE region, leading to an incorrect differentiation.
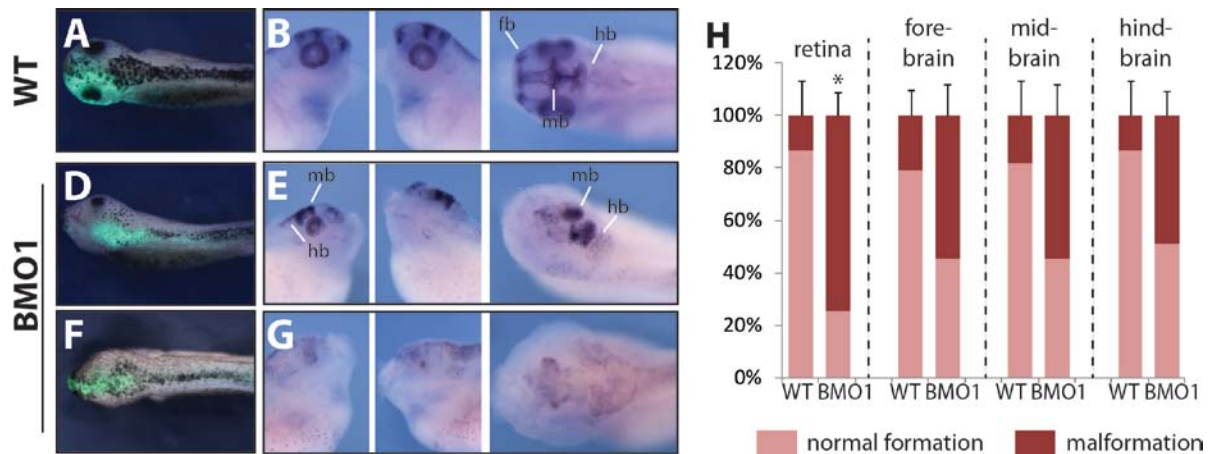
Figure 3.13: Transplantation of morphant BCNE leads to a loss of eye tissue and malformation of brain structures. Shown are embryos transplanted with either a WT BCNE (**A, B**) or morphant BCNE (**D-G**). In the left row a merge of the bright-field and the fluorescence picture is depicted in a dorsal view either for a WT transplant (**A**) or two morphant transplanted embryos (**D, F**). In **B**, **E** and **G** the embryos shown in **A**, **D** and **F** are stained for *otx2* expression and are shown in lateral and dorsal views. In the WT transplant the formation of the three brain structures: fore-, mid and hind-brain was distinguishable. Additionally *otx2* was expressed in the retina. In **D** and **E** an unilateral morphant transplant is shown. In **F** and **G** the result of a complete morphant BCNE is shown. In **H** the quantification of the *otx2* pattern is depicted. 17 WT transplants and 24 Brg1-morphant transplants were analyzed. fb, forebreain; mb, midbrain; hb, hindbrain. *, $p \leq 0.05$.

Although the WT transplants also displayed problems in retinal and also brain formation, the malformation in morphant transplants was clearly more severe. In 75% of the morphant transplants no or only rudiments of retinal *otx2* stain was observed. For all brain structures the malformation was around 50%. This finding underlines that morphant embryos did not only suffer from an eye defect but also brain tissue is unstructured and does not develop properly.

3.12 Brg1 knockdown impairs the transcriptional readout of wnt-and nodal inducers

In the last experiments the impact and necessity of the BCNE for later eye and brain development was analyzed and it was underlined that Brg1 plays a crucial role for gene expression of BCNE genes. Furthermore it revealed, that also other tissues outside the BCNE contribute to the full morphological phenotype, as the AP-axis was hardly reduced in the transplantation assay. The anterior mesendoderm, defined by a combination of wnt and nodal signaling, has a major impact on AP-axis establishment (Robertis & Kuroda, 2004). To investigate the effect of Brg1 knockdown on the two signal pathways, an animal cap assay was performed. For this purpose, embryos were radially injected with 40 ng BMO1 at the 2 cell stage. At the 8 cell stage either Wnt8 mRNA or Activin mRNA was injected into two animal blastomeres to induce wnt- or nodal- signaling, respectivley. The embryos were cultivated until blastula stage and then the animal part of the embryo was dissected

and cultured separately (Figure 3.14 A). When control embryos reached the gastrula stage (NF11) the animal caps were lysed for RNA preparation. The activation of two target genes per pathway was assessed by qRT-PCR. For both pathways two target genes were investigated, of which one responded upon Brg1 knockdown *in vivo* and one which did not respond (see Figure 3.8 and Figure 3.9). For wnt induced animal caps *siamois* and *xnr3* and for activin-induced animal caps *gsc* and *foxa4* for were examined.
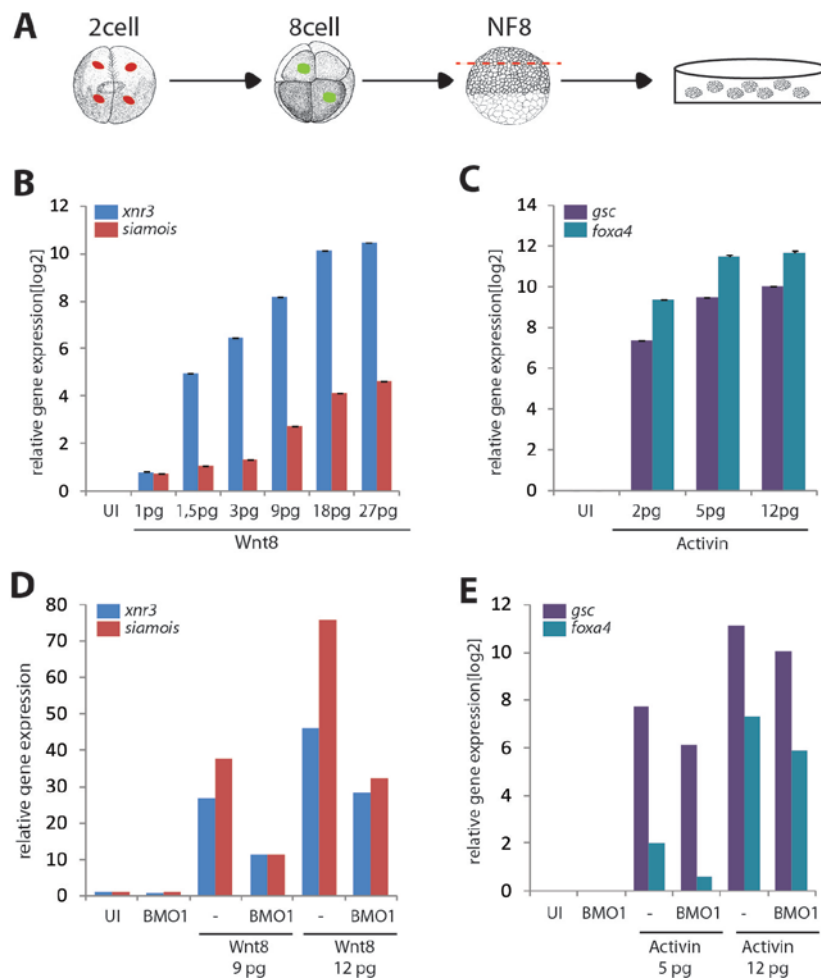
Figure 3.14: Loss of Brg1 leads to reduction of target genes after ectopical wnt and nodal induction in animal cap assay. Panel **A** shows the workflow of the animal cap assay. For details see Materials und Methods. In **B** and **C** qRT-PCR results of the titration for Wnt8 and Activin mRNA is shown. The mean of two independent experiments for each signal induction is shown. In **D** and **E** one representative qRT-PCR results out of 2-3 experiments of the induction assay is depicted. Coinjections with BMO1 led to a reduced induction of all analyzed genes. Please note the different scale on the y-axes.

From initial tests, two different doses of inducing RNA were chosen (see Figure 3.14 B and C). With regard to wnt signaling both target genes, *xnr3* and *siamois*, showed decreased gene expression

upon knockdown of Brg1 in both induction dosages. The same was true for Activin induction of *goosecoid* and *foxa4* transcription. This outcome was unexpected, since *siamois* as well as *goosecoid* transcription was not altered by reduced Brg1 protein level *in vivo*. Notably, the strength of the reduction differs among the two induction dosages. *Xnr3* and *foxa4* gene expression were halved in both inducing dosages. In contrast, the gene expression of *gsc* and *siamois* were halved in the lower induction dosages, but were less impaired in higher induction dosage. In total, these induction experiments indicate that Brg1 is required for the transcriptional readout of both, wnt and nodal-signaling. Presumably for some genes, a reduction can be overcome by stonger induction, which could explain the results of the *in vivo* analysis.

3.13   Genes outside the BCNE are affected by Brg1 knockdown

The data presented so far details crucial functions for Brg1 in brain and axes development. These functions can be traced back as early as blastula stage. Furthermore, Brg1 has a major impact on the BCNE, which is important for head development. As pointed out before, also other tissues are affected by Brg1 knockdown.

It is known that the anterior endomesoderm is contributing in head formation (Robertis & Kuroda, 2004). This tissue is defined by a combination of wnt and nodal signaling, which in the latter experiment both showed a regulation by Brg1. The combination of the two pathways induce factors like Cerberus, which functions as a secreted wnt,- nodal- and BMP-inhibitor (Piccolo et al, 1999b). Its expression pattern is confined to early mesendoderm and is located in a signaling center vegetally of the BCNE. This second signaling center at blastula is called the "Nieuwkoop center" (Robertis & Kuroda, 2004). In order to examine whether Brg1 also has an impact on genes outside the BCNE, BMO1 injections were performed at the 8 cell stage in either the dorso-animal (DA; BCNE) or dorso-vegetal (DV; Nieuwkoop center) cells. Besides *cerberus* also *hhex*, hematopoietically expressed homeobox, was analyzed. To directly compare the DV injections with the former Brg1 knockdown in BCNE, DA injections were performed side by side and assessed again for *chordin* and *noggin* expression.
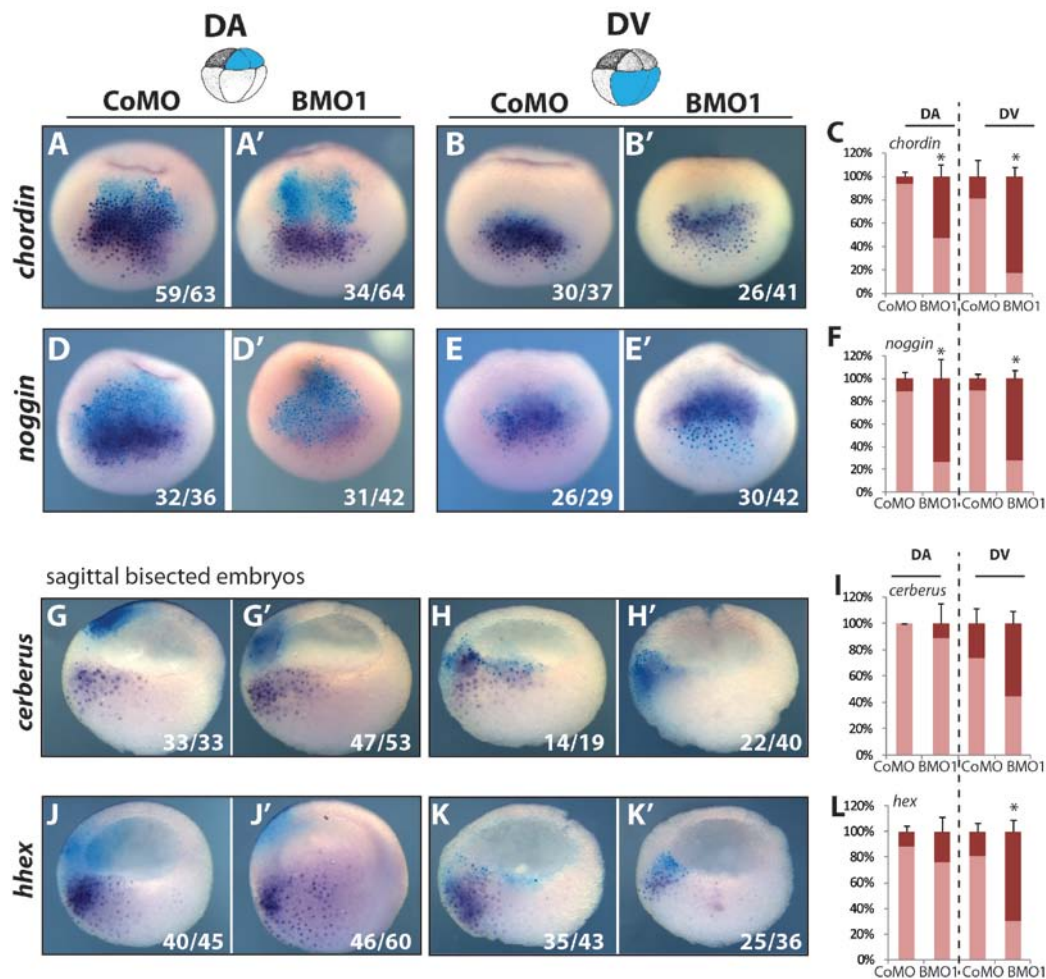
Figure 3.15: Dorso-vegetal genes do contribute to the observed phenotype in *X. laevis*. Embryos were injected at the 8 cell stage, either in the two dorso-animal blastomeres (DA) or the two dorso-vegetal blastomeres (DV) with 10 ng CoMO (**A-K**) or 10 ng BMO1 (**A'-K'**). To lineage-trace the injected cell progeny, 25 pg lacZ mRNA was coinjected. Embryos were cultivated until late blastula stage and afterwards analyzed for BCNE markers *chordin* (**A-B'**) and *noggin* (**D-E'**). As Nieuwkoop center genes *cerberus* (**G-H'**) and *hhex* (**J-K'**) were analyzed. **A-E'** show whole embryos, the animal pole is up. G-K' show bisected embryos, the animal pole is up. Numbers indicate the sum of 3-4 independent experiments. In **C, F, I, L** the quantifications for the indicated gene is depicted. *, $p < 0.05$.

In DA injections, *chordin* and *noggin* showed a clear reduction in gene expression, namely 50% or 73%, respectively (Figure 3.15 A, A'; B, B'; C; F). This expected result underlines the requirement of Brg1 in BCNE gene expression. In DA injections *cerberus* as well as *hhex* expression were not altered (Figure 3.15 I; L), because of missing spatial overlap as revealed by the lacZ lineage tracing stain (Figure 3.15 G, G' and J, J'). However, as the injections and the expression pattern of *cerberus* and *hhex* overlaped in DV injections, a loss of Brg1 caused a reduction in 55% and 69% of the embryos, respectively. This points out that Brg1 is required for gene transcription of distinct genes also in prospective mesendsoderm. Furthermore, when BCNE genes were analyzed in BMO1 DV injections, the embryos provided new informations. As the expression pattern perfectly matches with DV

injections, *chordin* and *noggin* mRNAs were tremendously reduced in the BCNE (Figure 3.15 B, B';
E, E'). For *chordin*, 80% of the injected embryos showed reduced gene expression. This was even
higher as in DA-injections. Regarding *noggin* the percentage of embryos with reduced gene
expression was comparable with DA-injections, namely 70%. These observations highlight a non
cell-autonomous function for Brg1 protein, which is required for the transcription of Nieuwkoop
center genes to unfold the RNA signature of the neighboring BCNE.

These results can be summarized as follows. Embryonic patterning requires the BCNE and
Nieuwkoop center signaling activities on the prospective dorsal side. Genes in both signaling centers
become induced by wnt activity and Brg1 helps to induce many, but not all of them. Furthermore,
autonomous and non-autonomous effects allow anterior neural differentiation of the head. Thus,
Brg1 behaves as a pleiotropic regulator of gene activation from midblastula stage on.

3.14 Brg1 knockdown in *Xenopus tropicalis*

In search for a possible common denominator that explains Brg1's target gene selectivity, a
genome-wide transcriptome analysis was undertaken. For this approach, the related species *Xenopus
tropicalis* is more suitable than *Xenopus laevis* for several reasons. First of all *Xenopus tropicalis* has a
diploid genome in contrast to the allotetraploid *Xenopus laevis*. This makes it easier to accomplish
protein knockdown in a reliable manner. A second big advantage offers the much better annotated
genome resource of *X. tropicalis*, which increases the number of transcripts that can be scored and
related to biological pathways depending on Brg1 function.

A first prerequisite was to demonstrate a comparable and specific morphological phenotype
upon Brg1 knockdown in *X. tropicalis*. BMO1 and BMO2 also fit to the Brg1 sequence of *X. tropicalis*
(Figure 3.16 A). This allows using the same morpholinos, thereby increasing the comparability of the
results obtained in the two species. For this purpose BMO1 and BMO2 were singly injected in one
dorsal blastomere at the 4 cell stage. After cultivating until NF40, the Eye-Size-Index (ESI) was
measured. The eye size was reduced and dorso-anterior structures were impaired upon both
morpholino injections to a comparable extent like in *X. laevis* by BMO1. This argues that Brg1 has a
similar role in *X. tropicalis* as in *X. laevis*. Again BMO1 was the more potent morpholino regarding the
strength of the phenotype. To nearly abolish eye development, 2.5 ng/blastomere of BMO1 was
sufficient whereas 10 ng/blastomere had to be injected in the case of BMO2 (Figure 3.16 B; E; D; G).
Although, four fold higher than BMO1, the latter dose is within the recommended dose range for
*Xenopus (*Heasman, 2002). In addition, both BMO1 and BMO2 were partially rescued by coinjections

of human Brg1 WT mRNA (Figure 3.16 C; F; D; G). These results provide the experimental grounds to investigate the genome wide contribution of Brg1 to the embryonic transcriptome.
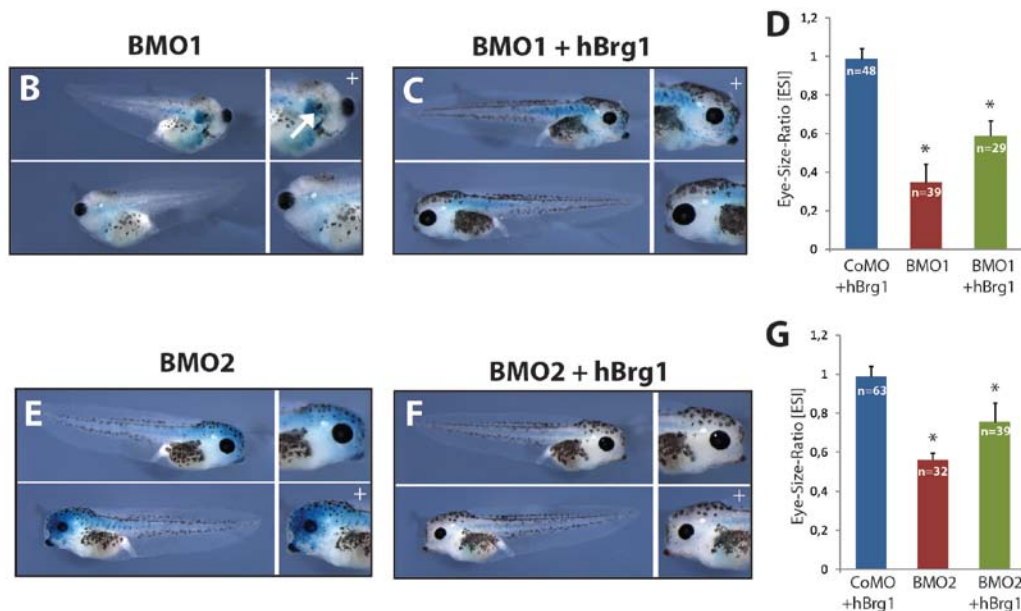
Figure 3.16: BMO targeting side and their effect on development. A shows the BMO targeting side in the *X. tropicalis* Brg1 mRNA sequence. In **B, C, E, F** lateral views of the morphological phenotype of BMO1 and BMO2 in *X. tropicalis* are shown. Embryos were injected in the DMZ of one dorsal blastomere at the 4 cell stage, cultivated until NF40 and the Eye-size-Index (ESI) were measured. In panel **B,** lateral views of a 2.5 ng/blastomere BMO1 injected embryo is shown. The eye on the injected side was hardly developed (white arrow). This could be partially rescued by coinjections with 1 ng/blastomere hBrg1 WT mRNA (**C**). The penetrance of the BMO1 phenotype under the different conditions is shown in panel **D**. In panel **E** an embryo injected with 10 g/blastomere BMO2 in lateral view is shown. On the injected side the eye size was reduced. This could be partially rescued with coinjections of 1 ng/blastomere hBrg1 WT mRNA (**F**). In panel **G** the quantification of the ESI is shown. Numbers indicate the sum of 3 independent experiments. +, injected site; *, $p \leq 0.05$.

3.15 BMO1 and BMO2 reduce Brg1 protein level at blastula and cause embryonic lethality during gastrulation

For the genome-wide transcriptome analysis, embryos were radially injected with either BMO1 or BMO2 oligonucleotide. Therefore a dose had to be defined that reduces the Brg1 protein levels as much as possible, while at the same time being non-toxic to the embryo. Since the studies in *X. laevis* indicate early functions for Brg1 from blastula stage onwards, the focus of the transcriptome analysis was set to the late blastula. This way, zygotic gene expression and transcriptional readout of early

signaling activities would be included. Titration experiments revealed for BMO1 a dose of 30 ng/embryo and for BMO2 a dose of 60 ng/embryo being most efficient in Brg1 knockdown. Two criteria influenced these experiments: The survival of the embryos and the efficiency of the knockdown. In the case of BMO1 already 30 ng/embryo injected radially led to embryonic lethality during gastrulation. Almost 90% of the injected embryos did not finish the gastrulation, whereas the lethality until late blastula stage was comparable to the control embryos (Figure 3.17 A). From the morphological analysis it was not clear, why BMO1 injected embryos were not able to proceed further in development. The protein level in BMO1 injected embryos at late blastula was reduced to an average of 0.48 of the compared control morphants (Figure 3.17 B). This finding indicates that it is not possible to produce a null situation presumably due to the maternal Brg1 protein stores. For BMO2 injected embryos the situation was not as severe. Whereas almost 80% of the injected embryo survived gastrulation, almost 50% died during neurulation (Figure 3.17 A). The embryos displayed reduced dorso-anterior structures, followed by death. In terms of protein inhibition, BMO2 was somewhat less efficient. On average a knockdown of 0.6%, compared to control morphants was created (Figure 3.17 B). In the Western Blot analysis, displayed in Figure 3.17 B, also the maternal Brg1 level (see lane "egg"), the preMBT Brg1 protein level (see lane "4cell") and the Brg1 protein level in late blastula uninjected embryos (see lane "UI") was analyzed. With this titration and characterization of the protein level the first steps towards a genome-wide analysis are made.
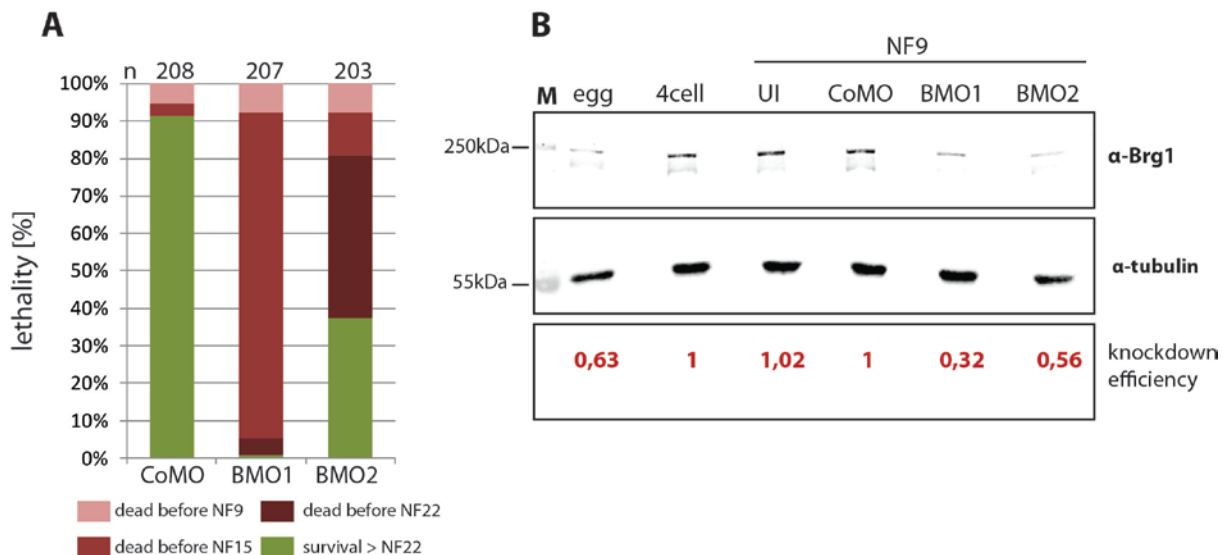
Figure 3.17: BMO1 and BMO2 injection decrease the Brg1 protein level at blastula stage but result in embryonic lethality. A shows the lethality rate of embryos injected with either 60 ng/embryo CoMO, 30 ng/embryo BMO1 or 60 ng/embryo BMO2. Numbers represent the sum of 8 independent experiments. In panel **B** a representative Western Blot analysis out of 4 independent experiments, is shown. As loading control the protein level for α-tubulin was investigated.The knockdown efficiency is the ratio between Brg1 and alpha-tubulin protein level. The ratios were normalized to the CoMO ratio. M, marker.

3.16 Morphant embryos are not delayed in development and do not activate apoptosis

After finding the right and tolerable dosages of the two morpholinos, some critical points had to be addressed. First of all it is important to determine that morphant embryos really pass beyond the MBT. To rule out that morphant embryos are not delayed, the MBT marker gene *gs*17 was analyzed in qRT-PCR analyses. The transcript levels of *chordin* and *cerberus*, shown to be reduced upon Brg1 knockdown, were also examined in these experiments. The gene expression of these three genes was related to the housekeeping gene *odc* and normalized to control morphant samples. Upon both BMO1 injections *gs*17 was reduced, but still robustly induced compared to the preMBT transcript levels (see Figure 3.18 A "4cell"). About 40 minutes after collecting the embryos in late blastula stage control morphants and Brg1 morphant embryos started to gastrulate, as evident from the simultaneous appearance of the dorsal blastoporus lip.
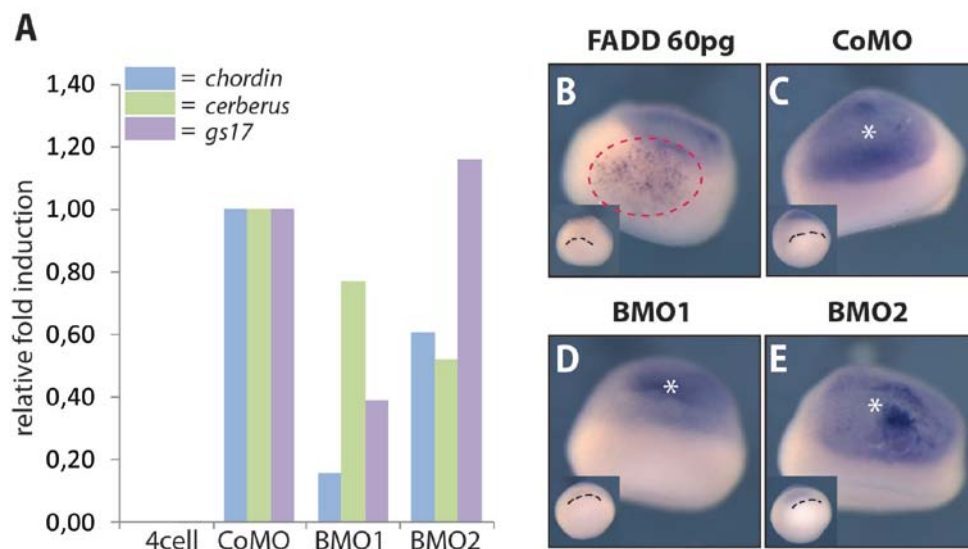
Figure 3.18: Morphant embryos are neither delayed in development nor do activate apoptosis. A shows one representative qRT-PCR analysis of NF9 embryos with MBT marker *gs*17, *chordin* and *cerberus* under the indicated conditions. Panel **B-E** display an ICC for activate Caspase-3. As positive control FADD-plasmid was injected in both dorsal blastomeres (DMZ) to ectopically induce apoptosis. CoMO, BMO1 and BMO2 injected embryos were radially injected. No activated Caspase-3 pattern was observed in morphant embryos. The dashed red line marks the area of active Caspase-3 staining in the positive control. The black dashed lines in the inserts depict the dorsal lip. The white asterisk indicates background staining in the blastocoel.

The embryonic lethality following from the Brg1 protein knockdown raised the concern, if the embryos were still healthy at the onset of the gastrulation or if they activated the apoptotic program already. This was investigated by immunostaining for active Caspase-3. Beginning of gastrulation, radially injected morphant and control embryos were collected and stained for activate Caspase-3.

As a positive control 60 pg of FADD plasmid was injected into the DMZ 4 cell stage (Figure 3.18 B). Whereas the positive control showed an accumulation of apoptotic cells, neither the control morphants nor the BMO-injected embryos showed apoptotic cells (Figure 3.18 C-E).

With these controls it can be stated that the embryos that are going to be analyzed in the genome-wide analysis have passed the MBT, are reduced in Brg1 protein level, show the typical reduction of *chordin* and *cerberus*, do not undergo apoptosis and are not delayed in development.

3.17 Genome-wide transcriptome analysis of BMO1 morphant embryos

For the genome-wide transcriptome analysis the Affymetrix GeneChip®*Xenopus Tropicalis* Genome Array was used. On this Chip over 59000 probe sets are spotted, which represent more than 25000 genes in *X. tropicalis*. In total, 12 genome arrays were performed. For each condition - CoMO, BMO1 and BMO2 - four biological replicates were analyzed. The quality of each RNA sample was tested on the Bioanalyzer. The RIN-values ranged between 8 and 8.6. The 12 RNA samples were handed over to the "Facility of functional genomics" at the Munich Gene Center, where the array hybridization was performed. The raw-data was sent to Dr. Tobias Straub, the head of the "Bioinformatics Core Unit" at the Adolf-Butenandt Institut, who performed the bioinformatic analysis described below.
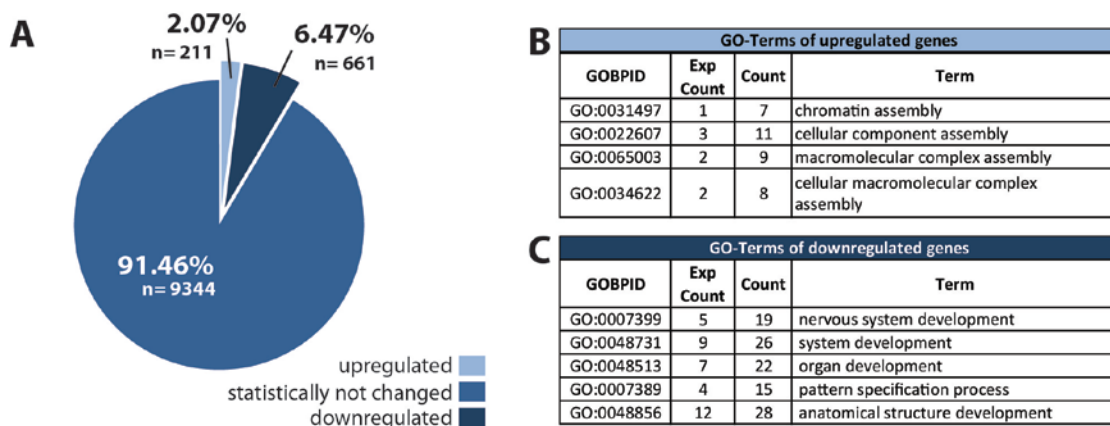
Figure 3.19: Brg1 knockdown causes minor changes in the transcriptome. A shows a pie chart of all 10216 genes that were active at NF9 and their response to Brg1 knockdown. For more details see text. The list in panel **B** shows the 5 most significant GO-terms for the upregulated gene cohort. In list **C** 5 significant enriched GO-terms of all downregulated genes are shown. Exp Count, expected count.

A cutoff was defined which binned the 25000 genes on the array in "active at late blastula" and "not-active at late blastula". 10216 of the spotted genes were active at this early developmental

stage. For statistical reasons the local false discovery rate (lfdr) was set to ≤ 0.2. After filtering, only 872 genes remained as responding to Brg1 knockdown. This indicates that 9344 genes, i.e. 91.46% of all active genes at late blastula were statistically not changed upon BMO1 knockdown. From the 872 altered genes 21 (2.07%) were upregulated and 661 (6.47%), were downregulated. These results are depicted in a pie chart of all active genes in Figure 3.19 A. This outcome was rather surprising, as a change in gene expression of only 8% of all genes obviously cause severe morphological phenotypes and embryonic lethality.

In order to classify the responding genes, a Gene Ontology search was carried out. Within the upregulated gene cohort terms like "chromatin assembly" or "macromolecular complex assembly", were overrepresented (Figure 3.19 B). Among the downregulated genes mainly developmental related genes were affected, like "nervous system development" and "pattern specification process" (Figure 3.19 C). This analysis leads to the conclusion that knockdown with BMO1 results rather selectively in changes on the transcription level but these changes are sufficient to perturb the embryonic program and cause embryonic lethality.

3.17.1 Genes related to "nervous system development" are affected in Brg1 morphants

Since the majority of misexpressed genes was downregulated and related to development, the focus was set on this gene cohort. First of all the most enriched sub-GO-term "nervous system development" was examined in detail. This GO-term lists 62 genes of which 19 were misregulated upon BMO1 injections. To validate the microarray results, another four independent biological replicates were performed and the gene expression of the 19 misregulated genes was re-investigated by quantitative RT-PCR. The results are shown in Figure 3.20. The gene expression levels of the analyzed genes were related to two house keeping genes, *ornithin decarboxylase* (*odc*) and *glycerinaldehyd-3-phosphate-dehydrogenase* (*gapdh*), and then normalized to control embryos. Genes that were downregulated more than 1.5 fold in the microarray analysis are depicted in red. From these 19 genes 15 could be verified to be significantly downregulated upon BMO1 injections, marked with the asterisk. This experiment underlines the significance of the microarray data and connects it to the morphological phenotype which was observed in DMZ targeted injections (see Figure 3.4).
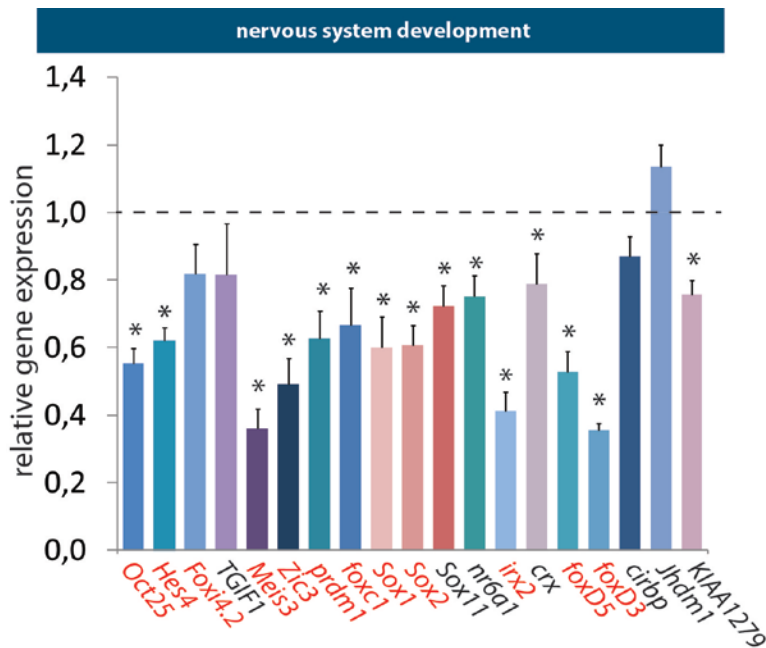
Figure 3.20: Genes in the GO-term "nervous system development" are highly affected upon BMO1 knockdown. qRT-PCR analysis of the tested 19 genes that showed reduced expression in the BMO1 morphant array. Genes which showed ≥ 1.5 fold change in the morphant microarray analysis are depicted in red. 15 genes within this group showed a significant reduction in gene expression. Shown is the mean of eight independent experiments. *,$p \leq 0.05$.

3.17.2 BMO1 affects a broad range of genes throughout all germ layers

The morphological analysis has identified a requirement for Brg1 in neuroectodermal differentiation, starting in the BCNE. Even though this requirement is underlined in the microarray analysis, it is not Brg1's only function. This becomes particularly clear in the morphological phenotype of BMO1 VMZ-injections. One third of these embryos displayed problems in the development of ventro-posterior structures (see Figure 3.4). This broader function is reflected in the microarray analysis, in which not only dorsal genes were affected but rather a broad range of general development related genes. In order to investigate the additional effects of BMO1 injections throughout germ layers, a selection of genes with broad functions in diverse developmental programs were further tested.

As mentioned before, *chordin*, *noggin*, *xnr3*, *siamois*, *twin* and *otx2* are expressed in the dorso-animal part of the embryo. Whereas *chordin* and *noggin* were significantly downregulated, *xnr3* was upregulated. This is not in accordance with the WMISH pattern observed in *X. laevis* and might reflect a regulatory difference between the two species (Figure 3.9). *Siamois* in contrast, is not responding in *X. laevis* while the paralogous gene *twin* is upregulated in *X. tropicalis* upon BMO1 injection. *Otx2* was marginally reduced in the microarray and qRT-PCR analysis, while its WMISH pattern in *X. laevis* gastrula embryos revealed a prominently reduced expression domain (Figure 3.8).

Follistatin, *cerberus*, *bmp4* and *sizzled* are all located in the dorso-vegetal halve of the developing embryo. Whereas *follistatin* and *cerberus* are important to specify head structures, *bmp4*

supports ventro-posterior fate. *Follistatin* and *bmp4* were reduced in their gene expression, whereas *cerberus* and *sizzled* did not respond to BMO1-mediated lower levels of Brg1 protein.

Important for neuroectodermal differentiation are the genes *zic1* and *zic3*. Both genes were downregulated upon knockdown of Brg1. In contrast, *zic2*, important for the maintenance of neuron-precursor genes, was not changed (Yan et al, 2009). Little information is available about *sox21* but it is believed to promote neuroectodermal differentiation. It was one of the strongest responder to Brg1 ablation in the microarray analysis. In contrast, epidermal fate promoting gene *foxi1* is upregulated upon Brg1 knockdown.
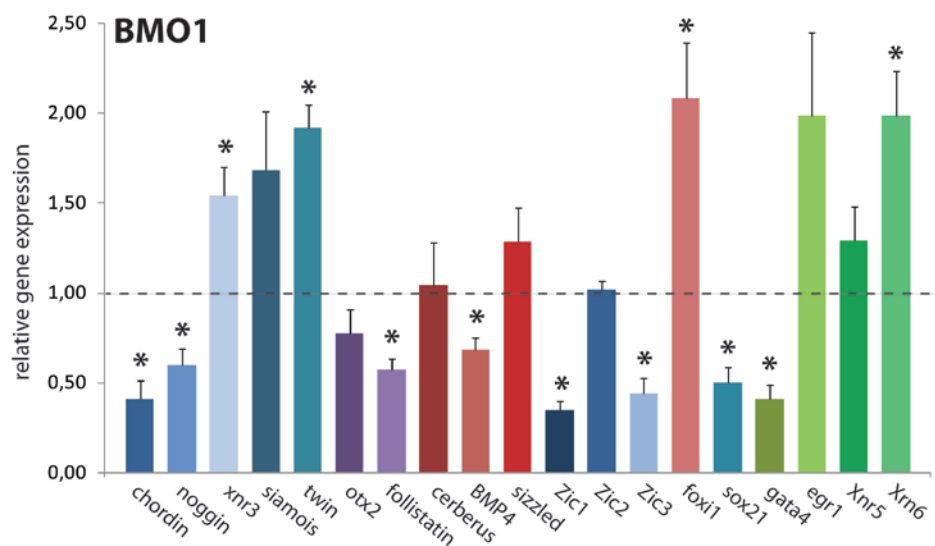
Figure 3.21: A broad range of genes are affected by the BMO1 injections. Shown is a qRT-PCR analysis of 19 genes, which are expressed in various tissues of the developing embryo and which define different germ layers. Shown is the mean of eight independent biological experiments. The asterisk marks statistical significance with $p \leq 0.05$.

The remaining genes that were investigated are all expressed in mesendodermal cells. *Gata4*, which is active in the dorsal and ventral mesendoderm, promotes differentiation of anterior mesoderm and was downregulated in morphant embryos. The gene early growth response 1, *egr1*, is transcribed mesodermal and later on also in posterior parts of neurula embryos. Even though this gene was upregulated in the microarray analysis, this result could not be verified by qRT-PCR. *Xnr5* and *xnr6* are both targets of the wnt and nodal pathway and are already expressed preMBT. As it was shown earlier in Figure 3.3 the preMBT expression of the genes were not changed, but in late blastula the gene expression are slightly upregulated in morphant embryos. This could be verified in the microarray analysis.

All together, the responses of this set of functionally diverse genes, crystallizes the notion that a loss of Brg1 protein activity has a broad impact on gene expression in the embryo. Given that these requirements are already visible at approximately 40-50% of the normal Brg1 level suggests that the full extent of Brg1's impact on gene transcription could be much larger and potentially even global.

3.18 Brg1 knockdown by BMO2 recapitulates the major changes in gene expression

To control for potential off target effects of the BMO1, the microarray analysis was repeated with a second morpholino, BMO2 (Figure 3.16 A). The pretest had indicated that the blocking efficiency of this morpholino was not as strong as BMO1, and consequently the morphological phenotype was milder.

As expected from the lower translation-blocking efficiency less genes responded to BMO2 in the microarray analysis. From the 10241 active genes at late blastula, 259 genes, 2.53%, were upregulated upon BMO2 knockdown. A minor fraction, namely 190 genes, 1.86%, was downregulated. The remaining 9792 genes, 95.62% did not pass the statistical cutoff of lfdr ≤ 0.2.
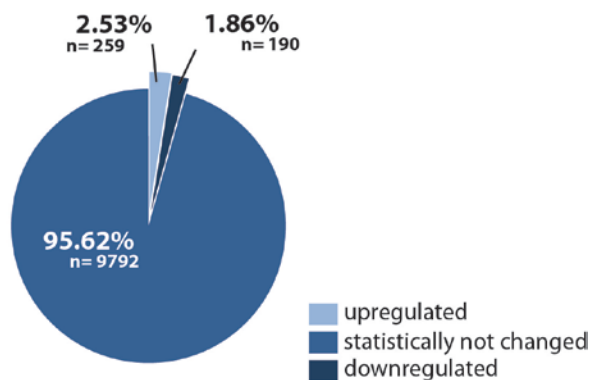
Figure 3.22: Microarray analysis for BMO2 injected embryos. Shown is a pie chart of all active genes at NF 9 and their response to Brg1 knockdown by BMO2.

With both classes of responders, upregulated and downregulated, a search in Gene Onthology was performed, but no statistical overrepresentation was found. This is quite unusual but points towards a rather global function of Brg1 rather than a specific functional annotation.

Despite the quite different outcome of BMO1 and BMO2 microarray data, also common responders were identified. As mentioned above in the BMO1 analysis various genes were chosen to be verified in qRT-PCR analysis. The same genes were tested also under BMO2 conditions. The result is displayed in Figure 3.23.

The BCNE genes *chordin* and *noggin* were only slightly downregulated in its gene expression but this reduction was not statistically significant over a mean of 7 independent biological replicates. In the dorso-animal group only *twin* was statistically reproduced among the two morpholino oligonucleotides. However, for all genes, except *xnr3*, the principal tendency was the same as with BMO1.
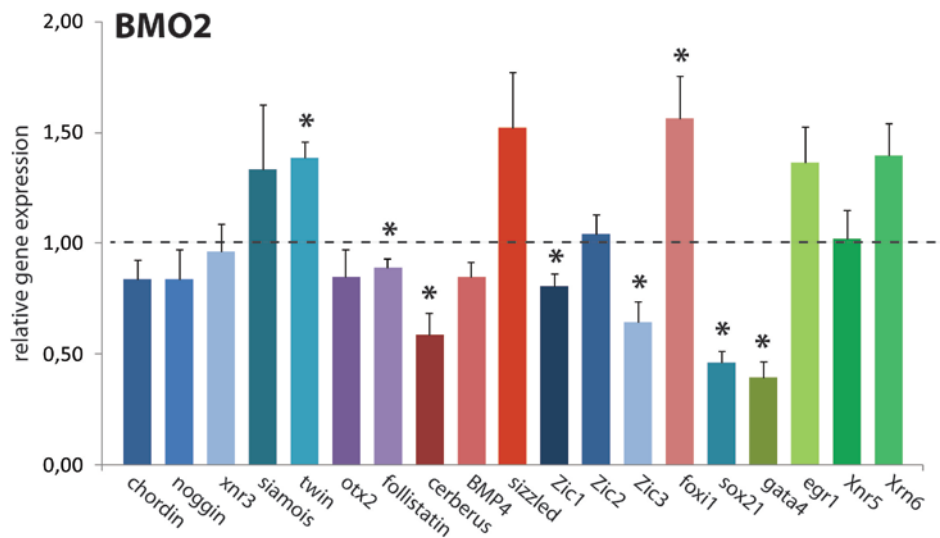
Figure 3.23: BMO2 microarray validation via qRT-PCR. A broad range of genes from various cell tissues and germ layers were analyzed in qRT-PCR analysis. 8 genes could be verified as statistically significant. In general, the investigated genes showed a similar tendency of misregulation for both morpholinos. Shown is the mean of seven independent experiments. *, $p \leq 0.05$.

The dorso-vegetal genes showed a diverse pattern in comparison to the BMO1. Whereas *follistatin* was downregulated, albeit to less extent than in the BMO1 morphants, *cerberus* gene expression was severely downregulated. This result was already observed in previous experiments (Figure 3.18). The two ventral genes, *bmp4* and *sizzled* are not changed upon BMO2 injections.

Regarding the neuroectodermal genes, the two morpholinos achieved comparable result, although again gene responses were weaker with BMO2. Neurogenesis promoting genes *zic1* and *zic3* were downregulated, neuronal progenitor maintenance factor *zic2* was unchanged, while *sox21* was severely reduced and epidermal fate promoting gene *foxi1* was upregulated.

Among the mesendodermal genes, only *gata4* was reduced under BMO2 knockdown. *Egr1* and *xnr6* were slightly upregulated but not in a statistically significant manner. *Xnr5* was not changed in its gene expression.

In total, the BMO2 morpholino displayed fewer changes on global gene expression level than BMO1. This was expected, because BMO2 also showed a lower translation blocking efficiency.

Finally, the validation of the same genes by qRT-PCR revealed similar tendencies. All together, the BMO2 data supports the results so far obtained for BMO1.

3.19 Global transcription changes at midblastula transition

The analysis revealed on morphological and molecular level that Brg1 is required especially during specification of dorsal structures. Nevertheless there is also evidence that Brg1 plays a role in ventral cell fate specification. Neither with the morphological features nor with the global transcriptome analysis a common denominator for Brg1 target genes has been revealed so far.

Due to the fact, that the earliest responders among dorsoventral Brg1 target genes can be traced back to the MBT, this stage was reinvestigated with the goal to define a potential role for Brg1 in zygotic genome activation. So far, only a few studies investigated the preMBT transcriptome in *Xenopus* (Blythe et al, 2010; Paranjpe et al, 2013; Yanai et al, 2011)*.* The majority of the published analyses examined genome-wide data after the MBT (Akkers et al, 2009; Bogdanovic et al, 2011; Bogdanovic et al, 2012; Schneider et al, 2011). Since the transcriptome undergoes major global changes at MBT, a comparison between the expression levels of preMBT and postMBT embryos would be very informative regarding the molecular events happening at the MBT. A simplified scheme in Figure 3.24 illustrates these changes.

In principal, three different classes of mRNAs are considered to be present at late blastula (NF9). One group of genes is maternally expressed and will be degraded with midblastula transition. This pool of RNA is depicted in blue. Other genes are already expressed maternally and with the MBT those gene transcripts get replaced with zygotic transcripts. Overall this pool of RNA, illustrated in green, may stay more or less constant in its abundance. The third class of mRNAs are the newly *de novo* gene transcripts, which are not present in the preMBT embryo. This class is shown in purple. In order to reveal a possible role for Brg1 in activating the newly zygotic genes, the purple class of mRNAs needs to be identified.
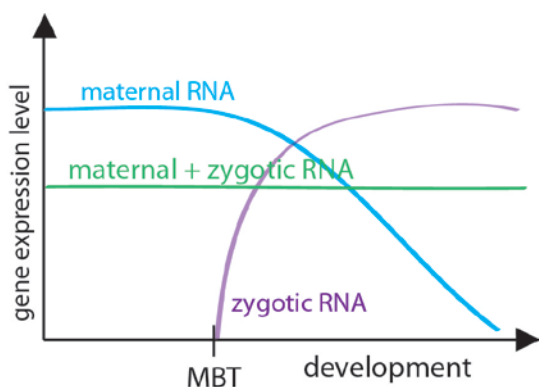
Figure 3.24: Simplified scheme of RNA classes and their dynamics during early development. In blue the maternal RNA class is visualized. It is defined as maternally present and the expression decreases after MBT. Depicted in green is the RNA class that is maternally and zygotically expressed with little changes in expression level. In purple are the transcripts classified that are absent maternally and get *de novo* transcribed with transition at the midblastula.

To examine this question a second microarray analysis was performed. The experimental workflow is shown in Figure 3.25 A. *Xenopus tropicalis* wild type embryos were collected in three phases: at the 4 cell stage; every 20 minutes over the MBT and in late blastula stage again every 20 minutes, until the pigmentation of the dorsal lip appeared. Then, to identify the preMBT sample closest prior to the MBT, the expression level of MBT marker *gs17* was analyzed in qRT-PCR. In Figure 3.25 B a representative qRT-PCR analysis is shown. The gene expression level of *gs17* was normalized to 4 cell stage embryos. Finally, the latest sample without *gs17* transcript was chosen as the preMBT sample for analysis.

The corresponding postMBT sample was the one collected ~40 minutes prior to appearance of the dorsal lip. This time point is in accordance to the time point of the BMO microarray analyses. To ensure the quality of the RNA the collected samples were run on the Bioanalyzer. The samples with the highest RIN score were chosen for the microarray analysis. In total, 3 pairs of independent pre- and postMBT samples were processed.
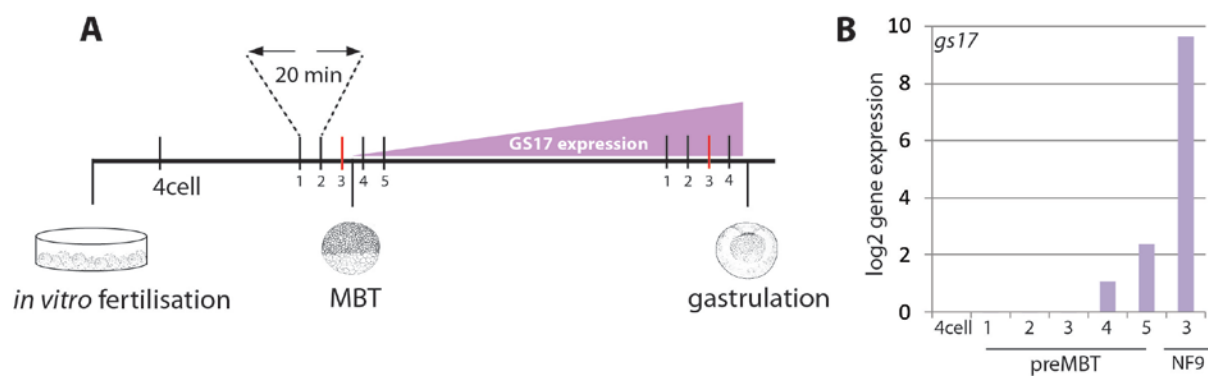
Figure 3.25: Experimental workflow to determine pre-and postMBT samples for microarray analysis. A shows a scheme of the experimental workflow. *X. tropicalis* WT embryos were *in vitro* fertilized and samples were collected at the 4 cell stage, whilst over the MBT in 20 min intervals and in late blastula again in 20 min intervals until the appearance of the dorsal lip. RNA was extracted and gene expression of MBT marker *gs17* was investigated by qRT-PCR. **B** shows a representative qRT-PCR analysis of *gs17* expression profile. The sample pair which was used for the microarray analysis is shown in red.

3.20 Comparison of pre- and postMBT transcriptomes

In the comparative microarray analysis, 10169 mRNAs from active genes were detected in either preMBT or postMBT. After setting the statistical cutoff of the "adjusted p-value" to ≤ 0.05, only 1357 genes remained, that are significantly. From this gene cohort 596 genes (5.86%) showed an upregulation of transcription and 761 genes (7.48%) a reduction of transcription between MBT and the late blastula. This result is depicted in the pie chart in Figure 3.26 A.

In Figure 3.26 B the enriched GO-terms for the upregulated gene class are listed. Besides the expected term "regulation of RNA metabolic process" and "transcription, DNA-dependent" also developmentally relevant terms like "pattern specification process" and "developmental process" emerged. The pattern specification process is of particular interest, as it was overrepresented in the downregulated responder genes cohort of the BMO1 microarray data set (Figure 3.19).

A 5.86% n=596 7.48% n=761 86.66% n=8812

- upregulated
- statistically not changed
- downregulated

B

GO-Terms of upregulated genes after MBT				
GOBPID	ExpCount	Count	size	Term
GO:0051252	10	46	293	regulation of RNA metabolic process
GO:0007389	2	22	53	pattern specification process
GO:0006351	11	46	304	transcription, DNA-dependent
GO:0010468	12	47	330	developmental process
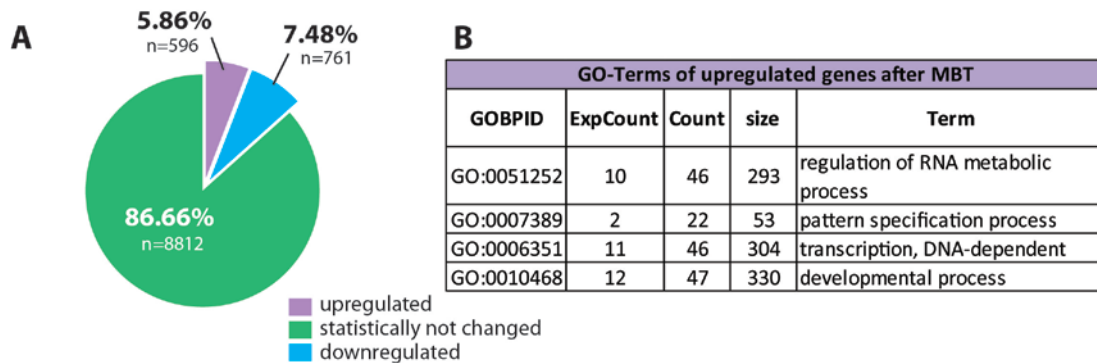
Figure 3.26: Gene expression changes of preMBT and postMBT embryos. A shows a pie chart with the three classes of RNA pools revealed from the comparative microarray analysis. In **B** the 5 most significant GO-terms for the "upregulated after MBT" cohort are shown.

3.21 Highly upregulated genes at MBT need Brg1 protein

As the GO-term "pattern specification process" was detected both in the downregulated GO-terms of the BMO1 morphant array and in the cohort of upregulated genes after MBT, this connection was further examined. The genes, present in this GO-Term, are listed in a heat map in Figure 3.27 according to the magnitude of activation at MBT, strongly activated genes are on top; less strongly activated genes are at the bottom. These genes were now compared to the list of BMO1 responding genes (see Figure 3.19). The genes which showed a downregulation more than 1.5 fold change in the BMO1 microarray analysis are marked with a red asterisk. Interestingly, the majority of the marked genes were among the strongest activated ones at MBT. In the GO-term "nervous system development" this distribution can be seen as well (data not shown). The genes that undergo strong upregulation after the MBT were among the genes that depend strongly on Brg1 protein.
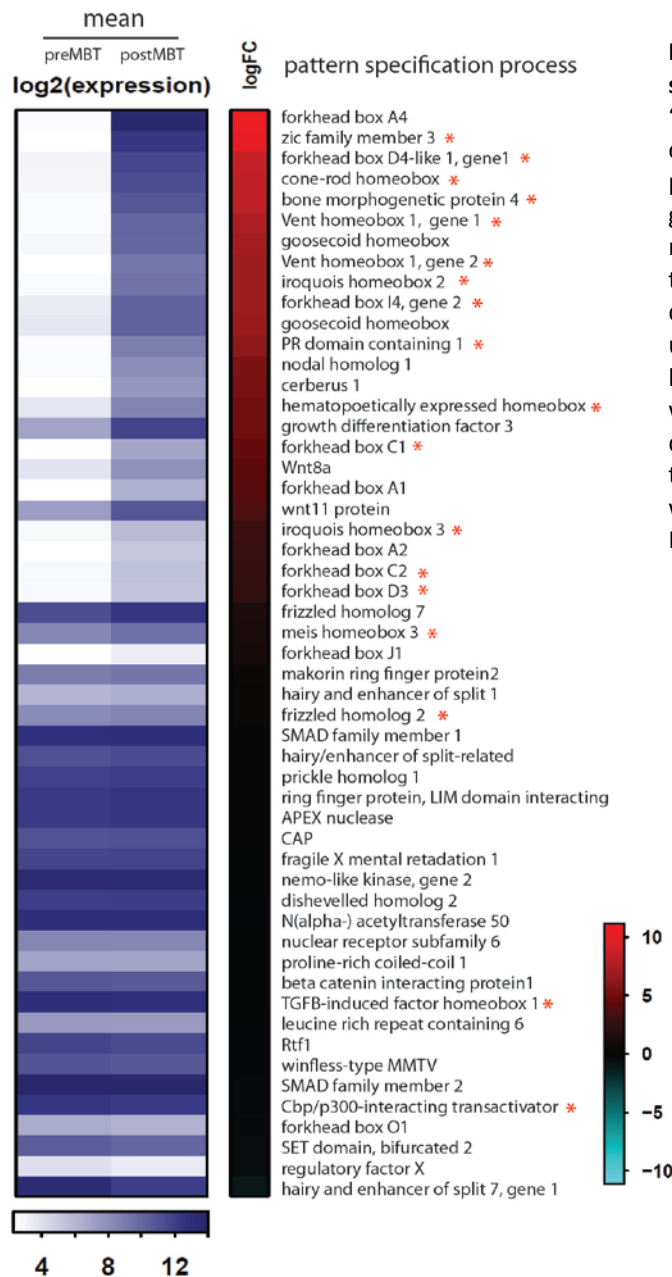
Figure 3.27: Heat map of GO-term "pattern specification process". The genes related to "pattern specification" are listed upon their changes in gene expression preMBT relative to postMBT. The first two columns describe the gene expression preMBT and postMBT, respectively. The deeper the blue the higher is the gene expression. The ratio for each gene is depicted in the logFC column. The genes that underwent the strongest changes have a high logFC value and are listed on top and genes which underwent no changes or downregulation are displayed in the bottom of the list. The red asterisk marks the genes that were downregulated more than 1.5 fold in the BMO1 morphant array.

In the BMO2 morphant microarray analysis this observation is not that explicit, but the trend is also apparent (data not shown). To verify further the hypothesis that a loss of Brg1 mainly affects the strongest upregulated genes after MBT- the "MBT-burst" gene class- was examined in detail. Defined as "MBT-burst" are genes, that show an upregulation at MBT higher than 5.65 fold change and this class of genes was separately compared with the responding genes of the BMO1 and BMO2 array data sets. In Figure 3.28 two pie charts display the response of the "MBT-burst" genes either under BMO1 knockdown or BMO2 knockdown conditions. For BMO1 324 genes were listed and almost 50% of them were misregulated. 135 genes were significantly downregulated and 9 genes were even upregulated upon Brg1 knockdown. The remaining 180 genes were not statistically significant with a local false discovery rate (lfdr ≥ 0 .2. Under BMO2 conditions, the same trend is seen, albeit less pronounced. 30 genes of the 352 "MBT-burst" genes showed a downregulation upon knockdown

with BMO2 and 11 genes showed an additional upregulation. For the vast majority, namely 311 genes, the changes in their expression level were not statistically significant. Nevertheless, the fact that more genes in this subset showed a downregulation rather than an upregulation is meaningful, because the overall trend of the transcriptome analysis upon BMO2 injections displayed rather an up- than a downregulation (Figure 3.22). This underlines the specificity of the finding that mostly genes that undergo a burst of transcription at the MBT require Brg1 protein.
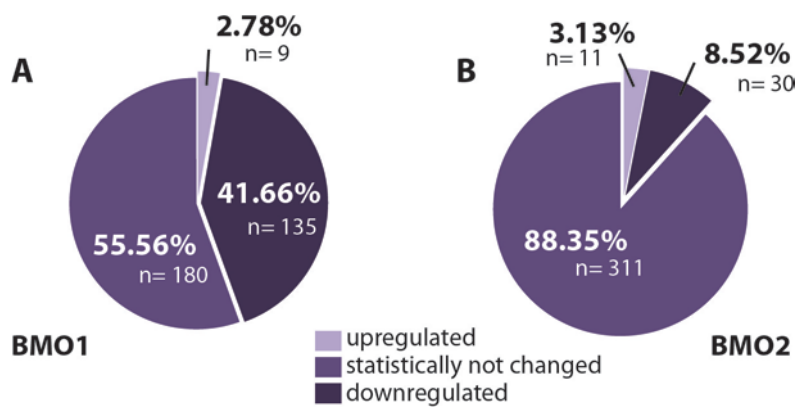
Figure 3.28: The "MBT-burst" genes require Brg1 protein function. The strongest upregulated genes at MBT were correlated to their gene expression upon either BMO1 knockdown (**A**) or BMO2 knockdown conditions (**B**) and visualized in a pie chart.

After revealing a relation between strong induction of gene expression at MBT and the necessity for concomitant presence of Brg1 protein, this hypothesis was further analyzed. Therefore, the genes of the preMBT/postMBT microarray analysis were devided into two classes. One class contains all genes that showed an upregulation in transcription at the MBT and the other class represents all genes that were either not changed between pre and postMBT or were downregulated at MBT.

Under both knockdown conditions, BMO1 and BMO2, the genes that underwent a upregulation at the MBT were reduced in their gene expression in comparison to the genes that did not undergo such a burst of transcription (Figure 3.29). The impairment of this transcriptional burst at MBT was more severe upon BMO1 knockdown than under BMO2 knockdown conditions. Given that BMO2 is less efficient in blocking the protein translation, this result is coherent. However, the tendency is clearly visible and statistically validated.
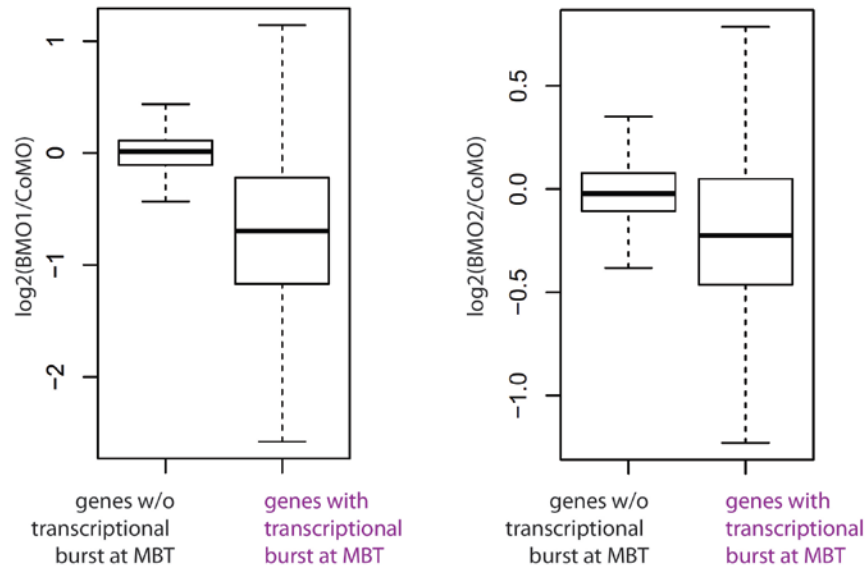
Figure 3.29: Brg1 protein function is needed for the transcriptional burst at MBT. In **A** the boxplot displays that genes which underwent an upregulation at MBT are strongly impaired in their expression level under BMO1 knockdown conditions in comparison to genes without an upregulation. **B** shows the same correlation under BMO2 knockdown conditions. w/o, without.

From this data it can be concluded, that Brg1 protein function is required to ensure the transcriptional burst at MBT. Additionally, the fact that two different morpholino oligonucleotides, with a minimum of overlap, result in a comparable morphological phenotype showing the same trend of correlation in the microarray sets, underlines the specificity of the finding.

4 Discussion

The development from a zygote to a multicellular organism is a profound process, which requires extensive arrangements on the cellular and genomic level. Each different cell type is the product of distinct signal gradients, inductive events or transcriptional restrictions in order to establish a unique transcriptional and cellular architectural state. Any developmental signal matters and even minor imbalances can lead to severe malformations up to embryonic lethality. Understandably, the earliest events in the life of an organism have to be tightly regulated and controlled. Chromatin modifying enzymes like methyltransferases or chromatin remodeling complexes have a pivotal role during these early events. By modulating the chromatin state, they cause changes on the transcriptional level, in particular stable on and off states ensuring a regulatory memory that stabilizes cell fates.

In this PhD thesis a crucial role for the chromatin remodeling ATPase Brg1 protein function during early *Xenopus* development has been revealed. A requirement for Brg1 during differentiation of neurons was already suggested. An additional role during neurogenesis and dorso-ventral patterning at earlier time points was discovered in this study. With a morpholino-based knockdown approach it was shown that Brg1 protein is essential for embryogenesis, since a loss of Brg1 caused embryonic lethality during gastrulation. Furthermore, the first misregulated genes under knockdown conditions were found in late blastula stage. Mainly the BCNE signaling center was affected but not all genes were equally impacted, which suggests some target specificity. In addition, also genes outside the BCNE were affected. The transcriptome analysis of morphant embryos at blastula stage revealed rather minor changes, though it was informative in terms of gene specificity. Two major considerations led to the investigation of Brg1 function during zygotic genome activation. The activation of the zygotic genome presumably requires large rearrangements within the chromatin structure which takes place at the MBT, meaning shortly before the first effects upon Brg1 knockdown were visible. Secondly, it was shown that Brg1 deficient mice die during implantation and that maternal Brg1 protein is needed for proper zygotic genome activation (Bultman et al, 2006). Taken this into consideration, the transcriptome of preMBT and postMBT wild type embryos were investigated and three different mRNA pools were defined. After comparing the mRNA subsets with the transcriptome analysis of Brg1 morphant embryos it became clear that the highly upregulated genes were specifically dependent on Brg1 activity. This suggests that Brg1 is required in *Xenopus* development for the burst of transcription at the MBT and that it is essential for a proper activation of zygotic genes, similar to what was shown in mouse development.

4.1 Morpholino efficiency and targeting behavior

In order to perform morpholino-based knockdown analyses, three different morpholinos against Brg1 mRNA were designed. As shown in Figure 3.2 the target sides differed among the three morpholinos. BMO1 targets only the coding region, beginning with the ATG. BMO2 is designed a bit upstream in the 5'UTR but reaching into the coding sequence. BMO3 targets only the 5'UTR and shares 14 bases with the BMO2. Although the targeting sides are in close proximity, the luciferase assay revealed differences in the translation blocking efficiency (see Figure 3.2). The optimal morpholino target is a 25 base sequence that lies within the region from the 5' cap to the first 25 bases of the coding region (www.gene-tools.com). Even if the company meanwhile recommend testing 2-3 morpholinos for the same mRNA, such a difference in blocking efficiency is rather unusual. The Kroll lab used a Brg1 morpholino targeting even further upstream of the minor efficient BMO3 tested in this study. Taken this into consideration, this could explain why they did not observe an earlier effect upon Brg1 knockdown. Although they investigated the Brg1 protein level by western blot analysis and clearly saw a downregulation, one has to keep in mind that their analysis regards embryos in neural stages (Seo et al, 2005). Presumably their morpholino was not efficient enough to reduce the protein level already at blastula stage in order to observe a misregulation. In the literature a correlation between morpholino efficiency and targeting side was not suggested so far. One paper, which investigates morpholino knockdown efficiency by a luciferase-based assay, correlated the inhibition efficiency with the strength of the phenotype in zebrafish upon Chordin knockdown. Two Chordin morpholinos were independently injected and indeed the more upstream morpholino showed lower penetrance (Kamachi et al, 2008). Overall such a correlation would be interesting and could presumably be explained by possible secondary structures, which leave the ATG-region accessible for ribosomes, whereas the 5'UTR forms loops.

In vivo, the Brg1 protein levels were examined in eggs, wild type 4 cell stage embryos and at late blastula stage in four different conditions: wild type, CoMO-, BMO1- and BMO2-injected. An increase in Brg1 protein level between eggs and 4cell stage was observed, whereas between the 4 cell stage and the late blastula stage (NF9) the protein level is more or less constant. Under knockdown conditions, BMO1 reduced the Brg1 protein level to less than 50%, whereas BMO2 reached a reduction up to 60%. Given that the time point of the genome-wide analysis is quite close to the MBT a complete reduction of Brg1 protein cannot be achieved, as the maternal Brg1 protein is still present. Though, a reduction only up to 40-50% already leads to embryonic lethality.

4.2 Phenotypic analysis of Brg1 morphant embryos

4.2.1 Morpholino based knockdown analyses

For genome-wide analysis *Xenopus tropicalis* embryos were radially injected. In BMO1 injections this led to embryonic lethality during gastrulation, while the majority of radial BMO2 injected embryos survived until neurulation. Most likely, this difference is explained by the different morpholino efficiencies. Regarding the embryonic lethality caused by BMO1 several mechanisms are possible that explain a unfinished gastrulation. First of all, SWI/SNF and Brg1 are known to be connected to cell cycle progression (Muchardt & Yaniv, 2001; Simone, 2006). A reduction of Brg1 therefore will lead to uncontrolled cell proliferation as some of the cell cycle check points are not functional anymore. This in turn leads to more and more DNA damages and especially in this early developmental stage the embryo cannot compensate for it, which in the end leads to developmental arrest. In case of BMO2 injected embryos the protein level is less reduced and probably sufficient to ensure in some degree a normal proceeding through gastrulation. Although an alteration within the cell cycle in Brg1 morphant embryos is valid, it is presumably not the cause of the embryonic lethality, as PMEFs deficient for Brg1 show no alterations in cell viability (Bultman et al, 2000). The second possible explanation is rather related to developmental specification processes, as it was revealed within this thesis that Brg1 is required for a proper transcriptional burst at the MBT. Among the genes, which were highly upregulated were mainly genes important for cell fate specification (Figure 3.19). Additionally, the germ layers and the body plan are specified during gastrulation. Given that after BMO injections the level of Brg1 was reduced, also the transcription of these genes was impaired and the specification process during gastrulation could not proceed in a proper way. In the case of BMO1, this was more severe than in BMO2 injections as the Brg1 protein level was lower and more genes were affected. This could be the cause of a cellular arrest as the cells lacked specific signals for differentiation. However, a tightly controlled study in morphant embryos investigating the morphological changes during gastrulation paired with apoptotic and proliferation markers would give further insight.

In targeted knockdown studies two different injections were performed. The marginal zones of either dorsal or ventral blastomeres were injected. BMO injections into the dorsal marginal zone led to severe dorso-anterior malformation. The phenotype ranged from a mild reduction of the eye up to a near complete loss of dorso-anterior structures (Figure 3.4). In order to classify morphological phenotypes in *Xenopus* the Dorso-Anterior-Index (DAI) is often used (Kao & Elinson, 1988). On this scale, the DMZ injected embryos classified as DAI 2–DAI 4, which is associated with a reduction of dorsalizing factors. As already pointed out in the introduction, the dorsalizing activity in *Xenopus*

embryos is mediated via ß-catenin signaling. A physical interaction in HEK239T cells between ß-catenin and Brg1 was already shown and a promoting function of Brg1 of wnt target genes was suggested. Additionally, a genetic interaction of Brahma and Armadillo was described in *Drosophila* (Barker et al, 2001). Furthermore, knockdown of maternal ß-catenin target genes, like *siamois*, *twin* or *chordin*, display similar dorso-anterior truncated phenotypes in *Xenopus* (Bae et al, 2011; Ishibashi et al, 2008; Kuroda et al, 2004). These described functions paired with the observation of the knockdown analysis of this study suggests a similar interconnection between ß-catenin and Brg1 also in *Xenopus*. This is a preferable explanation, but some results claim against it. The first experiment to verify such an interconnection was the secondary axis assay induced by Siamois. Although the secondary axis formation was minimally reduced on average, upon coinjections of BMO1, the DAI-value was not significantly reduced. This indicates that Brg1 is not essential to transmit the downstream dorsalizing activity of wnt target gene *siamois*. However, it does not exclude a genetic interaction between ß-catenin and Brg1 in *Xenopus* or a possible inducing feature of Brg1 on other ß-catenin target genes. In the end, the result of this experiment remains inconclusive. To resolve this question a CoIP or even better a ChIP at ß-catenin target genes should be performed. Noteworthy only *siamois* was analysed in this epistatis experiment, but the secondary axis formation potential is known for many more ß-catenin target genes (Carnac et al, 1996; De Robertis, 2006; Lemaire et al, 1995). A second hint that the role of Brg1 is beyond wnt/ß-catenin signaling suggested the animal cap assay (see Figure 3.14). Although both wnt-target genes, *siamois* and *xnr3*, were less induced by *wnt8* mRNA in the presence of BMO1, the same is also true for the two nodal-signal genes *goosecoid* and *foxa4*. Upon coinjections of Activin mRNA and BMO1 also these two genes showed a reduced gene expression. This suggests a more general role for Brg1 as a transcriptional activator, rather than a specific role in the ß-catenin signaling pathway. Though, the strongest argument, that Brg1 has a role beyond the ß-catenin signaling, is the fact that no enrichment for wnt target genes was detected within the microarray analysis (see Figure 3.19). In total, these results points towards a more general role for Brg1 in gene induction, with no pathway but gene target specificity.

BMO injections into the marginal zone of ventral blastomeres had a much weaker impact on development. About one third of the ventrally injected BMO1 morphants showed a malformed ventro-posterior development. Overall, it represented a mildly dorsalized phenotype, caused by a loss of ventral structures. Again there could be several explanations for that. Firstly, it could be that the outgrowth of the tail is impaired. However, this explanation is rather unlikely because in this late developmental stage Brg1 is restricted to neural structures and the outgrowth of the tail starts around NF27 (Beck & Slack, 2002; Seo et al, 2005). Loss of ventral tissue could also result from increased apoptotic cell death. As discussed above, Brg1 is connected to the cell cycle and a possible mechanism could be that a loss of Brg1 on the ventral side of the embryo causes uncontrolled cell

cycling. However, this would indicate different functions of Brg1 depending on its dorsal or ventral localization, which could be possible but is rather unlikely. As the phenotype looked like a mild dorsalized embryo, a further explanation could be that a loss of Brg1 leads to a reduction of ventral fate signaling. One possible candidate is Bmp4 protein. *Bmp4* is hardly maternally expressed but is quickly upregulated at late blastula, peaking in early gastrula (Hemmati-Brivanlou & Thomsen, 1995). Broadly expressed in the ecto- and mesoderm, *bmp4* expression is restricted during gastrulation to the ventrolateral marginal zone (Hemmati-Brivanlou & Thomsen, 1995). A knockdown study of Bmp4 revealed a mild dorsalization phenotype with major perturbation on ventral fin development (Reversade et al, 2005). This phenotype is morphologically very similar to the one observed in this study. The microarray analysis showed that *bmp4* indeed was reduced upon Brg1 knockdown (see Figure 3.21). Additionally, recently a physical interaction of Brg1 and Smad3 could be detected in several human cell lines. It was shown that the interaction between the two proteins promotes specific TGF-ß target genes (Xi et al, 2008). This study paired with the microarray data of this study suggests that Brg1 also positively affects the transcriptional level on the ventral side of the embryo, causing a loss of ventral factors in targeted morphant embryos.

All together, the data indicates, that Brg1 acts predominantly as a transcriptional coactivator in both dorsal and ventral tissues. Nevertheless, it is quite surprising that a loss of Brg1 on the dorsal side led to a strong reduction of dorso-anterior structures and a loss on the ventral side caused only mild reduction.

4.2.2 Overexpression of wild type Brg1

While the loss-of-function analysis shows the requirements of the gene, gain-of-functions analysis reveals what the gene can do. The ectopic overexpression of wild type Brg1 in one DMZ did not produce a phenotype. Surprisingly, the overexpression of wild type Brg1 in one ventral blastomere caused a truncated secondary body axis. This feature is the hallmark of genes expressed in the dorsal-marginal zone of a developing amphibian embryo. The majority of these genes are under the control of the maternal ß-catenin signaling pathway (De Robertis, 2006). Genes like *siamois* and *chordin* are known to produce full secondary body axes when overexpressed on the ventral side of an embryo (Oelgeschlager et al, 2003). Although the secondary axis produced by Brg1 overexpression contains skeletal muscles, a complete secondary axis, containing head and eye structures, was not generated (Figure 3.5). A possible explanation is an induction of Brg1 towards ß-catenin target genes. But the fact that in ventral cells ß-catenin is predominantly excluded from cell nuclei, makes this argument difficult to hold on (Schneider et al, 1996). Furthermore, Brg1 overexpression only

produced truncated secondary axes. Interestingly, an overexpression of a dominant-negative BMP receptor on the ventral side also results in truncated secondary axis (Suzuki et al, 1994). This leads to the idea that an excess of Brg1 either directly inhibits BMP receptors, represses BMP signals, or activates ventrally expressed BMP inhibitors, like *sizzled* or "BMP and activin membrane-bound inhibitor", *bambi*. Because Brg1 was also shown to be involved in transcriptional repression, a repression of positive regulating BMP signals could be possible (Murphy et al, 1999). In this scenario *bmp4* is again the most likely candidate. As described above, it mediates the development of ventral fate. However, as the morphological phenotype of ventral BMO injections resembles the knockdown of Bmp4, presumably Brg1 acts as an activator on *bmp4* rather as a repressor. A third hypothesis regards an activation of intrinsic BMP inhibitors. Bambi is a TGF-ß-family type I receptor lacking the intracellular kinase domain and therefore acts as a pseudoreceptor resulting in inhibiting BMP signaling (Onichtchouk et al, 1999). Moreover, Bambi is induced by BMP via the conserved BMP-responsive elements and via distinct Smad3 binding repeats and it is coexpressed with *bmp4* in *Xenopus* development (Onichtchouk et al, 1999; Sekiya et al, 2004b). In human colorectal tumor cell lines, an aberrant high expression of Bambi was observed, which is regulated by ß-catenin–TCF4, suggesting that besides BMP and smad signaling also wnt/ß-catenin signaling is involved in the regulation of Bambi (Sekiya et al, 2004a). Additionally, Bambi was slightly reduced upon Brg1 knockdown in the microarray analysis presented in this thesis. This makes Bambi a good candidate to be under a positive control of Brg1, which could be involved in forming a truncated secondary axis.

On the basis of the morphological phenotypes it is hard to define a clear role for Brg1 during development. A molecular marker screening after the various injections would have helped to identify the pathways through which Brg1 is acting. Especially in the gain-of-function experiment a WMISH at blastula or gastrula stage against either dorsalizing-promoting or BMP inhibitory genes would have given a better overview about the Brg1 mechanisms. However, in sum, the most feasible explanation points towards a general positive transcriptional regulation of Brg1 during development. This would explain all three morphological phenotypes generated in loss- and gain-of-function experiments.

4.3 Genome-wide transcriptome analysis of Brg1 morphant embryos

The embryonic lethality and the inconclusive morphological phenotype derived from targeted injections have led to an investigation of a genome-wide transcriptome analysis. The late blastula stage was chosen, because radial BMO1 and BMO2 injected embryos were still viable and the BMO1 morpholino caused already a of reduction in Brg1 protein level. Most importantly, the misregulated

BCNE genes *chordin*, *noggin* and also *cerberus* testified that Brg1 is functioning at this time and thus increasing the likelihood to investigate direct transcriptional effects. Additionally, the transcriptional aspects of axes formation are executed during blastula and gastrula time periods. These facts made a global investigation at this early developmental stage feasible. To underline the result, two morpholinos were individually injected. The different outcome of the two morphant microarray data sets can result from the different translation blocking efficiencies of both morpholinos. If the phenotype has a rather composite genetic underpinning, then interactions among genes, which are more dependent on Brg1 than other targets, will generate multiple intermediate states of DV-patterning in Brg1 morphants, which could lead to an apparently non-overlapping microarray result. This could be tested, by comparing the two morpholinos under comparable Brg1 protein ablation, rather than maximally achievable depletion conditions. Furthermore, many responder genes may show up as a mixture of maternal and zygotic transcripts, thus the real effect is masked by their maternal contributions. Therefore it is still possible that each morpholino generates a specific phenotype due to unknown off target effects. They are, however, not the major cause of the phenotypes, since both BMO1 and BMO2 effects were rescued by coinjections of human wild type Brg1 mRNA (see Figure 3.16).

A very helpful tool to classify such big data sets is the Gene Onthology analysis (GO). The group of responders, which are upregulated upon BMO1 injections, showed an enrichment for terms like "chromatin assembly" (GO:0031497), "cellular component assembly" (GO:0022607) or "macromolecular complex assembly" (GO:0065003). Even though the output of this analysis was rather small, it is obvious that the cell somehow tried to compensate the loss of a chromatin remodeling activity to keep up chromatin integrity. Interestingly, neither brahma nor any other chromatin remodeling ATPase subunit was upregulated upon Brg1 knockdown. This is in accordance with the results Nishant Singhal generated in his PhD thesis. Namely, the malformation of dorso-anterior structures upon Brg1 depletion were not rescued by coinjections of either hBrahma wild type mRNA or xISWI wild type mRNA. This indicates that other ATPase subunits cannot compensate a loss of Brg1 and it underlines the importance of Brg1 protein during early development. Notably, also none of the BAF proteins were upregulated upon loss of Brg1.

In contrast, the genes, which are downregulated upon BMO1 injections, were quite various. More than 50 GO-terms were enriched in the responders, whereof the majority is related to developmental processes. The most prominent terms are "nervous system development" (GO:0007399), "system development" (GO:0048731) and "pattern specification process" (GO:0007389). Interestingly, no distinct developmental signal pathway was found. This indicates that Brg1, as presumed, is not cooperating with one particular pathway, but rather has a role within

various developmental pathways. A loss of Brg1 affects many regulatory genes, whose misregulation lead to a dramatic malformation of the embryo and ultimately to its death.

4.4 Brg1 and its role in axes determination

4.4.1 Antero-posterior axis

The targeted Brg1 morphant embryos clearly were shorter along the antero-posterior body axis in comparison to control morphant embryos (Figure 3.4). In order to have a better estimation about the perturbed fragmentation, three AP-axis markers were examined in unilateral BMO1 injected embryos. The time point after neurulation was chosen as at this stage the AP-axis is determined. Surprisingly, a shift of one AP-segment was not observed.

The anterior marker *pax2* was reduced in a dose-dependent manner after BMO1 injections. If this reduction is direct or indirect is not known. Recently, it has been suggested that Pax2 interacts with Pax5 to induce the midbrain marker *engrailed2*. Therefore it is considered essential for brain formation in *Xenopus* (Koenig et al, 2010). In zebrafish a feedback mechanism between Eng2 and Pax2 was characterized in which the *eng2* gene is activated by Pax2, while Eng2 protein binds then to the *pax2* promoter region to maintain *pax2* gene expression (Picker et al, 2002). In the same year another study in *Xenopus* embryos revealed that orthodentricle homoebox 2, Otx2 directly activates *pax2* expression (Tour et al, 2002). From these studies it can be suggested that *pax2* is under the control of *otx2*, a gene which is already expressed in the organizer territory during gastrulation (Fletcher & Harland, 2008). A closer look at the microarray data sets revealed that *otx2* was downregulated upon Brg1 knockdown in both morpholino injections up to 1.4 fold change, albeit this could not be significantly verified in the qRT-PCR analysis afterwards. In contrast, *pax2* is not yet expressed in late blastula stages, as the microarray data indicate. This result paired with the WMISH gastrula analysis, in which the territory of *otx2* was diminished, makes it very likely that a loss of Brg1 results in reduction of *otx2* and consequently *pax2* is not fully induced.

Egr2, the second analyzed marker, is induced by a combination of Noggin protein and Fgf2 (fibroblast growth factor 2, formerly known as bFGF) at the start of gastrulation. Interestingly, Fgf2 induction alone induces posterior marker *hoxb9* in early gastrula embryos and Fgf2 alone is sufficient to induce *krox20* in late gastrulation embryos (Lamb & Harland, 1995). In essence, the Fgf2 signal helps to specify gene domains along the AP axis, but other factors, like Noggin, are needed at the right time to refine the AP-patterning. Unfortunately the Affymetrix microarray does not contain a *noggin* probe set, but in the qRT-PCR analysis *noggin* was reduced in both BMO1 and BMO2

morphants. Furthermore, it was shown that *chordin* gene expression regulates *egr2* expression in *Xenopus* neural explants. Upon Chordin knockdown, the neural explants did not express *egr2* anymore (Kuroda et al, 2004). This is not surprising, as *noggin* and *chordin* are coexpressed and both function as BMP inhibitors (Bachiller et al, 2000; Kuroda et al, 2004). A study in mice suggested that Egr2 not only induces cell segregation but also cell specification, as rhombomere r3 and r5 acquire the fates of neighboring rhombomeres in Egr2 depleted embryos (Voiculescu et al, 2001). Why rhombomere 5 was more prone to be reduced in comparison to rhombomere 3 upon loss of Brg1 in *Xenopus* is absolutely unclear. One suggestion is that during segmentation, r3 receives additional factors which stabilize the expression, while these are missing in rhombomere 5. In total, the results indicate that *egr2* is reduced in Brg1 morphant embryos by indirect effects, probably through reduced *noggin* gene expression.

As posterior marker *hoxb9* was analyzed. All Hox genes, which are expressed at this stage, are coexpressed in a similar pattern as the pan-mesodermal marker *xbra*. Besides Fgf2, also FGF-target gene Xbra is capable to induce *hoxb9* expression in *Xenopus* animal cap assays and *hoxb9* is reduced in Xbra downregulated embryos (Lamb & Harland, 1995; Wacker et al, 2004). Furthermore, Bmp4 obviously also has a regulatory effect on the Hox gene cluster, as a constitutive Bmp4 receptor leads to an expansion of posterior Hox gene expression, like *hoxb9* (Wacker et al, 2004). Given that Brg1 morphant embryos showed morphologically a ventralized phenotype, it was really surprising to see also *hoxb9* being reduced. Nevertheless, the positive interconnection between Brg1 and Bmp4, led to reduced *bmp4* expression in morphant embryos. This could explain why *hoxb9* expression was diminished, in particular because *fgf2* gene expression was not changed upon Brg1 knockdown.

Taken together, the outcome of this experiment is surprising, because an overall reduction of the all three analyzed tissues was observed. Conversely, in ventral targeted BMO injections a reduction of ventral structures was observed as well. This result underlines again a positive role of Brg1 in gene expression and that a knockdown of Brg1 results in reduced gene expression, which leads to a composite molecular phenotype.

4.4.2 Dorso-ventral patterning

The establishment of dorso-ventral patterning can be divided into 2 phases. The first phase takes place already in the blastula, in which the BCNE and the Nieuwkoop center are established. The second phase is the balancing between organizer and non-organizer signaling centers, a process

called dorsalization (Figure 3.8) (Dale & Slack, 1987; Forman & Slack, 1980). To gain an overview of this process in Brg1 morphants, both developmental stages were investigated by WMISH analyses.

The BCNE and Nieuwkoop center both are formed after the transcriptional burst at the MBT on the dorsal side of the embryo. Here, the expression of BCNE genes *chordin*, *noggin* and *xnr3* were investigated plus the more vegetal expressed *siamois*. All four genes are under the control of maternal wnt/ß-catenin signaling and the BCNE genes are characterized as BMP-inhibitors and required for neural differentiation (Kuroda et al, 2004; Wessely et al, 2001). Among the BCNE genes, *chordin* gave the strongest response to Brg1 knockdown, in WMISH analysis and in both microarray datasets. As mentioned above, also *noggin* gene expression was reduced upon Brg1 knockdown. In contrast to its WMISH pattern, *xnr3* was not reduced in the microarray analysis of BMO1 and BMO2, but rather showed a slight upregulation (see Figure 3.21 and Figure 3.23). However, one has to keep in mind that *xnr3* was the less responsive BCNE marker in the WMISH analyses and it was performed in *X. laevis*, whereas the microarray data was performed in *X. tropicalis*. A study, which investigated the differences in the gene profiles between these two related species, came to the conclusion that differences are rare, but if there are differences, they most likely appear during very early development (Yanai et al, 2011). The fact that *siamois* gene expression was not changed upon BMO1 and BMO2 injections is in perfect accordance to the earlier discussed results (see Figure 3.9 and Figure 3.10).

Another interesting observation was made in the targeted 8 cell injections (see Figure 3.15). DA-injections with BMO1 resulted in a reduction of *chordin* and *noggin* gene expression, which was expected. Surprisingly, also the Brg1 knockdown in DV-cells reduced the gene expression of these two genes. So far the dorsal A and B-blastomeres in *Xenopus* were thought to solely give rise to the BCNE tissue (Bauer et al, 1994; Kuroda et al, 2004). But with this analysis, it is shown that also C-blastomeres contribute to the formation of the BCNE and its gene expression, in a non-cell autonomously manner. This is at least true for late blastula stages embryo, in which the epiboly movements have shifted the BCNE more vegetally (Bauer et al, 1994).

The investigation of the Nieuwkoop center was represented by the genes *cerberus* and *hhex*. The BMO1 DA-injections did not interfere with gene expression of both genes, as expected because the expression domain and the injections did not overlap, visualized by the lacZ stain (Figure 3.15). This suggests a cell-autonomy behavior of the two genes. In the DV-injections, however, both genes are severely reduced upon Brg1 knockdown. This reduction was partially validated by the microarray analysis and qRT-PCR data. Under BMO1 and BMO2 conditions, *hhex* gene expression was reduced in the microarray analysis. This is different for *cerberus*. In the microarray and the qRT-PCR, *cerberus* gene expression was hardly changed upon BMO1 injections. However, its expression was significantly

reduced upon Brg1 knockdown generated by BMO2. But since *cerberus* expression has several different induction signals, it could well be that for *cerberus*, like in the case of *xnr3*, the differences between the two morpholinos and the two species stand out (Heasman, 2006; Yamamoto et al, 2003).

In summary, these analyses emphasize that Brg1 is needed as early as blastula stage to ensure proper dorso-ventral patterning. This is in particular visible in the BCNE and the Nieuwkoop center. Since the organizer develops from these two signaling centers on the dorsal side of the embryo, this perturbed expression is carried on to later stages.

In gastrula embryos, the gene expression domains of *otx2* and *vent2* are an exemplary couple, which represents the distribution of dorsal and ventral territories. Upon CoMO injections a clear organizer territory was seen in both expression patterns. *Otx2* was expressed in a broad area of the involuting mesoderm, the organizer, whereas *vent2* was expressed around the blastoporus but excluded from the organizer region (Figure 3.8). Upon BMO1 injections the organizer was diminished, shown by a reduced *otx2* expression and a much broader *vent2* gene expression. In essence, it can be stated: the organizer is weakened and the counteracting ventral factors expand into the organizer region. This shows that Brg1 morphant embryos were molecularly ventralized from this stage on. This behavior is seen in other tested genes as well. *Xnr3* and *foxa4* for example are both expressed at the dorsal lip and in the involuted mesodermal organizer region and were reduced upon BMO1 injections. In contrast, ventral gene *vent1*, coexpressed with *vent2*, was expanded in BMO1 injected embryos. This expansion fits perfectly to the morphological phenotype, but both genes are regulated by BMP-signaling and their expression is reduced in the microarray analysis upon Brg1 knockdown (Gawantka et al, 1995; Hata et al, 2000; Robertis & Kuroda, 2004). The only possible explanation for this discrepancy can be found within the different techniques. The microarray and qRT-PCR display the absolute quantification and the WMISH displays the distribution of the transcripts and quantitative information has to be taken with caution. Additionally, one has to keep in mind that the developmental stage, investigated in the two analyses, are different. Two possibilities arise from this data. Either, *bmp4* and the *vent* genes are not properly induced in late blastula and compensatory effects rescue the reduction until midgastrulation stage, or the absolute gene expression is still lowered in gastrula embryos, but the pattern spans a broader area compared to control embryos.

Vent1/vent2 and *goosecoid* homeobox genes are expressed in presumptive non-organizer and organizer territories, respectively, and have been shown to mutually repress each (Sander et al, 2007). The *goosecoid* promoter region is well described and it contains a wnt-signaling binding site, which is mediated through Twin and a nodal binding site, which in turn is mediated through Mixer (Watabe et al, 1995). Even though *goosecoid* is expressed in the organizer and is partially under the

control of the wnt signaling it seems not to be a target of Brg1, because the expression was not altered in gastrula morphant embryos (see Figure 3.8). Another explanation could be that compensatory effects between the two inducing pathways ensure a stable *goosecoid* expression in Brg1 morphants. In order to clarify this question more experiments have to be performed.

A similar phenomena is seen with *chordin*, which is expressed at the dorsal lip in gastrula embryos. In the case of a ventralized embryo, Chordin as a BMP-inhibitor should be reduced. But in BMO1 injected morphant gastrula embryos *chordin* expression was not altered. This is even more surprising since its expression was strongly reduced at blastula stages. However, similar to *goosecoid*, also *chordin* is induced by wnt/ß-catenin pathway and nodal signaling. During blastula stages *chordin* is expressed in the BCNE through maternal ß-catenin signaling but at gastrulation the induction and maintenance is mediated by nodal signaling, probably through Xnr1 (Reid et al, 2012; Wessely et al, 2001). In the microarray analysis of BMO1 injected embryos *twin* is upregulated, whereas *xnr1* is not changed. Presumably, some inducing signals were still present or even slightly overrepresented and this ensured a normal expression pattern of *chordin* at gastrula stage.

The panmesodermal marker *xbra* was not changed in WMISH analysis upon BMO1 injections, but was slightly reduced in the microarray analysis. Probably this has to do with Xbra's autocatalytic loop and its various regulatory factors. The primary induction may be lowered by a loss of Brg1 but the feedback loop and other inductive signals may compensate for a possible reduction (Loose & Patient, 2004). Two other genes that were investigated in gastrula morphant embryos are muscle-specific *myoD* and *myf5*. Both genes wre slightly reduced in gene expression, but in a very high penetrance, suggesting some compensatory effects, which ensured muscle formation in Brg1 morphant embryos.

4.5   Brg1 and its role in neurogenesis

Besides the function of Brg1 in axes patterning, the results obtained in this thesis and the so far published data on Brg1 also suggest a special impact of Brg1 during neurogenesis (Seo et al, 2005).

One of the strongest responder upon Brg1 knockdown at blastula was the BMP-inhibitor *chordin*. Furthermore, the early wave of *chordin* and *cerberus* in the blastula stage was shown to be important for later brain development (Kuroda et al, 2004). Two experiments underline first of all its early requirement for *chordin* gene expression and secondly the necessity of Brg1 to induce *chordin* gene expression: The morphological rescue with exogenous Chordin mRNA (Figure 3.11) and the transplantations assay (Figure 3.13). The morphological rescue with exogenous Chordin mRNA

implicates two findings. First, that Chordin is downstream of Brg1 and second that indeed the early *chordin* wave is important for later brain development. In the transplantation assay, a Brg1 deficient BCNE was transplanted into a wild type background and the embryos developed hardly eye tissue and had malformed brain structures. This proves in addition the requirement of Brg1 in the very early steps of specification and its role in brain development. Furthermore, this indicates that a wild type environment could not alleviate the differentiation capacity of the Brg1 morphant BCNE, which argues for a requirement of the BCNE in a cell-autonomous manner. Furthermore, a delay in neural tube closure was detected in the morphant transplants, even though it was not quantified.

Another aspect of Brg1 function in neurogenesis was revealed from the microarray data sets. Many genes important for "nervous system development" were significantly downregulated upon BMO1 injections. One of the severely reduced genes is *meis3*. *Meis homeobox 3* was first identified as a hindbrain marker and regulator downstream of the *zic* genes (Dibner et al, 2001; Gutkovich et al, 2010) In knockdown studies it was shown that *meis3* is important for the induction of several posterior *Hox* genes, like *hoxD1* during gastrulation. Additionally, in neural stages a loss of *meis3* causes a loss of primary neuron markers and neural crest cells (Gutkovich et al, 2010; In der Rieden et al, 2011). From the literature so far, an earlier role than during gastrulation was not shown. Nevertheless, a reduction already in late blastula stages could lead to a delay of target genes expression and successively lead to malformed brain structures or a defective Hox code, especially in the posterior part.

Another interesting candidate within the GO-term "nervous system development" was the gene *foxd5*. During recent years, a key regulatory function for *foxD5* in the neural differentiation network was suggested (Neilson et al, 2012; Yan et al, 2009). Furthermore is it expressed at blastula stages on the dorsal side of the embryo (Fetka et al, 2000). The regulatory network of *foxD5* is very complex and modulated depending on the developmental stage. This suggests that also other factors contribute to the network (Yan et al, 2009). At early gastrula stages loss of *foxD5* reduces the level of *zic1*, *zic3*, *sox2*. Other targets like *geminin* and *zic2* are not reduced in their expression, possibly because they are activated by maternal Foxd5 protein stores (Yan et al, 2009). The microarray data matched well with the proposed regulatory network. Whereas *geminin* and *zic2* were not changed upon loss of Brg1, the downstream neural differentiation genes like *zic1*, *zic3* and *sox2* were reduced. Presumably, this prevention of initial induction led later on to a composite effect and to the failure of cell differentiation. Even though it is known that the *zic* genes are expressed at MBT, very little is known about their function in these early stages. One major hint into this direction regards the balance between epidermal specification marker and neuroectodermal marker already at blastula stage. Whereas *zic1* and *zic3* were downregulated in Brg1 morphant embryos, their epidermal

antagonist *foxi1* was upregulated. This interdependence suggests that the *zic* genes help to prepattern the embryo already at blastula stage.

The Brg1 morphant phenotype described in the literature so far mainly affects an expansion of *sox2* domain in mid-neurula stages. Sox2 maintain the cells in a neuronal precursor state and inhibits further differentiation. Since different stages were investigated in this analysis, due to the higher degree of Brg1 depletion and the resulting embryonic lethality, it is difficult to compare or draw any conclusion from their finding. Based on the results obtained in this thesis, other explanations like a reduction of BCNE genes, are more likely to cause the impaired dorso-anterior development. In total, it seems that the neurogenic phenotype upon Brg1 knockdown consists rather of multiple additive effects.

4.6   Brg1 and its role during zygotic genome activation

The detailed analysis presented here indicates that Brg1 is required as early as the blastula stage. Upon its loss an imbalance in DV- and AP-patterning is generated. This led in mild phenotypes to a ventralized, antero-dorsal truncated embryo up to embryonic lethality in strongly affected specimen. In search for a common denominator that helps to understand the complex consequences of Brg1 depletion, its impact on the newly zygotic transcripts was examined. The newly transcribed gene pool was chosen, because the genome-wide analysis was performed in late blastula stage embryos, approximately only 3 hours after MBT's burst of transcription. In addition, the microarray data sets revealed a high impact of Brg1 on developmental required genes, of which the majority is highly upregulated at the MBT. In order to reveal the zygotic transcripts a further genome-wide analysis in wild type embryos was investigated. One study is published so far, in which the transcriptome preMBT and postMBT was investigated. However, this study focuses on the differences between X. *laevis* and *X. tropicalis* (Yanai et al, 2011). The analysis in this thesis is the first study, which puts a special focus on comparing the transcriptome of preMBT embryos with the transcriptome of postMBT embryos. With this data set it is possible to reveal which maternal genes will be degraded after MBT, which genes are upregulated and which genes do not change in their expression level.

The data of the three different RNA pools paired with the information gained from the two morphant microarray analysis suggests a common denominator for the Brg1 requirement in development: Genes, which are highly upregulated at MBT are sensitive to a loss of Brg1 in a dose-dependent manner. This indicates that the burst of transcription happening at the MBT requires Brg1 protein function as transcriptional activator (see Figure 4.1). Since several genes

important for embryonic development and pattern specification were among these highly upregulated genes, also the phenotypes that arose upon loss of Brg1 can be explained by this finding.
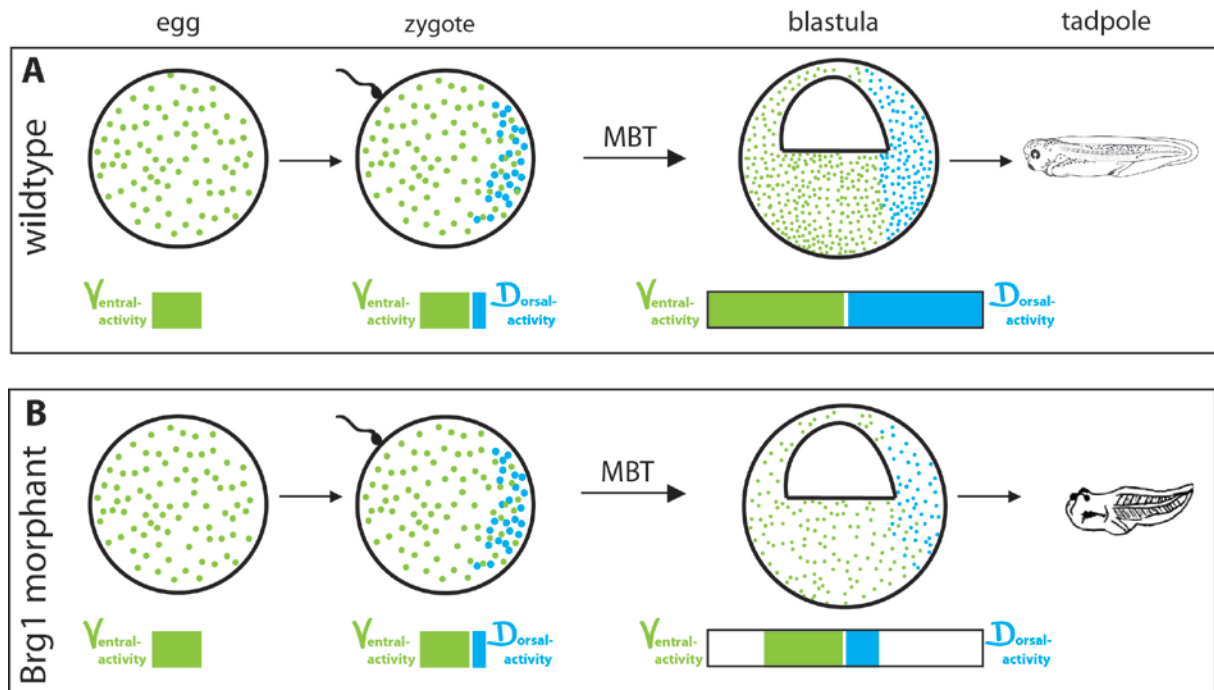
Figure 4.1: The MBT burst of transcription is diminished in Brg1 morphants. In **A** the wild type situation is shown. The matured *Xenopus* egg contains only active ventral promoting activity (depicted in green). With the sperm entry the cortex of the zygote is shifted and maternal dorsal promoting activity is activated on the prospective dorsal side (depicted in blue). At blastula stage the zygotic genome is activated and a transcriptional burst of ventralizing and dorsalizing factors is induced, so that the two counteracting entities shape the embryo. A normal tadpole develops. In **B** the Brg1 morphant situation is shown. The first steps are not affected, as the morpholino does not target maternal Brg1 protein. At blastula, the zygotic genome activation occurs but upon loss of zygotic Brg1 protein the transcriptional burst is impaired. This leads to lower dorsalizing but also to lower ventralizing activity. In the end this results in an imbalance between dorsal and ventral promoting activities and the DV pattern is shifted towards ventral fate. The embryo will develop a ventralized phenotype. MBT, midblastula transition

Presumably, the embryonic lethality is a result of an absence of inducing signals. During gastrulation, the germ layers and body axes are specified. If signals that are important for the specification process are lowered or absent, the embryo is not able to proceed in development. This fact also points out that not only dorsal-specific genes were reduced upon a loss of Brg1 but also ventral fate factors. If only dorsalizing factors would be missing the embryo would be strongly ventralized, like it is the case of UV-treated embryos (Kao & Elinson, 1988). But among the highly upregulated genes also ventralizing genes are identified, like *Bmp4*, which was upregulated 8 fold after MBT. As mentioned before, Bmp4 is an essential ventralizing factor and was reduced in BMO injected embryos. Apparently, the combined downregulation of dorsal and ventral specification factors led to embryonic death, probably by a developmental arrest during the gastrulation process. In the case of

targeted injections or milder knockdown conditions, an overall perturbation is not achieved and the morphant embryos succeeded to go on with development, although at the expense of teratogenic malformations. In those embryos, the misbalance between ventral to dorsal fate is shifted towards the ventral fate, i.e. the default state of the embryo prior to the MBT.

The secondary axes arising from ventral injections of Brg1 mRNA are more difficult to explain. As Brg1 acts independently from particular pathways but as a transcriptional activator, a combinatory effect is the most likely reason for the second body axis induction. As discussed above, also on the ventral side a transcriptional burst drives gene expression after MBT. Included in this burst is for example *sizzled*, a BMP-inhibitor, which was upregulated 27 fold. An overexpression of Brg1 could lead to an even stronger upregulation and thereby leading to a BMP-inhibitory effect which causes the secondary axis. However, *sizzled* is mildly upregulated upon Brg1 knockdown, which indicates, that sizzled is no direct target of Brg1. In the end two possibilities arise. Either, b*mp4* is upregulated upon Brg1 overexpression and thereby indirectly intrinsic BMP-inhibitors will be upregulated or Brg1 induces ectopically dorsalizing genes on the prospective ventral side during the burst of MBT.

4.7 Possible Brg1 mechanism at the burst of transcription

With the analysis of this thesis a new role for the chromatin remodeling ATPase Brg1 during early *Xenopus* development was revealed. The data presented here suggest a positive role of Brg1 on highly upregulated gene expression at MBT, which implies an additional selectivity of Brg1 to these genes. Nishant Singhal, a former PhD student who started the characterization of Brg1 during *Xenopus* development also investigated the capability of other remodeling ATPase to compensate for a loss of Brg1. He tested xISWI and hBrahma mRNAs, which both were not able to rescue the morphological phenotype generated by Brg1 knockdown (Singhal, 2005). This raised the question, what determines the Brg1 specificity to its target genes. One possibility could be a histone mark, which recruits Brg1 containing SWI/SNF complexes. A recent paper showed that the promoter of genes, which burst at the MBT are decorated with H3K16ac at preMBT stage (Blythe et al, 2010). This could be a recruiting signal for Brg1, since Brg1 contains a bromo-domain, which binds to acetylated histone tails. But for which purpose is Brg1 needed at these genes? In order to gain further information about the impact of the catalytic activity of Brg1, a dominant-negative protein can be used in loss-of-function studies. To investigate this, Nishant Singhal also performed this kind of loss-of-function approach. He mutated the catalytic domain of the ATPase and observed a comparable morphological phenotype as seen in morpholino injected embryos. From this data it can

be concluded that the enzymatic function of Brg1 is required for *Xenopus* development. (Singhal, 2005). This indicates that not only the presence of Brg1 is needed at MBT, but in particular the catalytic function is required for its role during the burst of transcription at MBT. One major function of chromatin remodeling complexes is the sliding of nucleosomes along the DNA. Furthermore, a hallmark of transcription is the nucleosome-free region at promoters of transcribed genes (Iyer, 2012). As the research of nucleosome sliding in the picture of development is poorly investigated, this fact leaves room for speculation. A mechanism by which Brg1 is recruited to promoters to open up or keep the TSS open, is likely. The mechanism of the upregulation of several hundred genes in a synchronous manner was investigated in *Drosophila* over the last years. Recently, several papers were published, which deal with genome-wide data at the onset of zygotic genome transcription. In the course of this, a common motif in the promoter region of the newly transcribed genes was revealed and shortly after, the transcription factor Zelda, was found (Harrison et al, 2011; Liang et al, 2008). Additionally, by genome-wide data in *Drosophila* it was shown that the synchrony of gene transcription in various tissue is accomplished by RNA polymerase II pausing (Lagha et al, 2013). Another recent study revealed that Brg1 in human cell lines is needed to overcome a nucleosomal barrier during RNA polymerase II elongation (Subtil-Rodriguez & Reyes, 2010). A hypothesis, which combines these studies and the findings presented here, could be: Genes, which undergo a burst of transcription, are marked preMBT with the acetlyation of H3K16. Maternal Brg1 protein, which is not targeted by the morpholino injections binds to it and recruits additional transcription factors. By this, RNA polymerase II is recruited and starts with a minimal transcription, causing a poising of these genes. With the onset of the zygotic transcription, maternal Brg1 or a recruited factor helps to release the paused RNA polymerase II in order to ensure proper transcription. To assure such a high transcriptional upregulation, which is needed at MBT, the promoter has to be kept open, additional RNA polymerase II has to be recruited and the genes have to be rapidly transcribed. Presumably, these steps are under the control of zygotic Brg1 and are impaired upon BMO injections in *Xenopus*.

4.8   Conclusions and future directions

It is shown, that *Xenopus* Brg1 protein is needed much earlier in development than described before, namely as early as the blastula stage. Furthermore, it was revealed that Brg1 has a gene specific role as transcriptional activator during the onset of the zygotic genome transcription. A loss of zygotic Brg1 leads to a reduced transcriptional burst at the MBT, which leads to the reduction of patterning signals resulting in embryonic lethality during gastrulation. Upon milder knockdown conditions or in targeted injections, a misbalance between dorsal and ventral signals impairs development, since the majority of the high upregulated genes at MBT are dorsalizing factors.

Nevertheless, further experiments are necessary to describe Brg1 function during early vertebrate development. It would be interesting to know, which genes are directly regulated by Brg1 and which genes are indirectly affected by Brg1. Therefore, an experiment with Cycloheximide would be appropriated. It inhibits the protein translation and in combination with Brg1 overexpression only the direct target genes are expressed. The experiment goes hand in hand with the examination of the truncated secondary axes. Is this mediated by an upregulation of dorsalizing genes or an upregulation of intrinsic BMP-inhibitors? To further prove gene specificity, a ChIP-qPCR could be performed. Especially, as ChIP-Seq data of a chromatin remodeling factor is rather difficult to obtain as it has so many functions which are carried out over large fractions of the genome.

Experiments, which reveal the mechanism behind Brg1 function at MBT would be very important. First of all, deletion mutants of Brg1 could show, if Brg1 is targeted via the H3K16ac histone mark to its target genes. ChIP-Seq data of paused RNA polymerase II at the MBT could show if the highly upregulated genes are really poised and whether Brg1 is colocalized. Furthermore, an investigation of other SWI/SNF complex proteins is necessary to reveal if Brg1 needs the presence of other complex components in order to function properly. In the same line it would be interesting, if at MBT a special SWI/SNF complex is present, like it was shown for ES-cells (Ho et al, 2009).

Another profound data set, which was generated within this thesis, is the genome-wide transcriptome analysis, comparing pre and postMBT embryos. These data sets reveal insights into the tremendous changes on the transcriptional level and underline the necessity of a spatial and tight regulation to ensure embryonic patterning and development in *Xenopus*.

Abbreviations

AP-axis	antero-posterior axis
AP-buffer	alkaline phosphatase buffer
Baf	brahma associated factors
Bambi	BMP and Activin Membrane-Bound Inhibitor
BCIP	5-Bromo-4-chlor-3-indoxylphosphat
BCNE	blastula Chordin- and Noggin-expression center
BMO	Brg1-morpholino
BMP	bone morphogenic protein
Brg1	brahma related gene 1
Brm	brahma
bzw.	beziehungsweise
cDNA	complementary DNA
CHD	chromodomain helicase DNA-binding
ChIP	chromatin immunoprecipitation
ChIP-Seq	ChIP-DNA sequencing
CNS	central nervous system
CoIP	Co-immunoprecipitation
CoMO	control morpholino
DA	dorso-animal
DAI	Dorsal-Anterior-Index
dig-labeled	digoxigenin-labeled
DNA	deoxyribonucleic acid
DMZ	dorsal marginal zone
DV	dorso-vegetal
e.g.	exempli gratia
egr2	early growth response 2
esBAF	embryonic stem cell BAF complex
ES cells	Embryonic stem cells
ESI	eye-size-index
EtOH	ethanol
FADD	Fas-Associated protein with Death Domain
foxa4	forkhead box A4
gapdh	glyceraldehyde-3-phosphate dehydrogenase
gs17	gastrula specific 17
gsc	goosecoid
GO	Gene onthology
h	hour
hCG	human chorionic gonadotropin
HDAC	histone deacytelase
hhex	hematopoietically expressed homeobox
hoxb9	homeobox B9
ICC	immunocytochemistry
i.e.	id est

ISWI	Imitation SWI
lfdr	local false discovery rate
MBS	Modified Barth Solution
MBT	Midblastula transition
MEMFA	MEM Formaldehyde
MeOH	methanol
min	minute
mRNA	messengerRNA
nBAF	neuron-specific BAF-complex
NBT	Nitro Blue Tetrazolium
NF	Nieuwkoop and Faber stage
NuRD	Nucleosome Remodeling Deacetlyase
odc	ornithine decarboxylase
o/n	over night
otx2	orthodenticle homeobox 2
pax2	paired box 2
PBS	Phosphate Buffered Saline
PMEF	primary mouse embryonic fibroblast
Pol II	Polymerase II
PRMT	protein arginine methyltransferase
PTM	posttranslational modification
RNA	ribonucleic acid
rpm	revolutions per minute
RT	room temperatur
SSC	Saline-sodium citrate
SWI/SNF	SWItch/Sucrose NonFermentable
TGF-ß	transforming growth factor beta
TSS	transcriptional startside
UI	uninjected
UTR	untranslated region
UV	ultra-violett
VMZ	ventral marginal zone
WMISH	whole mount *in situ* hybridization
w/o	without
WT	wild type
xnr	*xenopus* nodal-related
ZGA	zygotic genome activation

References

Agius E, Oelgeschlager M, Wessely O, Kemp C, De Robertis EM (2000) Endodermal Nodal-related signals and mesoderm induction in Xenopus. *Development* **127:** 1173-1183

Akkers RC, van Heeringen SJ, Jacobi UG, Janssen-Megens EM, Francoijs KJ, Stunnenberg HG, Veenstra GJ (2009) A hierarchy of H3K4me3 and H3K27me3 acquisition in spatial gene regulation in Xenopus embryos. *Developmental cell* **17:** 425-434

Allis CD, Jenuwein T, Reinberg D (2007) *Epigenetics*, Cold Spring Harbor, N.Y.: Cold Spring Harbor Laboratory Press.

Azuara V, Perry P, Sauer S, Spivakov M, Jorgensen HF, John RM, Gouti M, Casanova M, Warnes G, Merkenschlager M, Fisher AG (2006) Chromatin signatures of pluripotent cell lines. *Nature cell biology* **8:** 532-538

Bachiller D, Klingensmith J, Kemp C, Belo JA, Anderson RM, May SR, McMahon JA, McMahon AP, Harland RM, Rossant J, De Robertis EM (2000) The organizer factors Chordin and Noggin are required for mouse forebrain development. *Nature* **403:** 658-661

Bae S, Reid CD, Kessler DS (2011) Siamois and Twin are redundant and essential in formation of the Spemann organizer. *Dev Biol* **352:** 367-381

Bajpai R, Chen DA, Rada-Iglesias A, Zhang J, Xiong Y, Helms J, Chang CP, Zhao Y, Swigut T, Wysocka J (2010) CHD7 cooperates with PBAF to control multipotent neural crest formation. *Nature* **463:** 958-962

Barker N, Hurlstone A, Musisi H, Miles A, Bienz M, Clevers H (2001) The chromatin remodelling factor Brg-1 interacts with beta-catenin to promote target gene activation. *The EMBO journal* **20:** 4935-4943

Baroux C, Autran D, Gillmor CS, Grimanelli D, Grossniklaus U (2008) The maternal to zygotic transition in animals and plants. *Cold Spring Harbor symposia on quantitative biology* **73:** 89-100

Bauer DV, Huang S, Moody SA (1994) Cleavage stage origin of spemanns organizer: analysis of the movements of blastomere clones before and during gastrulation in Xenopus. *Development* **120:** 1179-1189

Bayramov AV, Eroshkin FM, Martynova NY, Ermakova GV, Solovieva EA, Zaraisky AG (2011) Novel functions of Noggin proteins: inhibition of Activin/Nodal and Wnt signaling. *Development* **138:** 5345-5356

Beck CW, Slack JM (2002) Notch is required for outgrowth of the Xenopus tail bud. *The International journal of developmental biology* **46:** 255-258

Becker PB, Horz W (2002) ATP-dependent nucleosome remodeling. *Annual review of biochemistry* **71:** 247-273

Bedford MT, Clarke SG (2009) Protein arginine methylation in mammals: who, what, and why. *Molecular cell* **33:** 1-13

Bhaumik SR, Smith E, Shilatifard A (2007) Covalent modifications of histones during development and disease pathogenesis. *Nature structural & molecular biology* **14:** 1008-1016

Blythe SA, Cha SW, Tadjuidje E, Heasman J, Klein PS (2010) beta-Catenin primes organizer gene expression by recruiting a histone H3 arginine 8 methyltransferase, Prmt2. *Developmental cell* **19:** 220-231

Bogdanovic O, Long SW, van Heeringen SJ, Brinkman AB, Gomez-Skarmeta JL, Stunnenberg HG, Jones PL, Veenstra GJ (2011) Temporal uncoupling of the DNA methylome and transcriptional repression during embryogenesis. *Genome research* **21:** 1313-1327

Bogdanovic O, van Heeringen SJ, Veenstra GJ (2012) The epigenome in early vertebrate development. *Genesis* **50:** 192-206

Bouwmeester T, Kim S, Sasai Y, Lu B, De Robertis EM (1996) Cerberus is a head-inducing secreted factor expressed in the anterior endoderm of Spemann's organizer. *Nature* **382:** 595-601

Brizuela BJ, Elfring L, Ballard J, Tamkun JW, Kennison JA (1994) Genetic analysis of the brahma gene of Drosophila melanogaster and polytene chromosome subdivisions 72AB. *Genetics* **137:** 803-813

Bultman S, Gebuhr T, Yee D, La Mantia C, Nicholson J, Gilliam A, Randazzo F, Metzger D, Chambon P, Crabtree G, Magnuson T (2000) A Brg1 null mutation in the mouse reveals functional differences among mammalian SWI/SNF complexes. *Molecular cell* **6:** 1287-1295

Bultman SJ, Gebuhr TC, Pan H, Svoboda P, Schultz RM, Magnuson T (2006) Maternal BRG1 regulates zygotic genome activation in the mouse. *Genes Dev* **20:** 1744-1754

Cao R, Zhang Y (2004) The functions of E(Z)/EZH2-mediated methylation of lysine 27 in histone H3. *Current opinion in genetics & development* **14:** 155-164

Carnac G, Kodjabachian L, Gurdon JB, Lemaire P (1996) The homeobox gene Siamois is a target of the Wnt dorsalisation pathway and triggers organiser activity in the absence of mesoderm. *Development* **122:** 3055-3065

Chen L, Widom J (2005) Mechanism of transcriptional silencing in yeast. *Cell* **120:** 37-48

Collart C, Allen GE, Bradshaw CR, Smith JC, Zegerman P (2013) Titration of four replication factors is essential for the Xenopus laevis midblastula transition. *Science* **341:** 893-896

Dale L, Slack JM (1987) Regional specification within the mesoderm of early embryos of Xenopus laevis. *Development* **100:** 279-295

Dambacher S, Hahn M, Schotta G (2013) The compact view on heterochromatin. *Cell cycle* **12:** 2925-2926

de la Serna IL, Ohkawa Y, Imbalzano AN (2006) Chromatin remodelling in mammalian differentiation: lessons from ATP-dependent remodellers. *Nature reviews Genetics* **7:** 461-473

De Renzis S, Elemento O, Tavazoie S, Wieschaus EF (2007) Unmasking activation of the zygotic genome using chromosomal deletions in the Drosophila embryo. *PLoS biology* **5:** e117

De Robertis EM (2006) Spemann's organizer and self-regulation in amphibian embryos. *Nature reviews Molecular cell biology* **7:** 296-302

De Robertis EM, Larrain J, Oelgeschlager M, Wessely O (2000) The establishment of Spemann's organizer and patterning of the vertebrate embryo. *Nature reviews Genetics* **1:** 171-181

Detivaud L, Pascreau G, Karaiskou A, Osborne HB, Kubiak JZ (2003) Regulation of EDEN-dependent deadenylation of Aurora A/Eg2-derived mRNA via phosphorylation and dephosphorylation in Xenopus laevis egg extracts. *Journal of cell science* **116:** 2697-2705

Dibner C, Elias S, Frank D (2001) XMeis3 protein activity is required for proper hindbrain patterning in Xenopus laevis embryos. *Development* **128:** 3415-3426

Durston AJ, Jansen HJ, Wacker SA (2010) Review: Time-space translation regulates trunk axial patterning in the early vertebrate embryo. *Genomics* **95:** 250-255

Fetka I, Doederlein G, Bouwmeester T (2000) Neuroectodermal specification and regionalization of the Spemann organizer in Xenopus. *Mechanisms of development* **93:** 49-58

Filion GJ, van Bemmel JG, Braunschweig U, Talhout W, Kind J, Ward LD, Brugman W, de Castro IJ, Kerkhoven RM, Bussemaker HJ, van Steensel B (2010) Systematic protein location mapping reveals five principal chromatin types in Drosophila cells. *Cell* **143:** 212-224

Fletcher RB, Harland RM (2008) The role of FGF signaling in the establishment and maintenance of mesodermal gene expression in Xenopus. *Developmental dynamics : an official publication of the American Association of Anatomists* **237:** 1243-1254

References

Forcales SV, Albini S, Giordani L, Malecova B, Cignolo L, Chernov A, Coutinho P, Saccone V, Consalvi S, Williams R, Wang K, Wu Z, Baranovskaya S, Miller A, Dilworth FJ, Puri PL (2012) Signal-dependent incorporation of MyoD-BAF60c into Brg1-based SWI/SNF chromatin-remodelling complex. *The EMBO journal* **31:** 301-316

Forman D, Slack JM (1980) Determination and cellular commitment in the embryonic amphibian mesoderm. *Nature* **286:** 492-494

Gawantka V, Delius H, Hirschfeld K, Blumenstock C, Niehrs C (1995) Antagonizing the Spemann organizer: role of the homeobox gene Xvent-1. *The EMBO journal* **14:** 6268-6279

Gerhart J, Danilchik M, Doniach T, Roberts S, Rowning B, Stewart R (1989) Cortical rotation of the Xenopus egg: consequences for the anteroposterior pattern of embryonic dorsal development. *Development* **107 Suppl:** 37-51

Giudicelli F, Taillebourg E, Charnay P, Gilardi-Hebenstreit P (2001) Krox-20 patterns the hindbrain through both cell-autonomous and non cell-autonomous mechanisms. *Genes Dev* **15:** 567-580

Godsave S, Dekker EJ, Holling T, Pannese M, Boncinelli E, Durston A (1994) Expression patterns of Hoxb genes in the Xenopus embryo suggest roles in anteroposterior specification of the hindbrain and in dorsoventral patterning of the mesoderm. *Dev Biol* **166:** 465-476

Guenther MG, Levine SS, Boyer LA, Jaenisch R, Young RA (2007) A chromatin landmark and transcription initiation at most promoters in human cells. *Cell* **130:** 77-88

Gutkovich YE, Ofir R, Elkouby YM, Dibner C, Gefen A, Elias S, Frank D (2010) Xenopus Meis3 protein lies at a nexus downstream to Zic1 and Pax3 proteins, regulating multiple cell-fates during early nervous system development. *Dev Biol* **338:** 50-62

Hansen CS, Marion CD, Steele K, George S, Smith WC (1997) Direct neural induction and selective inhibition of mesoderm and epidermis inducers by Xnr3. *Development* **124:** 483-492

Hardin J, Keller R (1988) The behaviour and function of bottle cells during gastrulation of Xenopus laevis. *Development* **103:** 211-230

Hargreaves DC, Crabtree GR (2011) ATP-dependent chromatin remodeling: genetics, genomics and mechanisms. *Cell research* **21:** 396-420

Harrison MM, Li XY, Kaplan T, Botchan MR, Eisen MB (2011) Zelda binding in the early Drosophila melanogaster embryo marks regions subsequently activated at the maternal-to-zygotic transition. *PLoS genetics* **7:** e1002266

References
_____

Hassan AH, Prochasson P, Neely KE, Galasinski SC, Chandy M, Carrozza MJ, Workman JL (2002) Function and selectivity of bromodomains in anchoring chromatin-modifying complexes to promoter nucleosomes. *Cell* **111:** 369-379

Hata A, Seoane J, Lagna G, Montalvo E, Hemmati-Brivanlou A, Massague J (2000) OAZ uses distinct DNA- and protein-binding zinc fingers in separate BMP-Smad and Olf signaling pathways. *Cell* **100:** 229-240

Heasman J (2002) Morpholino oligos: making sense of antisense? *Dev Biol* **243:** 209-214

Heasman J (2006) Patterning the early Xenopus embryo. *Development* **133:** 1205-1217

Heller N, Brandli AW (1997) Xenopus Pax-2 displays multiple splice forms during embryogenesis and pronephric kidney development. *Mechanisms of development* **69:** 83-104

Hemmati-Brivanlou A, Thomsen GH (1995) Ventral mesodermal patterning in Xenopus embryos: expression patterns and activities of BMP-2 and BMP-4. *Developmental genetics* **17:** 78-89

Ho L, Ronan JL, Wu J, Staahl BT, Chen L, Kuo A, Lessard J, Nesvizhskii AI, Ranish J, Crabtree GR (2009) An embryonic stem cell chromatin remodeling complex, esBAF, is essential for embryonic stem cell self-renewal and pluripotency. *Proceedings of the National Academy of Sciences of the United States of America* **106:** 5181-5186

Holliday R (1994) Epigenetics: an overview. *Developmental genetics* **15:** 453-457

Houston DW (2012) Cortical rotation and messenger RNA localization in Xenopus axis formation. *Wiley interdisciplinary reviews Developmental biology* **1:** 371-388

Howe JA, Newport JW (1996) A developmental timer regulates degradation of cyclin E1 at the midblastula transition during Xenopus embryogenesis. *Proceedings of the National Academy of Sciences of the United States of America* **93:** 2060-2064

In der Rieden PM, Jansen HJ, Durston AJ (2011) XMeis3 is necessary for mesodermal Hox gene expression and function. *PloS one* **6:** e18010

Ishibashi H, Matsumura N, Hanafusa H, Matsumoto K, De Robertis EM, Kuroda H (2008) Expression of Siamois and Twin in the blastula Chordin/Noggin signaling center is required for brain formation in Xenopus laevis embryos. *Mechanisms of development* **125:** 58-66

Iyer VR (2012) Nucleosome positioning: bringing order to the eukaryotic genome. *Trends in cell biology* **22:** 250-256

Jenuwein T, Allis CD (2001) Translating the histone code. *Science* **293:** 1074-1080

Kamachi Y, Okuda Y, Kondoh H (2008) Quantitative assessment of the knockdown efficiency of morpholino antisense oligonucleotides in zebrafish embryos using a luciferase assay. *Genesis* **46:** 1-7

Kane DA, Kimmel CB (1993) The zebrafish midblastula transition. *Development* **119:** 447-456

Kao KR, Elinson RP (1988) The Entire Mesodermal Mantle Behaves as Spemann's Organizer in Dorsoanterior Enhanced Xenopus laevis Embryos. *Developmental Biology* **127:** 64-77

King ML, Messitt TJ, Mowry KL (2005) Putting RNAs in the right place at the right time: RNA localization in the frog oocyte. *Biology of the cell / under the auspices of the European Cell Biology Organization* **97:** 19-33

Knochel S, Lef J, Clement J, Klocke B, Hille S, Koster M, Knochel W (1992) Activin A induced expression of a fork head related gene in posterior chordamesoderm (notochord) of Xenopus laevis embryos. *Mechanisms of development* **38:** 157-165

Koenig SF, Brentle S, Hamdi K, Fichtner D, Wedlich D, Gradl D (2010) En2, Pax2/5 and Tcf-4 transcription factors cooperate in patterning the Xenopus brain. *Dev Biol* **340:** 318-328

Krieg PA, Melton DA (1985) Developmental regulation of a gastrula-specific gene injected into fertilized Xenopus eggs. *The EMBO journal* **4:** 3463-3471

Kuroda H, Wessely O, De Robertis EM (2004) Neural induction in Xenopus: requirement for ectodermal and endomesodermal signals via Chordin, Noggin, beta-Catenin, and Cerberus. *PLoS biology* **2:** E92

Lagha M, Bothma JP, Esposito E, Ng S, Stefanik L, Tsui C, Johnston J, Chen K, Gilmour DS, Zeitlinger J, Levine MS (2013) Paused Pol II coordinates tissue morphogenesis in the Drosophila embryo. *Cell* **153:** 976-987

Lamb TM, Harland RM (1995) Fibroblast growth factor is a direct neural inducer, which combined with noggin generates anterior-posterior neural pattern. *Development* **121:** 3627-3636

Larabell CA, Torres M, Rowning BA, Yost C, Miller JR, Wu M, Kimelman D, Moon RT (1997) Establishment of the dorso-ventral axis in Xenopus embryos is presaged by early asymmetries in beta-catenin that are modulated by the Wnt signaling pathway. *The Journal of cell biology* **136:** 1123-1136

Laurent BC, Treitel MA, Carlson M (1991) Functional interdependence of the yeast SNF2, SNF5, and SNF6 proteins in transcriptional activation. *Proceedings of the National Academy of Sciences of the United States of America* **88:** 2687-2691

References

Lee HX, Ambrosio AL, Reversade B, De Robertis EM (2006) Embryonic dorsal-ventral signaling: secreted frizzled-related proteins as inhibitors of tolloid proteinases. *Cell* **124:** 147-159

Lemaire P, Garrett N, Gurdon JB (1995) Expression cloning of Siamois, a Xenopus homeobox gene expressed in dorsal-vegetal cells of blastulae and able to induce a complete secondary axis. *Cell* **81:** 85-94

Lessard JA, Crabtree GR (2010) Chromatin regulatory mechanisms in pluripotency. *Annual review of cell and developmental biology* **26:** 503-532

Liang HL, Nien CY, Liu HY, Metzstein MM, Kirov N, Rushlow C (2008) The zinc-finger protein Zelda is a key activator of the early zygotic genome in Drosophila. *Nature* **456:** 400-403

Lickert H, Takeuchi JK, Von Both I, Walls JR, McAuliffe F, Adamson SL, Henkelman RM, Wrana JL, Rossant J, Bruneau BG (2004) Baf60c is essential for function of BAF chromatin remodelling complexes in heart development. *Nature* **432:** 107-112

Loose M, Patient R (2004) A genetic regulatory network for Xenopus mesendoderm formation. *Dev Biol* **271:** 467-478

Luger K, Dechassa ML, Tremethick DJ (2012) New insights into nucleosome and chromatin structure: an ordered state or a disordered affair? *Nature reviews Molecular cell biology* **13:** 436-447

Luger K, Mader AW, Richmond RK, Sargent DF, Richmond TJ (1997) Crystal structure of the nucleosome core particle at 2.8 A resolution. *Nature* **389:** 251-260

Mayor R, Morgan R, Sargent MG (1995) Induction of the prospective neural crest of Xenopus. *Development* **121:** 767-777

Meshorer E, Yellajoshula D, George E, Scambler PJ, Brown DT, Misteli T (2006) Hyperdynamic plasticity of chromatin proteins in pluripotent embryonic stem cells. *Developmental cell* **10:** 105-116

Muchardt C, Yaniv M (2001) When the SWI/SNF complex remodels...the cell cycle. *Oncogene* **20:** 3067-3075

Mueller-Planitz F, Klinker H, Becker PB (2013a) Nucleosome sliding mechanisms: new twists in a looped history. *Nature structural & molecular biology* **20:** 1026-1032

Mueller-Planitz F, Klinker H, Ludwigsen J, Becker PB (2013b) The ATPase domain of ISWI is an autonomous nucleosome remodeling machine. *Nature structural & molecular biology* **20:** 82-89

Murphy DJ, Hardy S, Engel DA (1999) Human SWI-SNF component BRG1 represses transcription of the c-fos gene. *Molecular and cellular biology* **19:** 2724-2733

References

Neilson KM, Klein SL, Mhaske P, Mood K, Daar IO, Moody SA (2012) Specific domains of FoxD4/5 activate and repress neural transcription factor genes to control the progression of immature neural ectoderm to differentiating neural plate. *Dev Biol* **365:** 363-375

Newport J, Kirschner M (1982a) A major developmental transition in early Xenopus embryos: I. characterization and timing of cellular changes at the midblastula stage. *Cell* **30:** 675-686

Newport J, Kirschner M (1982b) A major developmental transition in early Xenopus embryos: II. Control of the onset of transcription. *Cell* **30:** 687-696

Nieuwkoop PD, Faber J (1994) *Normal table of Xenopus laevis (Daudin) : a systematical and chronological survey of the development from the fertilized egg till the end of metamorphosis*, New York: Garland Pub.

Ninomiya H, Elinson RP, Winklbauer R (2004) Antero-posterior tissue polarity links mesoderm convergent extension to axial patterning. *Nature* **430:** 364-367

Nishino Y, Eltsov M, Joti Y, Ito K, Takata H, Takahashi Y, Hihara S, Frangakis AS, Imamoto N, Ishikawa T, Maeshima K (2012) Human mitotic chromosomes consist predominantly of irregularly folded nucleosome fibres without a 30-nm chromatin structure. *The EMBO journal* **31:** 1644-1653

Oelgeschlager M, Kuroda H, Reversade B, De Robertis EM (2003) Chordin is required for the Spemann organizer transplantation phenomenon in Xenopus embryos. *Developmental cell* **4:** 219-230

Onichtchouk D, Chen YG, Dosch R, Gawantka V, Delius H, Massague J, Niehrs C (1999) Silencing of TGF-beta signalling by the pseudoreceptor BAMBI. *Nature* **401:** 480-485

Onichtchouk D, Glinka A, Niehrs C (1998) Requirement for Xvent-1 and Xvent-2 gene function in dorsoventral patterning of Xenopus mesoderm. *Development* **125:** 1447-1456

Pannese M, Polo C, Andreazzoli M, Vignali R, Kablar B, Barsacchi G, Boncinelli E (1995) The Xenopus homologue of Otx2 is a maternal homeobox gene that demarcates and specifies anterior body regions. *Development* **121:** 707-720

Pannetier M, Julien E, Schotta G, Tardat M, Sardet C, Jenuwein T, Feil R (2008) PR-SET7 and SUV4-20H regulate H4 lysine-20 methylation at imprinting control regions in the mouse. *EMBO reports* **9:** 998-1005

Paranjpe SS, Jacobi UG, van Heeringen SJ, Veenstra GJ (2013) A genome-wide survey of maternal and embryonic transcripts during Xenopus tropicalis development. *BMC genomics* **14:** 762

References

Piccolo S, Agius E, Leyns L, Bhattacharyya S, Grunz H, Bouwmeester T, De Robertis EM (1999a) The head inducer Cerberus is a multifunctional antagonist of Nodal, BMP and Wnt signals. *Nature* **397:** 707-710

Piccolo S, Agius E, Leyns L, Bhattacharyya S, Grunz H, Bouwmeester T, Robertis EMD (1999b) The head inducer Cerberus is a multifunctional antagonist of nodal BMP and Wnt signaling. *Nature* **397:** 707-710

Picker A, Scholpp S, Bohli H, Takeda H, Brand M (2002) A novel positive transcriptional feedback loop in midbrain-hindbrain boundary development is revealed through analysis of the zebrafish pax2.1 promoter in transgenic lines. *Development* **129:** 3227-3239

Reid CD, Zhang Y, Sheets MD, Kessler DS (2012) Transcriptional integration of Wnt and Nodal pathways in establishment of the Spemann organizer. *Dev Biol* **368:** 231-241

Reversade B, Kuroda H, Lee H, Mays A, De Robertis EM (2005) Depletion of Bmp2, Bmp4, Bmp7 and Spemann organizer signals induces massive brain formation in Xenopus embryos. *Development* **132:** 3381-3392

Reyes JC, Barra J, Muchardt C, Camus A, Babinet C, Yaniv M (1998) Altered control of cellular proliferation in the absence of mammalian brahma (SNF2alpha). *The EMBO journal* **17:** 6979-6991

Robertis EMD, Kuroda H (2004) Dorsal-Ventral patterning and neural induction in Xenopus Embryos. *Annu Rev Cell Dev Biol* **20:** 285-308

Robinson PJ, Fairall L, Huynh VA, Rhodes D (2006) EM measurements define the dimensions of the "30-nm" chromatin fiber: evidence for a compact, interdigitated structure. *Proceedings of the National Academy of Sciences of the United States of America* **103:** 6506-6511

Rozario T, Dzamba B, Weber GF, Davidson LA, DeSimone DW (2009) The physical state of fibronectin matrix differentially regulates morphogenetic movements in vivo. *Dev Biol* **327:** 386-398

Sander V, Reversade B, De Robertis EM (2007) The opposing homeobox genes Goosecoid and Vent1/2 self-regulate Xenopus patterning. *The EMBO journal* **26:** 2955-2965

Sasai Y, Lu B, Steinbeisser H, Geissert D, Gont LK, Robertis EMD (1994) Xenopus chordin: A novel dorsalizing Factor Actovated by Organizer-Specific homeobox Genes. *Cell* **79:** 779-790

Schmitt SM, Gull M, Brandli AW (2014) Engineering Xenopus embryos for phenotypic drug discovery screening. *Advanced drug delivery reviews*

Schneider S, Steinbeisser H, Warga RM, Hausen P (1996) Beta-catenin translocation into nuclei demarcates the dorsalizing centers in frog and fish embryos. *Mechanisms of development* **57:** 191-198

Schneider TD, Arteaga-Salas JM, Mentele E, David R, Nicetto D, Imhof A, Rupp RA (2011) Stage-specific histone modification profiles reveal global transitions in the Xenopus embryonic epigenome. *PloS one* **6:** e22548

Schotta G, Lachner M, Sarma K, Ebert A, Sengupta R, Reuter G, Reinberg D, Jenuwein T (2004) A silencing pathway to induce H3-K9 and H4-K20 trimethylation at constitutive heterochromatin. *Genes Dev* **18:** 1251-1262

Schuettengruber B, Ganapathi M, Leblanc B, Portoso M, Jaschek R, Tolhuis B, van Lohuizen M, Tanay A, Cavalli G (2009) Functional anatomy of polycomb and trithorax chromatin landscapes in Drosophila embryos. *PLoS biology* **7:** e13

Sekiya T, Adachi S, Kohu K, Yamada T, Higuchi O, Furukawa Y, Nakamura Y, Nakamura T, Tashiro K, Kuhara S, Ohwada S, Akiyama T (2004a) Identification of BMP and activin membrane-bound inhibitor (BAMBI), an inhibitor of transforming growth factor-beta signaling, as a target of the beta-catenin pathway in colorectal tumor cells. *The Journal of biological chemistry* **279:** 6840-6846

Sekiya T, Oda T, Matsuura K, Akiyama T (2004b) Transcriptional regulation of the TGF-beta pseudoreceptor BAMBI by TGF-beta signaling. *Biochemical and biophysical research communications* **320:** 680-684

Semotok JL, Cooperstock RL, Pinder BD, Vari HK, Lipshitz HD, Smibert CA (2005) Smaug recruits the CCR4/POP2/NOT deadenylase complex to trigger maternal transcript localization in the early Drosophila embryo. *Current biology : CB* **15:** 284-294

Seo S, Richardson GA, Kroll KL (2005) The SWI/SNF chromatin remodeling protein Brg1 is required for vertebrate neurogenesis and mediates transactivation of Ngn and NeuroD. *Development* **132:** 105-115

Simone C (2006) SWI/SNF: the crossroads where extracellular signaling pathways meet chromatin. *Journal of cellular physiology* **207:** 309-314

Singhal N (2005) The role of Xenopus BRG1, a conserved subunit of SWI/SNF class of remodeling complexes, during early frog development. *Dissertation, LMU München: Fakultät für Biologie*

Singhal N, Esch D, Stehling M, Scholer HR (2014) BRG1 Is Required to Maintain Pluripotency of Murine Embryonic Stem Cells. *BioResearch open access* **3:** 1-8

Singhal N, Graumann J, Wu G, Arauzo-Bravo MJ, Han DW, Greber B, Gentile L, Mann M, Scholer HR (2010) Chromatin-Remodeling Components of the BAF Complex Facilitate Reprogramming. *Cell* **141:** 943-955

Smibert CA, Wilson JE, Kerr K, Macdonald PM (1996) smaug protein represses translation of unlocalized nanos mRNA in the Drosophila embryo. *Genes Dev* **10:** 2600-2609

References

Smith WC, McKendry R, Jr. SR, Harland RM (1995) A nodal related Gene Defines a Physical and Fuunctional Domain within the Spemann Organizer. *Cell* **82**

Subtil-Rodriguez A, Reyes JC (2010) BRG1 helps RNA polymerase II to overcome a nucleosomal barrier during elongation, in vivo. *EMBO reports* **11:** 751-757

Suzuki A, Thies RS, Yamaji N, Song JJ, Wozney JM, Murakami K, Ueno N (1994) A truncated bone morphogenetic protein receptor affects dorsal-ventral patterning in the early Xenopus embryo. *Proceedings of the National Academy of Sciences of the United States of America* **91:** 10255-10259

Tadros W, Lipshitz HD (2009) The maternal-to-zygotic transition: a play in two acts. *Development* **136:** 3033-3042

Tamkun JW, Deuring R, Scott MP, Kissinger M, Pattatucci AM, Kaufman TC, Kennison JA (1992) brahma: a regulator of Drosophila homeotic genes structurally related to the yeast transcriptional activator SNF2/SWI2. *Cell* **68:** 561-572

Tour E, Pillemer G, Gruenbaum Y, Fainsod A (2002) Otx2 can activate the isthmic organizer genetic network in the Xenopus embryo. *Mechanisms of development* **110:** 3-13

van Steensel B (2011) Chromatin: constructing the big picture. *The EMBO journal* **30:** 1885-1895

Voiculescu O, Taillebourg E, Pujades C, Kress C, Buart S, Charnay P, Schneider-Maunoury S (2001) Hindbrain patterning: Krox20 couples segmentation and specification of regional identity. *Development* **128:** 4967-4978

Wacker SA, McNulty CL, Durston AJ (2004) The initiation of Hox gene expression in Xenopus laevis is controlled by Brachyury and BMP-4. *Dev Biol* **266:** 123-137

Wang K, Sengupta S, Magnani L, Wilson CA, Henry RW, Knott JG (2010) Brg1 is required for Cdx2-mediated repression of Oct4 expression in mouse blastocysts. *PloS one* **5:** e10622

Watabe T, Kim S, Candia A, Rothbacher U, Hashimoto C, Inoue K, Cho KW (1995) Molecular mechanisms of Spemann's organizer formation: conserved growth factor synergy between Xenopus and mouse. *Genes & Development* **9:** 3038-3050

Wessely O, Agius E, Oelgeschlager M, Pera EM, De Robertis EM (2001) Neural induction in the absence of mesoderm: beta-catenin-dependent expression of secreted BMP antagonists at the blastula stage in Xenopus. *Dev Biol* **234:** 161-173

Wong AK, Shanahan F, Chen Y, Lian L, Ha P, Hendricks K, Ghaffari S, Iliev D, Penn B, Woodland AM, Smith R, Salada G, Carillo A, Laity K, Gupte J, Swedlund B, Tavtigian SV, Teng DH, Lees E (2000) BRG1,

a component of the SWI-SNF complex, is mutated in multiple human tumor cell lines. *Cancer research* **60:** 6171-6177

Xanthos JB, Kofron M, Wylie C, Heasman J (2001) Maternal VegT is the initiator of a molecular network specifying endoderm in Xenopus laevis. *Development* **128:** 167-180

Xi Q, He W, Zhang XH, Le HV, Massague J (2008) Genome-wide impact of the BRG1 SWI/SNF chromatin remodeler on the transforming growth factor beta transcriptional program. *The Journal of biological chemistry* **283:** 1146-1155

Xie W, Schultz MD, Lister R, Hou Z, Rajagopal N, Ray P, Whitaker JW, Tian S, Hawkins RD, Leung D, Yang H, Wang T, Lee AY, Swanson SA, Zhang J, Zhu Y, Kim A, Nery JR, Urich MA, Kuan S, Yen CA, Klugman S, Yu P, Suknuntha K, Propson NE, Chen H, Edsall LE, Wagner U, Li Y, Ye Z, Kulkarni A, Xuan Z, Chung WY, Chi NC, Antosiewicz-Bourget JE, Slukvin I, Stewart R, Zhang MQ, Wang W, Thomson JA, Ecker JR, Ren B (2013) Epigenomic analysis of multilineage differentiation of human embryonic stem cells. *Cell* **153:** 1134-1148

Yamamoto S, Hikasa H, Ono H, Taira M (2003) Molecular link in the sequential induction of the Spemann organizer: direct activation of the cerberus gene by Xlim-1, Xotx2, Mix.1, and Siamois, immediately downstream from Nodal and Wnt signaling. *Dev Biol* **257:** 190-204

Yan B, Neilson KM, Moody SA (2009) foxD5 plays a critical upstream role in regulating neural ectodermal fate and the onset of neural differentiation. *Dev Biol* **329:** 80-95

Yanai I, Peshkin L, Jorgensen P, Kirschner MW (2011) Mapping gene expression in two Xenopus species: evolutionary constraints and developmental flexibility. *Developmental cell* **20:** 483-496

Yoo AS, Crabtree GR (2009) ATP-dependent chromatin remodeling in neural development. *Current opinion in neurobiology* **19:** 120-126

Zhan X, Shi X, Zhang Z, Chen Y, Wu JI (2011) Dual role of Brg chromatin remodeling factor in Sonic hedgehog signaling during neural development. *Proceedings of the National Academy of Sciences of the United States of America* **108:** 12758-12763

Zhu J, Adli M, Zou JY, Verstappen G, Coyne M, Zhang X, Durham T, Miri M, Deshpande V, De Jager PL, Bennett DA, Houmard JA, Muoio DM, Onder TT, Camahort R, Cowan CA, Meissner A, Epstein CB, Shoresh N, Bernstein BE (2013) Genome-wide chromatin state transitions associated with developmental and environmental cues. *Cell* **152:** 642-654

Appendix

BMO1 microarray analysis

Listed are all genes, upreglulated ≥ 1.5 fold change and with a local false discovery rate ≤ 0.2.

Set-probe number	fold change [log2]	gene name	symbol
StrEns.5201.1.S1_s_at	3,719	WNT1-inducible-signaling pathway protein 3-like	LOC100488354
Str.40271.2.S1_a_at	3,227	Hypothetical protein LOC550005	LOC550005
Str.9570.1.S1_at	3,080	ribophorin II	rpn2
Str.27732.1.S1_at	2,895	GTP binding protein 5 (putative)	gtpbp5
Str.20978.1.S1_at	2,344	Hypothetical protein LOC100158502	LOC100158502
Str.51787.1.S1_at	2,153	histone cluster 1, H2ah	hist1h2ah
Str.51882.1.S1_at	2,094	chromosome 20 open reading frame 29	c20orf29
Str.40271.1.S1_at	2,005	Hypothetical protein LOC549623	TGas006m08.1
Str.16459.1.S1_at	1,698	hect (homologous to the E6-AP (UBE3A) carboxyl terminus) domain and RCC1 (CHC1)-like domain (RLD) 1	herc1
Str.3409.1.A1_at	1,583	GTP binding protein 2	gtpbp2
Str.24465.1.S1_at	1,562	mal, T-cell differentiation protein 2	mal2
Str.1273.1.S1_at	1,499	histone H4-like	LOC100496593
StrJgi.934.1.S1_s_at	1,452	protein kinase (cAMP-dependent, catalytic) inhibitor gamma	pkig
Str.18904.1.S1_at	1,433	junctophilin 1	jph1
Str.27312.1.S1_at	1,356	histone cluster 2, H2ab	hist2h2ab
Str.2030.1.A1_at	1,250	Frizzled homolog 3	fzd3
StrEns.12239.1.S1_s_at	1,230	hypothetical protein hypothetical protein	LOC100491313 LOC100496030
Str.5781.1.A1_at	1,199	Hypothetical protein MGC147532	MGC147532
Str.25548.1.A1_at	1,150	amyloid protein-binding protein 2-like	LOC100487715
StrEns.8996.1.S1_a_at	1,142	hypothetical protein LOC100496030	LOC100496030

Str.41102.1.S1_at	1,047	CCAAT/enhancer binding protein (C/EBP), delta	cebpd
Str.37449.1.A1_at	1,007	poly (ADP-ribose) polymerase family, member 4	parp4
Str.8423.1.S1_at	1,004	chromosome 6 open reading frame 211	c6orf211
Str.3950.1.S2_at	0,989	integrin alpha-5-like	LOC100492002
Str.8642.1.S1_at	0,987	trans-1,2-dihydrobenzene-1,2-diol dehydrogenase	dhdh
StrAffx.105.1.S1_s_at	0,975	synaptotagmin 7	syt7
Str.6540.2.A1_at	0,967	Vac14 homolog	vac14
Str.51459.1.S1_at	0,966	neurobeachin	nbea
Str.16785.2.S1_at	0,954	oxidase (cytochrome c) assembly 1-like	oxa1l
Str.50909.1.S1_at	0,953	activating transcription factor 7	atf7
Str.14144.2.A1_at	0,934	zinc finger and BTB domain containing 5	zbtb5
Str.21484.1.A1_s_at	0,907	pyruvate dehyrogenase phosphatase catalytic subunit 1	pdp1
Str.11152.1.S2_at	0,904	cornichon homolog 4	cnih4
Str.10066.1.S1_at	0,904	mesendoderm nuclear factor, gene 1	menf.1
Str.2681.1.S1_at	0,897	SMG1 homolog, phosphatidylinositol 3-kinase-related kinase	smg1
Str.36162.1.A1_at	0,848	hypothetical protein LOC100498210	LOC100498210
Str.31142.1.S1_at	0,847	transmembrane protein, adipocyte asscociated 1	tpra1
Str.14124.1.S2_at	0,846	sestrin 1	sesn1
StrEns.6148.1.S1_a_at	0,842	peptide chain release factor 1, mitochondrial-like	LOC100486280
Str.101.1.S1_at	0,833	replication factor C (activator 1) 5, 36.5kDa	rfc5
Str.564.1.S1_at	0,824	DNZDHHC/NEW1 zinc finger protein 11	dnz1
Str.33322.1.S1_at	0,818	chromosome 16 open reading frame 68	c16orf68
Str.11519.1.S2_at	0,815	spermine oxidase	smox
Str.9548.3.A1_at	0,806	28S ribosomal protein S25, mitochondrial-like	LOC100494871
Str.4065.1.S1_at	0,805	ATG4 autophagy related 4 homolog A	atg4a

Str.27290.1.S1_at	0,804	ribonuclease H2, subunit A	rnaseh2a
Str.33694.1.S1_at	0,801	round spermatid basic protein 1	rsbn1
Str.2504.2.S1_at	0,797	RNA binding motif protein 6	rbm6
Str.40497.1.S1_at	0,794	ras-related C3 botulinum toxin substrate 3 (rho family, small GTP binding protein Rac3)	rac3
Str.20705.2.A1_a_at	0,789	uncharacterized protein C8orf41-like	LOC100487242
Str.40433.1.S1_at	0,789	vasoactive intestinal polypeptide receptor-like	LOC100497291
Str.8281.1.S1_at	0,763	small subunit of serine palmitoyltransferase A-B-like	LOC100495839
Str.27561.1.S1_at	0,758	TSPY-like 2	tspyl2
Str.32322.1.S1_at	0,755	nucleosome assembly protein 1-like 4	nap1l4
Str.31445.1.S1_at	0,753	inhibitor of growth family, member 1	ing1
Str.28870.1.S1_at	0,752	Hypothetical protein LOC779512	LOC779512
Str.27848.1.S1_at	0,750	egl nine homolog 3	egln3
Str.25272.1.S1_at	0,726	retinoid X receptor, gamma	rxrg
Str.7571.2.S1_a_at	0,726	hypothetical LOC100491590 hypothetical LOC100491682 hypothetical LOC100493923	LOC100491590 LOC100491682 LOC100493923
Str.5120.1.S1_at	0,719	adaptor-related protein complex 2, sigma 1 subunit	ap2s1
Str.27693.1.S1_at	0,701	SCY1-like 3	scyl3
Str.10400.2.S1_at	0,696	biogenesis of lysosomal organelles complex-1, subunit 1	bloc1s1
Str.27324.1.S2_at	0,695	ras-related protein ras-dva	ras-dva
Str.849.2.A1_at	0,686	Hypothetical protein MGC75957	MGC75957
Str.39705.1.S1_s_at	0,677	integrator complex subunit 12	ints12
Str.30835.3.S1_a_at	0,671	Interleukin-15	il-15
Str.2145.1.S1_at	0,668	laminin, gamma 1	lamc1
Str.26914.1.S1_at	0,666	UTP11-like, U3 small nucleolar ribonucleoprotein	utp11l
Str.13906.1.S1_a_at	0,657	low molecular weight neuronal intermediate filament	nif
Str.51698.1.S1_at	0,650	zinc finger protein 64 homolog	zfp64

Str.29188.1.S1_at	0,647	chromosome 1 open reading frame 89	c1orf89
Str.32445.1.S1_at	0,644	tubulin alpha-1D chain-like MGC97820 protein	LOC100487867 MGC97820
Str.3482.1.S1_at	0,640	dual specificity phosphatase 22	dusp22
Str.27186.1.S1_s_at	0,637	histone H3.2-like	LOC100496129
Str.44813.1.S1_s_at	0,632	oligophrenin 1	ophn1
Str.27520.1.A1_at	0,629	dedicator of cytokinesis 3	dock3
Str.31215.1.S1_s_at	0,625	septin 12	Sep 12
Str.216.1.S1_at	0,624	Hypothetical protein MGC76116	MGC76116
Str.26671.2.A1_a_at	0,624	similar to candidate tumor suppressor OVCA2	ovca2
Str.18325.1.A1_at	0,619	leucine rich repeat neuronal 1	lrrn1
Str.42318.1.A1_at	0,611	GH3 domain-containing protein-like	LOC100488130
Str.22588.1.S1_at	0,610	chromosome 11 open reading frame 2	c11orf2
Str.10971.1.S1_at	0,609	OTU domain-containing protein 1-like	LOC100493984
Str.40156.1.S1_at	0,608	probable tubulin polyglutamylase TTLL1-like	LOC100495095
Str.37703.1.S1_at	0,608	transportin 1	tnpo1
StrJgi.4435.1.S1_s_at	0,606	DnaJ (Hsp40) homolog, subfamily C, member 27	dnajc27
Str.16298.1.S1_at	0,602	nucleotide binding protein-like	nubpl
Str.52172.1.S1_at	0,600	procollagen-lysine, 2-oxoglutarate 5-dioxygenase 3	plod3
Str.8414.1.S1_at	0,590	nucleoporin 85kDa	nup85
Str.38351.1.S1_at	0,590	acyl-CoA synthetase family member 3	acsf3
Str.42612.1.S1_at	0,590	ATPase, H+ transporting, lysosomal 34kDa, V1 subunit D	atp6v1d

Listed are all genes downregulated ≥ 1.5 fold change with a local false discovery rate ≤ 0.2.

Set-probe number	fold change [log2]	gene name	symbol
Str.1716.1.S1_x_at	-3,945	purinergic receptor P2Y, G-protein coupled, 2	p2ry2
Str.5336.1.S1_at	-2,985	symplekin	sympk
Str.31377.1.S1_at	-2,793	microsomal triglyceride transfer protein, gene 2	mttp.2
Str.27013.1.S1_a_at	-2,699	uroplakin 3B	upk3b
Str.11165.7.S1_at	-2,579	sarcoplasmic/endoplasmic reticulum calcium ATPase 2-like	LOC100489059
Str.4354.1.S1_at	-2,467	signal transducing adaptor molecule (SH3 domain and ITAM motif) 2	stam2
StrEns.8369.1.S1_at	-2,460	growth/differentiation factor 2-like	LOC100485289
Str.13147.1.A1_at	-2,432	zinc finger protein 219-like	LOC100495520
StrEns.7683.1.S1_at	-2,365	zona pellucida sperm-binding protein 4-like	LOC100494768
Str.15007.1.S1_at	-2,343	gastrula-specific protein 17	gs17
Str.19278.2.S1_at	-2,318	hypothetical protein LOC100491368	LOC100491368
Str.5826.1.S1_at	-2,272	non-metastatic cells 2, protein (NM23B) expressed in	nme2
Str.6718.1.S1_at	-2,204	hypothetical LOC100494381	LOC100494381
Str.9193.1.A1_a_at	-2,189	UPF0632 protein C2orf89-like	LOC100491951
Str.2177.1.A1_a_at	-2,181	sphingosine-1-phosphate receptor 5	s1pr5
Str.21595.1.A1_at	-2,172	cyclin-dependent kinase 5	cdk5
Str.5015.1.A1_at	-2,168	neural precursor cell expressed, developmentally down-regulated 9	nedd9
Str.16322.1.S1_at	-2,131	Sp9 transcription factor homolog	sp9
Str.31367.1.A1_at	-2,128	coronin-7-like	LOC100492934
Str.21613.1.S1_a_at	-2,121	Calponin 2	cnn2
Str.17625.1.S1_at	-2,107	hypothetical LOC100495344	LOC100495344
Str.8191.1.S2_at	-2,082	phospholipase A2, group XIIB	pla2g12b
Str.6681.1.S1_a_at	-2,071	keratin	krt
Str.9958.1.S1_at	-2,051	chromosome 7 open reading frame 11	c7orf11
Str.7434.3.S1_at	-2,050	La ribonucleoprotein domain family, member 1	larp1

Str.10944.1.S1_at	-2,038	Zic family member 1 (odd-paired homolog)	zic1
Str.1956.1.S1_at	-2,019	eukaryotic translation initiation factor 3, subunit H	eif3h
Str.11087.1.S1_at	-1,993	distal-less homeobox 5	dlx5
Str.15072.2.A1_a_at	-1,975	delta-like 1	dll1
Str.40060.1.S1_at	-1,923	solute carrier family 25 (mitochondrial carrier, phosphate carrier), member 25	slc25a25
Str.24376.1.S1_at	-1,867	heart and neural crest derivatives expressed 2	hand2
Str.1920.1.S2_a_at	-1,864	hypothetical protein LOC549355	LOC549355
Str.6151.1.S1_at	-1,826	ATPase, Na+/K+ transporting, beta 2 polypeptide	atp1b2
Str.10072.1.S2_at	-1,802	Solute carrier family 2 (facilitated glucose transporter), member 2	slc2a2
Str.34177.1.A1_s_at	-1,774	tumor necrosis factor receptor superfamily, member 21	tnfrsf21
Str.15669.1.S1_at	-1,764	nuclear receptor subfamily 2, group F, member 1	nr2f1
Str.1093.1.S1_at	-1,757	ADP-ribosylation factor-like 4C	arl4c
Str.30624.1.S1_at	-1,746	ephrin-A3	efna3
Str.20569.1.S1_at	-1,740	Hypothetical protein LOC100127613	LOC100127613
Str.8471.1.S1_at	-1,739	oxysterol binding protein-like 11	osbpl11
Str.16419.1.S1_at	-1,732	DNA-damage-inducible transcript 3	ddit3
Str.643.1.S1_a_at	-1,728	hypothetical LOC100486597	LOC100486597
Str.8459.1.S1_at	-1,726	baculoviral IAP repeat-containing 2	birc2
Str.4773.2.S1_s_at	-1,716	hypothetical protein LOC100488209	LOC100488209
Str.6630.1.S2_at	-1,710	X-box binding protein 1	xbp1
Str.29344.1.S1_at	-1,706	neurogenin 3	neurog3
Str.26164.1.S1_at	-1,705	protocadherin 18	pcdh18
Str.7073.1.S1_at	-1,648	iroquois homeobox 2	irx2
Str.11719.1.S1_at	-1,644	tissue factor-like	LOC100489511
Str.6889.1.A1_at	-1,631	vav 2 oncogene	LOC733982
Str.11302.1.S1_at	-1,631	forkhead box D3	foxd3
Str.16957.1.S2_at	-1,623	fused in sarcoma	fus

Str.20470.1.S2_at	-1,609	cyclin E2	ccne2
Str.49050.1.S1_at	-1,590	Fast skeletal myosin light chain 2	TNeu107a14.1
StrEns.3882.1.S1_at	-1,583	forkhead box protein D5-C-like	LOC100485983
Str.21868.1.S1_at	-1,582	macrophage stimulating 1 receptor (c-met-related tyrosine kinase)	mst1r
Str.10727.1.S1_at	-1,579	deoxyribonuclease gamma-like	LOC100497175
StrEns.9993.1.S1_at	-1,573	succinate dehydrogenase complex, subunit B, iron sulfur (Ip)	sdhb
Str.9762.1.S1_at	-1,571	stimulated by retinoic acid gene 6 homolog	stra6
Str.10076.1.S1_at	-1,571	angiomotin like 2	amotl2
Str.954.1.S1_at	-1,555	potassium channel tetramerisation domain containing 15	kctd15
Str.15587.1.S1_at	-1,554	hypothetical protein LOC100487200	LOC100487200
Str.2103.1.S1_at	-1,546	anaphase promoting complex subunit 11	anapc11
Str.6201.1.S1_at	-1,546	SRY (sex determining region Y)-box 2	sox2
Str.10659.1.S1_at	-1,544	transcription factor AP-2 epsilon (activating enhancer binding protein 2 epsilon)	tfap2e
Str.6731.1.S1_at	-1,525	zinc finger protein 750	znf750
Str.18694.2.S1_x_at	-1,525	hypothetical protein LOC100498107	LOC100498107
Str.3344.1.S1_at	-1,520	novel protein similar to hatching enzymes	LOC594901
Str.34138.1.A1_at	-1,518	WD repeat domain 24	wdr24
Str.14655.1.S2_at	-1,517	LIM homeobox 5	lhx5
Str.16688.1.S1_at	-1,513	RNA pseudouridylate synthase domain containing 3	rpusd3
Str.12012.1.S1_at	-1,490	ankyrin repeat domain 10	ankrd10
Str.29569.1.S1_at	-1,486	Meningioma (disrupted in balanced translocation) 1, gene 1	mn1.1
Str.15223.4.S1_a_at	-1,463	eukaryotic translation initiation factor 4A2	eif4a2
Str.6185.1.S1_at	-1,463	cornifelin homolog	cnfn
Str.21522.1.S1_at	-1,449	uroplakin 2	upk2
Str.49514.1.S1_at	-1,419	T-box 3	tbx3

Str.23519.2.S1_a_at	-1,416	Death inducer-obliterator 1	dido1
Str.7428.1.S2_at	-1,408	centromere protein N	cenpn
Str.51988.1.S1_at	-1,397	serine/arginine-rich splicing factor 11	srsf11
Str.37707.1.A1_at	-1,396	fibronectin-like	LOC100492420
Str.27213.1.S1_a_at	-1,391	myeloid/lymphoid or mixed-lineage leukemia (trithorax homolog); translocated to, 4	mllt4
Str.5401.1.S1_at	-1,381	retinal pigment epithelium-specific protein 65kDa	rpe65
Str.1047.1.S1_at	-1,379	prohibitin 2	phb2
Str.6900.1.S2_s_at	-1,378	ER degradation enhancer, mannosidase alpha-like 1 /// angiopoietin-related protein 1-like	edem1 /// LOC100491105
Str.39270.1.A1_at	-1,373	bone morphogenetic protein 15-like	LOC100485893
Str.10293.1.S1_at	-1,363	SEC22 vesicle trafficking protein-like 2 (S. cerevisiae)	sec22l2
Str.125.1.S1_at	-1,361	cytochrome b-561	cyb561
Str.3124.1.S1_at	-1,358	UbiA prenyltransferase domain containing 1	ubiad1
Str.7820.2.S1_a_at	-1,358	immediate early response gene 2 protein-like	LOC100491464
Str.16252.1.S1_at	-1,356	SRY (sex determining region Y)-box 1	sox1
Str.44939.1.A1_s_at	-1,354	RAN binding protein 3	ranbp3
Str.784.1.A1_at	-1,353	rap1 GTPase-GDP dissociation stimulator 1-A-like	LOC100486041
Str.21559.2.S1_at	-1,352	Y box binding protein 2	ybx2
Str.15005.1.S1_at	-1,349	hairy and enhancer of split 3, gene 1	hes3.1
Str.51845.1.A1_at	-1,337	hypothetical protein MGC69473	MGC69473
Str.10716.1.S1_at	-1,315	forkhead box D4-like 1, gene 1	foxd4l1.1
Str.37993.1.S1_at	-1,315	uncharacterized protein KIAA0319-like	LOC100492839
Str.14504.1.S1_at	-1,314	rho GTPase-activating protein 39-like	LOC100485974
Str.27681.1.S1_at	-1,313	protease, serine 27	prss27
Str.11402.1.A1_at	-1,298	protein phosphatase 1, regulatory (inhibitor) subunit 3C, gene 1	ppp1r3c.1
Str.40874.1.S1_at	-1,293	ring finger protein 222	rnf222

Str.15297.1.S1_at	-1,292	glyoxylate reductase/hydroxypyruvate reductase, gene 2	grhpr.2
Str.1890.1.S1_at	-1,288	39S ribosomal protein L10, mitochondrial-like	LOC100496025
Str.18694.1.S1_at	-1,269	uncharacterized protein ywlC-like	LOC100497798
Str.3160.2.S1_a_at	-1,256	serine/arginine-rich splicing factor 6	srsf6
Str.30747.1.A1_at	-1,254	regulator of G-protein signaling 16	rgs16
Str.8142.1.A1_at	-1,245	TSC22 domain family, member 3	tsc22d3
Str.3146.2.A1_at	-1,243	hypothetical LOC100491246	LOC100491246
Str.11483.1.S1_at	-1,231	leucine-rich repeat-containing protein 8C-like leucine rich repeat containing 8 family, member C	LOC100488426 lrrc8c
Str.18694.2.S1_a_at	-1,221	uncharacterized protein ywlC-like	LOC100497798 LOC100498107
Str.21593.1.S1_at	-1,209	H1 histone family, member X	h1fx
Str.916.1.S1_at	-1,205	lin-28 homolog A (C. elegans)	lin28a
Str.24820.1.S1_at	-1,202	regulator of nonsense transcripts 1	upf1
Str.1440.1.S2_at	-1,190	solute carrier family 25 (mitochondrial carrier; peroxisomal membrane protein, 34kDa), member 17	slc25a17
StrJgi.4201.1.S1_s_at	-1,188	mitogen-activated protein-binding protein-interacting protein-like /// roadblock domain containing 3	LOC100489368 /// robld3
AFFX-Str-gapdh-M_at	-1,186	glyceraldehyde-3-phosphate dehydrogenase	gapdh
Str.420.1.S1_at	-1,185	ABO blood group (transferase A, alpha 1-3-N-acetylgalactosaminyltransferase; transferase B, alpha 1-3-galactosyltransferase)	abo
Str.38280.1.S1_at	-1,185	leucine rich repeat containing 24	lrrc24
Str.15044.1.S1_at	-1,183	bolA homolog 2	bola2
Str.17465.2.S1_a_at	-1,181	hypothetical LOC100493277	LOC100493277
Str.52067.1.S1_s_at	-1,180	zinc finger protein 568	znf568
Str.1183.1.S1_at	-1,180	transmembrane protein 127	tmem127
Str.6117.1.S1_at	-1,174	max interactor 1	mxi1

Str.7447.2.A1_at	-1,173	Heterogeneous nuclear ribonucleoprotein D-like	hnrpdl
Str.10535.1.S1_at	-1,165	hypothetical LOC100495377	LOC100495377
Str.13720.1.S1_at	-1,162	GTP-binding protein 10 (putative)	gtpbp10
Str.6659.1.S1_at	-1,160	nerve growth factor receptor	ngfr
Str.3502.1.S1_at	-1,158	roadblock domain containing 3	robld3
Str.10455.1.S1_at	-1,156	hypothetical LOC100495538	LOC100495538
Str.14040.1.A1_at	-1,151	hypothetical LOC100490704	LOC100490704
Str.52193.1.S1_at	-1,150	High-mobility group nucleosomal binding domain 2	TEgg003n10.1
Str.24811.1.S2_at	-1,148	myelin expression factor 2	myef2
Str.9615.1.A1_at	-1,147	tyrosine kinase, non-receptor, 2	tnk2
Str.5386.1.S1_at	-1,143	phosphoglucomutase 1	pgm1
Str.16319.2.S1_at	-1,138	hypothetical protein LOC100489354	LOC100489354
Str.51828.1.S1_a_at	-1,129	ribosomal protein L9	rpl9
Str.11288.1.S1_at	-1,128	hypothetical LOC100486074	LOC100486074
Str.303.1.S1_at	-1,125	G protein-coupled receptor, family C, group 5, member C	gprc5c
Str.7693.2.S1_at	-1,118	VENT homeobox 1, gene 1	ventx1.1
Str.51981.1.S1_s_at	-1,114	formin binding protein 4	LOC734003
Str.12750.1.A1_at	-1,107	LIM homeobox 1	lhx1
Str.7116.1.S1_at	-1,104	succinate-CoA ligase, alpha subunit	suclg1
Str.4741.1.S1_at	-1,101	peroxisomal biogenesis factor 11 beta	pex11b
Str.17679.1.S1_at	-1,097	chromosome 13 open reading frame 15	c13orf15
Str.10984.1.S1_at	-1,096	S100 calcium binding protein A11	s100a11
Str.15740.1.A1_at	-1,093	MAP kinase interacting serine/threonine kinase 2	mknk2
Str.17253.1.S1_at	-1,093	DnaJ (Hsp40) homolog, subfamily C, member 5 gamma	dnajc5g
Str.6879.1.A2_at	-1,084	myeloid cell leukemia sequence 1 (BCL2-related)	mcl1
StrJgi.784.1.S1_s_at	-1,083	retinoblastoma-like 1 (p107)	rbl1
StrJgi.5287.1.S1_s_at	-1,076	kin of IRRE like 2	kirrel2
Str.43062.1.A1_at	-1,074	hypothetical LOC100135121	LOC100135121

Str.24440.1.S2_at	-1,052	transcription factor 7-like 1 (T-cell specific, HMG-box)	tcf7l1
Str.27418.2.A1_at	-1,050	DENN/MADD domain containing 2C	dennd2c
Str.6578.1.S2_a_at	-1,047	serine/arginine-rich splicing factor 1	srsf1
Str.2004.1.S1_at	-1,043	frizzled homolog 2	fzd2
Str.27441.1.S1_at	-1,041	dyslexia susceptibility 1 candidate 1	dyx1c1
Str.8403.1.S1_at	-1,040	ribosomal RNA processing 12 homolog	rrp12
Str.10058.1.S2_at	-1,035	syntaxin 19	stx19
Str.37908.1.S1_a_at	-1,030	DNA-directed RNA polymerase, mitochondrial-like	LOC100488061
Str.26578.1.S1_a_at	-1,029	Cbp/p300-interacting transactivator, with Glu/Asp-rich carboxy-terminal domain, 4	cited4
Str.5673.1.S1_at	-1,028	high density lipoprotein binding protein (vigilin)	hdlbp
Str.10008.1.S1_at	-1,022	hypothetical protein LOC100487199	LOC100487199
Str.10236.1.S1_at	-1,021	receptor-interacting serine-threonine kinase 4	ripk4
Str.10362.1.A1_at	-1,018	hypothetical LOC100493109	LOC100493109
Str.37633.1.S1_at	-1,015	aminopeptidase-like 1	npepl1
Str.2049.3.S1_a_at	-1,007	solute carrier family 25 (mitochondrial carrier; phosphate carrier), member 3	slc25a3
Str.28803.2.S1_a_at	-1,005	hypothetical LOC100486098	LOC100486098
Str.1861.3.S1_s_at	-1,005	DEAD (Asp-Glu-Ala-Asp) box polypeptide 6	ddx6
Str.20062.1.S1_at	-0,997	phosphoglycerate dehydrogenase	phgdh
Str.52227.2.A1_a_at	-0,993	hypothetical protein	LOC100484994 LOC100486020 LOC100489931 LOC100490293 LOC100492588 LOC100498560
Str.22118.1.S1_at	-0,992	hypothetical protein LOC100038295	LOC100038295
Str.1881.1.S1_at	-0,990	hypothetical protein LOC100497165	LOC100497165

Str.1933.1.S1_at	-0,990	mitochondrial ribosomal protein L12	mrpl12
Str.6229.1.A1_at	-0,989	POU class V protein oct-25	Oct25
Str.22855.1.S1_at	-0,988	pleckstrin homology-like domain, family A, member 1	phlda1
Str.15274.1.S1_at	-0,985	Meis homeobox 3	meis3
Str.11630.1.A1_s_at	-0,985	XPA binding protein 2	xab2
Str.6222.1.S1_at	-0,984	annexin A2	anxa2
Str.79.2.S1_at	-0,984	POU domain, class 5, transcription factor 1.2-like	LOC100498076
Str.20248.1.S1_at	-0,980	sema domain, immunoglobulin domain (Ig), short basic domain, secreted, (semaphorin) 3F	sema3f
Str.10351.1.S1_at	-0,977	G protein-coupled receptor 161	gpr161
Str.21546.1.S1_at	-0,976	chromosome 14 open reading frame 179	c14orf179
Str.8453.1.S1_at	-0,975	chromatin modifying protein 1A	chmp1a
Str.6874.1.S1_at	-0,974	RAB11A, member RAS oncogene family	rab11a
Str.3045.1.S1_at	-0,972	musashi homolog 1	msi1
Str.7693.2.S1_a_at	-0,967	VENT homeobox 1, gene 1 VENT homeobox 1, gene 2	ventx1.1 ventx1.2
Str.9076.1.S1_at	-0,967	mitochondrial ribosomal protein S2	mrps2
Str.3002.1.A1_at	-0,965	Hypothetical protein LOC779546	LOC779546
Str.37570.1.S1_at	-0,964	solute carrier family 7 (cationic amino acid transporter, y+ system), member 3	slc7a3
Str.51678.1.S1_at	-0,962	ribosomal protein S17	rps17
Str.6544.1.S1_at	-0,961	DEP domain containing 7	depdc7
Str.51323.1.S1_at	-0,960	hairy and enhancer of split 2	hes2
Str.7709.1.S2_at	-0,957	RCD1 required for cell differentiation1 homolog	rqcd1
Str.37157.1.S1_at	-0,956	phosphatidylinositol 4-kinase type 2 alpha	pi4k2a
StrEns.4639.1.S1_s_at	-0,951	arachidonate 5-lipoxygenase-activating protein	alox5ap
Str.17801.1.A1_at	-0,951	hypothetical protein LOC100488783	LOC100488783
Str.7111.1.S1_at	-0,949	nucleophosmin/nucleoplasmin 2	npm2

Str.27139.1.S1_at	-0,945	PR domain containing 1, with ZNF domain	prdm1
Str.37891.2.S1_at	-0,939	hypothetical protein LOC100498385	LOC100498385
Str.7002.1.S1_at	-0,935	hypothetical LOC100497373	LOC100497373
StrJgi.754.1.S1_s_at	-0,931	G2/M-phase specific E3 ubiquitin protein ligase	g2e3
Str.19642.1.S1_at	-0,923	ATG16 autophagy related 16-like 1	atg16l1
Str.51307.2.S1_s_at	-0,922	hypothetical protein LOC100485101	LOC100485101
Str.5058.1.S1_at	-0,916	rhabdoid tumor deletion region gene 1	rtdr1
Str.6021.1.S1_at	-0,915	hypothetical protein MGC75753	MGC75753
StrJgi.6490.1.S1_s_at	-0,913	nischarin	nisch
Str.27191.2.S1_at	-0,912	putative ferric-chelate reductase 1-like	LOC100489839
Str.16697.1.S1_at	-0,912	nuclear receptor subfamily 1, group D, member 1	nr1d1
Str.10814.1.S1_a_at	-0,910	T, brachyury homolog	t
Str.15841.2.S1_at	-0,905	ras homolog gene family, member V	rhov
Str.10791.1.S1_at	-0,901	F-box protein 5	fbxo5
Str.29354.1.A1_at	-0,896	integrator complex subunit 4-like	LOC100498633
Str.4240.1.S1_at	-0,896	catechol-O-methyltransferase	comt
Str.37794.1.S1_at	-0,895	lysophosphatidic acid receptor 6	lpar6
Str.8913.1.S3_at	-0,890	C-terminal binding protein 2	ctbp2
Str.5871.1.S1_at	-0,888	cyclin-dependent kinase inhibitor xic1	cdknx
Str.11206.1.S1_a_at	-0,885	hypothetical LOC100496939	LOC100496939
Str.42508.1.A1_at	-0,882	v-kit Hardy-Zuckerman 4 feline sarcoma viral oncogene homolog	kit
Str.6167.1.S1_at	-0,880	phosphorylase, glycogen, muscle	pygm
Str.41326.1.S1_s_at	-0,875	hairy and enhancer of split 6, gene 1	hes6.1
StrEns.3083.1.S1_s_at	-0,873	angel homolog 2	angel2
Str.27368.1.S1_at	-0,864	HCLS1-associated protein X-1-like	LOC100485912
Str.42404.1.A1_at	-0,864	Smg-5 homolog, nonsense mediated mRNA decay factor	smg5

Str.10780.1.S1_at	-0,860	ATP synthase, H+ transporting, mitochondrial F1 complex, delta subunit	atp5d
Str.50368.2.S1_at	-0,858	retinoic acid receptor gamma-A-like	LOC100485387
StrEns.6535.1.S1_s_at	-0,857	hormonally up-regulated Neu-associated kinase	hunk
StrAffx.22.1.S1_at	-0,855	hypothetical protein LOC100486038 /// hypothetical protein LOC100487146	LOC100486038 /// LOC100487146
Str.6401.1.S1_a_at	-0,854	cullin 4B	cul4b
Str.292.1.S1_at	-0,853	KIAA0907	kiaa0907
Str.4669.1.S1_at	-0,851	hypothetical protein LOC100494135	LOC100494135
Str.4856.1.S1_at	-0,846	folate receptor 1 (adult)	folr1
Str.538.2.A1_at	-0,844	chordin	chrd
StrJgi.4129.1.S1_at	-0,844	ATPase inhibitory factor 1	atpif1
Str.169.2.S1_a_at	-0,840	sal-like 1	sall1
Str.24427.1.A1_at	-0,838	ran-binding protein 3-like	LOC100498481
Str.14235.1.S1_at	-0,835	coenzyme Q10 homolog B	coq10b
Str.16683.1.A1_at	-0,834	phosphatidylinositol 4-kinase, catalytic, alpha	pi4ka
Str.19092.2.A1_at	-0,830	RAB11 family interacting protein 1 (class I)	rab11fip1
Str.511.2.S1_at	-0,829	activating transcription factor 5	atf5
Str.31799.1.S1_at	-0,829	hypothetical protein LOC100124772	LOC100124772
Str.38847.3.S1_at	-0,827	chromosome 19 open reading frame 66	c19orf66
Str.31289.2.S1_at	-0,825	oocyte zinc finger protein XlCOF7.1-like	LOC100496553
Str.50363.2.S1_at	-0,825	COX10 homolog, cytochrome c oxidase assembly protein, heme A: farnesyltransferase	cox10
Str.10916.1.S1_at	-0,823	NADH dehydrogenase (ubiquinone) 1 beta subcomplex 4	ndufb4
Str.11181.1.S1_at	-0,823	transmembrane protein 49	tmem49
Str.471.1.S1_a_at	-0,822	ubiquitin-conjugating enzyme E2I (UBC9 homolog)	ube2i
Str.15327.1.S1_at	-0,821	chromosome 3 open reading frame 32	c3orf32
Str.37502.1.S1_at	-0,820	lipase A, lysosomal acid, cholesterol esterase	lipa

Str.10764.1.S1_a_at	-0,811	transmembrane protein 183A	tmem183a
Str.27547.1.S3_at	-0,810	hypothetical protein LOC550042	LOC550042
Str.24913.1.S1_at	-0,810	CLPTM1-like	clptm1l
Str.488.1.S1_at	-0,802	hypothetical protein MGC76328	MGC76328
Str.3639.2.S1_s_at	-0,797	ankyrin repeat domain 11	ankrd11
Str.26831.1.S1_s_at	-0,791	bone morphogenetic protein 4	bmp4
Str.4537.1.S1_at	-0,788	alpha-ketoglutarate-dependent dioxygenase alkB homolog 3-like	LOC100495476
Str.8680.1.S1_at	-0,786	lactate dehydrogenase B	ldhb
Str.26963.1.S1_at	-0,782	Hypothetical protein LOC100145127	LOC100145127
Str.3361.1.S1_at	-0,780	MAK16 homolog	mak16
Str.4965.1.S1_at	-0,777	minichromosome maintenance complex component 6	mcm6.2
StrEns.171.1.S1_s_at	-0,776	phosphatidic acid phosphatase type 2B	ppap2b
Str.6623.1.S1_at	-0,774	hypothetical protein LOC733945	LOC733945
Str.6018.1.S1_at	-0,774	hairy and enhancer of split 4	hes4
Str.15770.1.S1_at	-0,773	prostaglandin-endoperoxide synthase 2	ptgs2
Str.15499.1.S1_at	-0,772	oxysterol binding protein	osbp
Str.24757.1.S1_at	-0,764	nipsnap homolog 3A	nipsnap3a
Str.1347.1.A1_at	-0,761	integrin-linked kinase	ilk
Str.24893.1.S1_at	-0,760	SPRY domain-containing SOCS box protein 4-like	LOC100496912
Str.10257.1.S1_at	-0,756	28S ribosomal protein S18b, mitochondrial-like	LOC100489063
Str.10270.1.S1_at	-0,755	hydroxysteroid (17-beta) dehydrogenase 12	hsd17b12
StrEns.9037.1.S1_s_at	-0,755	WD repeat domain 91	wdr91
Str.16160.1.S1_at	-0,755	forkhead box I4, gene 2	foxi4.2
Str.21592.1.S1_at	-0,754	Rho/Rac guanine nucleotide exchange factor (GEF) 2	arhgef2
Str.1370.1.S1_s_at	-0,752	zinc finger, HIT-type containing 1	znhit1
Str.51820.1.S1_at	-0,749	cyclin F	ccnf
Str.34332.1.A1_s_at	-0,744	heme oxygenase (decycling) 2	hmox2
Str.2761.1.S1_at	-0,739	CD81 molecule	cd81

Str.49437.1.S1_at	-0,737	Hypothetical protein LOC100144964	LOC100144964
Str.10129.1.S1_at	-0,736	Novel solute carrier family 18 (vesicular monoamine) slca18 protein	LOC733714
Str.43415.1.S1_at	-0,731	Coiled-coil domain containing 92	ccdc92
Str.10123.1.S1_at	-0,731	glucose-fructose oxidoreductase domain containing 1	gfod1
Str.16503.1.S1_at	-0,729	adaptor-related protein complex 2, alpha 2 subunit	ap2a2
StrEns.6699.1.S1_at	-0,729	tRNA pseudouridine synthase-like 1-like	LOC100497905
Str.46269.1.A1_s_at	-0,728	chromosome 19 open reading frame 60	c19orf60
Str.19440.1.S1_a_at	-0,728	B-cell translocation gene 5	btg5
Str.381.2.A1_a_at	-0,727	ubiquilin 4	ubqln4
Str.34312.1.A1_at	-0,725	hypothetical protein LOC100492765	LOC100492765
Str.50958.1.S1_s_at	-0,721	THAP domain containing 4	thap4
Str.2540.1.S1_at	-0,714	SMAD family member 6	smad6
Str.22075.1.S1_at	-0,711	mitochondrial ribosomal protein L33	mrpl33
Str.37581.1.S1_at	-0,708	hypothetical protein LOC100489670	LOC100489670
Str.31764.1.A1_at	-0,706	neurofilament, light polypeptide	nefl
Str.5440.1.S1_at	-0,705	ariadne homolog, ubiquitin-conjugating enzyme E2 binding protein, 1	arih1
Str.49709.1.A1_s_at	-0,704	intraflagellar transport 52 homolog	ift52
Str.6196.1.S2_at	-0,704	hypothetical protein MGC75626	MGC75626
Str.11467.1.S1_at	-0,703	ferredoxin reductase	fdxr
Str.34173.3.S1_s_at	-0,703	chromosome 2 open reading frame 42	c2orf42
Str.27369.1.S2_at	-0,702	homeobox B3	hoxb3
Str.6282.1.A1_x_at	-0,702	filamin C, gamma	flnc
Str.18831.1.S1_at	-0,701	zinc finger protein 567-like	LOC100495895
Str.563.1.S1_at	-0,700	inositol-3-phosphate synthase 1	isyna1
Str.10174.1.A1_at	-0,698	single-strand-selective monofunctional uracil-DNA glycosylase 1	smug1

Str.3944.1.S1_at	-0,695	hypothetical protein LOC733539	LOC733539
StrEns.1418.1.S1_s_at	-0,695	Bloom syndrome, RecQ helicase-like	blm
Str.10015.1.S1_at	-0,694	transmembrane protein 41B	tmem41b
Str.27247.1.S2_s_at	-0,692	serine peptidase inhibitor, Kunitz type, 2	spint2
Str.29917.1.A1_at	-0,689	HMG box-containing protein	hbcx
Str.7564.2.S1_a_at	-0,689	diazepam binding inhibitor (dbi)	dbi
Str.9089.2.S1_a_at	-0,688	trans-2,3-enoyl-CoA reductase	tecr
Str.15911.1.A1_at	-0,688	hypothetical protein MGC145685	MGC145685
Str.6712.1.S1_s_at	-0,681	ribosomal protein S2	rps2
Str.6262.1.A1_at	-0,681	phosphatase and actin regulator 4	phactr4
Str.51838.1.S1_at	-0,680	leucine-rich repeats and WD repeat domain containing 1	lrwd1
Str.20309.1.A1_at	-0,677	cyclin-dependent kinase 6	cdk6
StrAffx.136.1.S1_s_at	-0,674	family with sequence similarity 160, member B2	fam160b2
Str.24290.1.S1_at	-0,674	hypothetical protein MGC147490	MGC147490
Str.32043.1.A1_at	-0,670	hypothetical protein MGC147507	MGC147507
Str.2514.1.S1_a_at	-0,668	NIMA (never in mitosis gene a)-related kinase 2	nek2
Str.21553.1.S1_at	-0,667	zinc finger protein 740	znf740
Str.862.1.S1_at	-0,664	transcription factor CP2	tfcp2
Str.1699.1.S1_at	-0,664	malate dehydrogenase 2, NAD (mitochondrial)	mdh2
StrJgi.162.1.S1_at	-0,663	serine palmitoyltransferase, long chain base subunit 3	sptlc3
Str.15129.1.S1_at	-0,660	alkB, alkylation repair homolog 5	alkbh5
Str.8533.1.A1_s_at	-0,655	caveolin 2	cav2
Str.7025.2.S2_at	-0,654	hypothetical LOC100496454	LOC100496454
Str.5456.2.A1_s_at	-0,653	arsA arsenite transporter, ATP-binding, homolog 1 (bacterial)	asna1
Str.28989.1.A1_at	-0,651	72 kDa inositol polyphosphate 5-phosphatase-like	LOC100486470
Str.7586.3.S1_a_at	-0,650	MAPK scaffold protein 1	mapksp1
Str.6355.1.S1_at	-0,648	RAD51 associated protein 1	rad51ap1

Str.10998.1.S1_at	-0,644	CNDP dipeptidase 2 (metallopeptidase M20 family)	cndp2
Str.464.1.S1_at	-0,643	radial spoke head 9 homolog	rsph9
Str.11870.1.S1_at	-0,643	collagen, type IX, alpha 3	col9a3
Str.17125.1.S1_at	-0,643	Rho family GTPase 3	rnd3
Str.17056.1.S1_a_at	-0,643	H3 histone, family 3B (H3.3B)	h3f3b
Str.28075.1.S1_s_at	-0,642	translocator protein (18kDa)	tspo
Str.8911.1.S1_at	-0,642	hippocampus abundant transcript 1	hiat1
Str.5375.2.S1_a_at	-0,640	uridine monophosphate synthetase	umps
Str.3.1.S1_a_at	-0,633	nanos homolog 1	nanos1
Str.24671.1.S1_a_at	-0,633	tubulin tyrosine ligase-like family, member 4	ttll4
Str.11129.1.S1_at	-0,631	ubiquitin-conjugating enzyme E2B (RAD6 homolog)	ube2b
Str.26863.1.S1_at	-0,631	mitochondrial ribosomal protein L40	mrpl40
Str.8957.1.A1_at	-0,630	ATG2 autophagy related 2 homolog A	atg2a
Str.21719.1.S1_at	-0,627	mitochondrial ribosomal protein L52	mrpl52
Str.6511.1.S1_at	-0,624	transmembrane protein 11	tmem11
Str.52134.1.S1_s_at	-0,620	PQ loop repeat containing 3	pqlc3
Str.31657.1.S1_at	-0,619	hypothetical protein LOC100494403	LOC100494403
Str.10064.2.S1_a_at	-0,618	MTERF domain containing 1	mterfd1
StrJgi.4070.1.S1_s_at	-0,616	glycoprotein-N-acetylgalactosamine 3-beta-galactosyltransferase 1-like	LOC100487794
Str.15041.1.S1_at	-0,616	regulator of chromosome condensation (RCC1) and BTB (POZ) domain containing protein 2	rcbtb2
Str.8025.1.S1_a_at	-0,615	keratin 18	krt18
Str.16910.1.S1_at	-0,615	activating transcription factor 4 (tax-responsive enhancer element B67)	atf4
Str.1806.1.S1_at	-0,614	Hypothetical protein MGC146711	MGC146711
Str.37447.1.S1_at	-0,613	hypothetical protein LOC100487171	LOC100487171
Str.4820.1.S2_at	-0,610	eukaryotic translation elongation factor 1 alpha 1, oocyte form	eef1a1o

Str.21822.1.S1_at	-0,610	AFG3 ATPase family gene 3-like 2 (S. cerevisiae)	afg3l2
Str.2054.1.S1_at	-0,610	YTH domain family, member 1	ythdf1
Str.6670.1.S1_at	-0,609	aldolase A, fructose-bisphosphate	aldoa
Str.11968.1.A1_at	-0,606	RAS, dexamethasone-induced 1	rasd1
Str.6981.1.S1_at	-0,606	growth arrest and DNA-damage-inducible, gamma	gadd45g
Str.7658.1.S1_at	-0,603	maternal embryonic leucine zipper kinase	melk
Str.2080.1.S1_at	-0,601	ribonuclease P 14kDa subunit	rpp14
Str.27246.1.S1_at	-0,600	SRY (sex determining region Y)-box 11	sox11
Str.1379.1.S1_at	-0,598	cell division cycle associated 7	cdca7
StrEns.9103.1.S1_at	-0,598	zinc finger homeobox protein 3-like	LOC100489378
StrEns.8056.1.S1_at	-0,598	solute carrier family 45 member 3-like	LOC100496642
Str.52196.1.S1_at	-0,598	enolase-phosphatase 1	enoph1
Str.10330.1.S2_at	-0,596	sprouty homolog 1, antagonist of FGF signaling	spry1
AFFX-Str-ef1a-5_at	-0,594	eukaryotic translation elongation factor 1 alpha 1	eef1a1
Str.27580.1.S1_at	-0,594	cat eye syndrome chromosome region, candidate 5 homolog (human)	cecr5
Str.5136.1.S1_at	-0,592	TGFB-induced factor homeobox 1	tgif1

BMO2 microarray analysis

Listed are all genes, upreglulated ≤ 1.5 fold change and with a local false discovery rate ≤ 0.2.

Set-probe number	fold change [log2]	gene name	symbol
Str.9570.1.S1_at	3,814	ribophorin II	rpn2
Str.37672.2.S1_at	3,324	LON peptidase N-terminal domain and ring finger 3	lonrf3
Str.27732.1.S1_at	3,160	GTP binding protein 5 (putative)	gtpbp5
Str.21604.1.S1_at	2,113	5'-nucleotidase, cytosolic III	nt5c3
Str.11279.1.S1_at	2,102	unc-45 homolog B	unc45b
Str.51882.1.S1_at	2,061	chromosome 20 open reading frame 29	c20orf29
Str.4820.1.S2_at	1,858	eukaryotic translation elongation factor 1 alpha 1, oocyte form	eef1a1o
Str.7641.1.S3_at	1,754	B-cell translocation gene 1, anti-proliferative	btg1
Str.11402.1.A1_at	1,747	protein phosphatase 1, regulatory (inhibitor) subunit 3C, gene 1	ppp1r3c.1
Str.27919.1.A1_at	1,669	nuclear factor, interleukin 3 regulated	nfil3
Str.52226.1.S2_at	1,613	chromosome 1 open reading frame 93	c1orf93
Str.21588.1.S1_at	1,548	T, brachyury homolog, gene 2	t2
Str.8423.1.S1_at	1,484	chromosome 6 open reading frame 211	c6orf211
Str.16459.1.S1_at	1,483	hect (homologous to the E6-AP (UBE3A) carboxyl terminus) domain and RCC1 (CHC1)-like domain (RLD) 1	herc1
Str.51692.1.S1_at	1,305	novel protein-like	LOC733728
Str.37449.1.A1_at	1,273	poly (ADP-ribose) polymerase family, member 4	parp4
Str.2357.1.S1_at	1,204	forkhead box I1	foxi1
Str.20514.1.S1_at	1,180	FBJ murine osteosarcoma viral oncogene homolog	fos
Str.52097.1.S1_at	1,169	ATPase type 13A5	atp13a5
Str.25548.1.A1_at	1,161	amyloid protein-binding protein 2-like	LOC100487715
Str.11288.1.S1_at	1,105	hypothetical LOC100486074	LOC100486074

Str.16957.1.S2_at	1,071	fused in sarcoma	fus
Str.21032.2.S1_a_at	1,069	MGC89871 protein	MGC89871
Str.3485.1.S1_at	1,067	rho GTPase-activating protein 11A-like	LOC100495220
Str.49500.1.S2_at	1,056	stearoyl-CoA desaturase (delta-9-desaturase)	scd
Str.16732.1.S2_at	1,046	v-myc myelocytomatosis viral related oncogene, neuroblastoma derived	mycn
Str.11260.1.S1_at	1,045	hairy and enhancer of split 5, gene 1	hes5.1
Str.21086.2.S1_s_at	1,038	glutamate receptor, ionotropic, N-methyl D-aspartate-like 1A	grinl1a
Str.6857.1.S2_at	1,004	eukaryotic translation termination factor 1	etf1
Str.17056.1.S1_a_at	0,980	H3 histone, family 3B (H3.3B)	h3f3b
Str.5851.1.S1_at	0,978	PDZ binding kinase	pbk
Str.27186.1.S1_s_at	0,955	histone H3.2-like	LOC100496129
Str.22588.1.S1_at	0,950	chromosome 11 open reading frame 2	c11orf2
Str.14144.2.A1_at	0,946	zinc finger and BTB domain containing 5	zbtb5
Str.21295.1.S1_a_at	0,901	nudix (nucleoside diphosphate linked moiety X)-type motif 16	nudt16
Str.51420.1.S1_at	0,895	iron-sulfur cluster assembly 2 homolog	isca2
Str.27913.1.S1_at	0,867	acidic repeat containing	acrc
Str.1999.1.S1_at	0,863	superoxide dismutase 1, soluble	sod1
Str.27324.1.S2_at	0,858	ras-related protein ras-dva	ras-dva
Str.27848.1.S1_at	0,848	egl nine homolog 3	egln3
Str.15757.1.S1_at	0,836	dihydrofolate reductase	dhfr
Str.27290.1.S1_at	0,816	ribonuclease H2, subunit A	rnaseh2a
Str.17024.1.S1_at	0,809	X-ray repair complementing defective repair in Chinese hamster cells 3	xrcc3
Str.51912.1.S1_at	0,806	S100P binding protein	s100pbp
Str.15137.1.S1_at	0,804	ADP-ribosylation factor-like 6 interacting protein 1	arl6ip1
Str.51459.1.S1_at	0,798	neurobeachin	nbea
Str.51053.2.A1_s_at	0,789	human immunodeficiency virus type I enhancer binding protein 2	hivep2

Str.40497.1.S1_at	0,785	ras-related C3 botulinum toxin substrate 3 (rho family, small GTP binding protein Rac3)	rac3
Str.51787.1.S1_at	0,782	histone cluster 1, H2ah	hist1h2ah
StrEns.3693.1.S1_s_at	0,766	hypothetical protein EGF-like module-containing mucin-like hormone receptor-like 1-like	LOC100490769 LOC100490939
StrEns.6148.1.S1_a_at	0,763	peptide chain release factor 1, mitochondrial-like	LOC100486280
Str.8101.1.S1_at	0,758	ferritin, heavy polypeptide 1	fth1
Str.20232.1.S1_at	0,757	Hypothetical protein LOC100144290	LOC100144290
Str.37700.1.S1_at	0,751	nuclear factor of kappa light polypeptide gene enhancer in B-cells inhibitor, zeta	nfkbiz
StrAffx.238.1.S1_at	0,740	integrator complex subunit 12	ints12
Str.15265.1.S1_at	0,725	novel helix-loop-helix DNA binding domain protein	LOC733709
Str.17731.1.S1_at	0,724	general transcription factor 3A	gtf3a
Str.6900.1.S2_s_at	0,717	ER degradation enhancer, mannosidase alpha-like 1 angiopoietin-related protein 1-like	edem1 LOC100491105
Str.13001.1.S1_at	0,717	MAD2 mitotic arrest deficient-like 1	mad2l1
Str.24585.1.S1_at	0,713	apolipoprotein O	apoo
Str.32445.1.S1_at	0,706	tubulin alpha-1D chain-like MGC97820 protein	LOC100487867 MGC97820
Str.31142.1.S1_at	0,704	transmembrane protein, adipocyte asscociated 1	tpra1
Str.101.1.S1_at	0,703	replication factor C (activator 1) 5, 36.5kDa	rfc5
Str.27997.1.S1_at	0,701	hypothetical protein LOC100498215	LOC100498215
Str.21484.1.A1_s_at	0,701	pyruvate dehyrogenase phosphatase catalytic subunit 1	pdp1
Str.7662.1.S1_at	0,700	fatty acid 2-hydroxylase	fa2h
Str.34983.1.A1_s_at	0,698	Hypothetical protein LOC779512	LOC779512
Str.39187.1.S1_at	0,697	mTERF domain-containing protein 3, mitochondrial-like	LOC100485703

Str.26008.1.S1_at	0,688	hypothetical protein LOC100498571	LOC100498571
Str.38888.1.S1_at	0,679	transcription factor AP-1-like	LOC100493911
Str.40052.1.S1_at	0,677	promethin-A-like	LOC100486925
Str.40271.2.S1_a_at	0,674	Hypothetical protein LOC550005	LOC550005
Str.52018.1.S1_at	0,673	zinc finger protein 16	znf16
Str.45299.1.A1_s_at	0,670	hypothetical LOC548351	LOC548351
Str.26767.1.S1_at	0,663	dual serine/threonine and tyrosine protein kinase	dstyk
Str.37936.1.A1_at	0,660	fibroblast growth factor 20	fgf20
Str.15499.1.S1_at	0,649	oxysterol binding protein	osbp
Str.18904.1.S1_at	0,646	junctophilin 1	jph1
StrEns.10243.1.S1_at	0,642	thyrotropin subunit beta-like	LOC100496349
Str.9548.3.A1_at	0,639	28S ribosomal protein S25, mitochondrial-like	LOC100494871
Str.13245.1.S1_at	0,633	heat shock 70kDa protein 9 (mortalin)	hspa9
Str.25272.1.S1_at	0,626	retinoid X receptor, gamma	rxrg
Str.27358.1.S1_at	0,622	transmembrane protease, serine 11F	tmprss11f
Str.7160.3.A1_at	0,618	ubiquinone biosynthesis methyltransferase COQ5, mitochondrial-like	LOC100495452
Str.29780.1.A1_at	0,617	Fanconi anemia, complementation group D2	fancd2
Str.20243.1.S1_at	0,607	SET and MYND domain containing 4	smyd4
Str.31445.1.S1_at	0,606	inhibitor of growth family, member 1	ing1
Str.28441.1.S1_at	0,605	SNF related kinase	snrk

Listed are all genes, downreglulated ≤ 1.5 fold change and with a local false discovery rate ≤ 0.2.

Set-probe number	fold change [log2]	gene name	symbol
Str.24244.1.S1_at	-1,344	SRY (sex determining region Y)-box 21	sox21
Str.24947.1.S1_at	-1,308	ADP-ribosylation factor 4	arf4
Str.11939.1.S1_at	-1,303	l-amino-acid oxidase-like	LOC100496394
Str.5401.1.S1_at	-1,235	retinal pigment epithelium-specific protein 65kDa	rpe65
Str.15587.1.S1_at	-1,230	hypothetical protein LOC100487200	LOC100487200
Str.11165.7.S1_at	-1,206	sarcoplasmic/endoplasmic reticulum calcium ATPase 2-like	LOC100489059
Str.6222.1.S1_at	-1,120	annexin A2	anxa2
Str.10362.1.A1_at	-1,111	hypothetical LOC100493109	LOC100493109
Str.15223.9.A1_at	-1,110	14 kDa phosphohistidine phosphatase-like	LOC100497662
Str.10659.1.S1_at	-1,110	transcription factor AP-2 epsilon (activating enhancer binding protein 2 epsilon)	tfap2e
Str.17388.1.S1_at	-1,078	hypothetical LOC100495861	LOC100495861
Str.42272.1.A1_at	-1,035	Zinc finger, CCHC domain containing 2	zcchc2
StrEns.6291.1.S1_s_at	-1,029	nucleoporin 155kDa	nup155
Str.21950.1.S1_at	-1,021	hypothetical LOC100488570	LOC100488570
Str.420.1.S1_at	-1,008	ABO blood group (transferase A, alpha 1-3-N-acetylgalactosaminyltransferase; transferase B, alpha 1-3-galactosyltransferase)	abo
StrEns.8369.1.S1_at	-0,961	growth/differentiation factor 2-like	LOC100485289
Str.6623.1.S1_at	-0,953	hypothetical protein LOC733945	LOC733945
Str.7820.2.S1_a_at	-0,952	immediate early response gene 2 protein-like	LOC100491464
StrEns.12689.1.S1_s_at	-0,910	ERGIC and golgi 2	ergic2
StrJgi.8475.1.S1_s_at	-0,908	SNAP-associated protein	snapin
Str.8913.1.S3_at	-0,905	C-terminal binding protein 2	ctbp2
Str.27847.1.A1_at	-0,899	hypothetical protein LOC100493690	LOC100493690
Str.12012.1.S1_at	-0,894	ankyrin repeat domain 10	ankrd10

Str.31510.1.S1_at	-0,894	Hypothetical protein MGC146314	MGC146314
Str.4321.1.S1_at	-0,888	RNA pseudouridylate synthase domain containing 4	LOC734064
Str.21559.2.S1_x_at	-0,868	Y box binding protein 2	ybx2
Str.36616.1.A1_at	-0,844	haloacid dehalogenase-like hydrolase domain containing 3	hdhd3
Str.10535.1.S1_at	-0,841	hypothetical LOC100495377	LOC100495377
Str.6659.1.S1_at	-0,820	nerve growth factor receptor	ngfr
Str.11483.1.S1_at	-0,808	leucine-rich repeat-containing protein 8C-like leucine rich repeat containing 8 family, member C	LOC100488426 lrrc8c
Str.643.1.S1_a_at	-0,792	hypothetical LOC100486597	LOC100486597
Str.26763.1.S1_at	-0,779	chromosome 15 open reading frame 44	c15orf44
Str.51988.1.S1_at	-0,771	serine/arginine-rich splicing factor 11	srsf11
Str.21643.1.S1_at	-0,767	serpin peptidase inhibitor, clade I (neuroserpin), member 1	serpini1
StrJgi.1740.1.S1_at	-0,764	Na+/H+ exchanger domain containing 2	nhedc2
Str.27583.2.S1_at	-0,763	COX assembly mitochondrial protein homolog	cmc1
Str.1431.1.S1_at	-0,753	hypothetical protein LOC100124857	LOC100124857
Str.21898.1.S1_at	-0,710	NADH dehydrogenase (ubiquinone) 1 alpha subcomplex, 11, 14.7kDa	ndufa11
Str.21613.1.S1_a_at	-0,705	Calponin 2	cnn2
Str.39270.1.A1_at	-0,694	bone morphogenetic protein 15-like	LOC100485893
Str.1984.1.S1_at	-0,689	solute carrier family 9 (sodium/hydrogen exchanger), member 3 regulator 1	slc9a3r1
Str.3624.1.S1_at	-0,682	APEX nuclease (apurinic/apyrimidinic endonuclease) 2	apex2
Str.17660.1.S1_at	-0,679	interferon-related developmental regulator 1	ifrd1
Str.15669.1.S1_at	-0,673	nuclear receptor subfamily 2, group F, member 1	nr2f1

Str.10016.1.S1_at	-0,661	cdc42 effector protein (Rho GTPase binding) 4	cdc42ep4
Str.51981.1.S1_s_at	-0,659	formin binding protein 4	LOC734003
Str.39300.1.S2_at	-0,657	MGC97787 protein	MGC97787
Str.27368.1.S1_at	-0,653	HCLS1-associated protein X-1-like	LOC100485912
Str.5388.1.S1_a_at	-0,652	calcium homeostasis modulator 2	calhm2
Str.5015.1.A1_at	-0,638	neural precursor cell expressed, developmentally down-regulated 9	nedd9
Str.37633.1.S1_at	-0,635	aminopeptidase-like 1	npepl1
StrJgi.1688.1.S1_at	-0,626	hypothetical protein LOC100495013	LOC100495013
Str.8618.1.S1_a_at	-0,620	ATPase, H+ transporting, lysosomal 14kDa, V1 subunit F	atp6v1f
Str.21553.1.S1_at	-0,613	zinc finger protein 740	znf740
Str.27567.1.S2_at	-0,606	polymerase (RNA) III (DNA directed) polypeptide E (80kD)	polr3e
Str.1806.1.S1_at	-0,605	Hypothetical protein MGC146711	MGC146711
Str.28803.2.S1_a_at	-0,603	hypothetical LOC100486098	LOC100486098

Pre/postMBT microarray analysis

Listed are all genes, upreglulated ≥ 5.65 fold change and with an adjusted *p*-value ≤ 0.05.

Set-probe number	fold change [log2]	gene name	symbol
Str.14985.1.S1_at	11,53	eomesodermin	eomes
Str.20300.1.S1_a_at	11,38	mix-like endodermal regulator	mixer
Str.1534.1.S1_at	11,09	hypothetical LOC100487344	LOC100487344
Str.6030.1.S1_at	11,09	forkhead box A4	foxa4
Str.15007.1.S1_at	10,74	gastrula-specific protein 17	gs17
Str.10688.1.S1_at	10,28	hypothetical protein LOC100170595 putative nuclease HARBI1-like	LOC100170595 LOC100492963
Str.37794.1.S1_at	10,24	lysophosphatidic acid receptor 6	lpar6
Str.112.1.S1_at	10,12	Brachyury-inducible homeobox 1, gene 1 homeobox protein Mix.1-like	bix1.1 LOC100491743
Str.10234.1.S2_at	10,10	Zic family member 3 (odd-paired homolog)	zic3
Str.10066.1.S1_at	10,07	mesendoderm nuclear factor, gene 1	menf.1
Str.113.1.S1_at	10,02	mix1 homeobox	mix1
Str.30719.1.A1_s_at	9,97	ras homolog gene family, member V	rhov
Str.11884.1.S1_at	9,86	anti-dorsalizing morphogenic protein	admp
Str.17224.1.S1_at	9,83	Zic family member 1 (odd-paired homolog)	zic1
Str.10058.1.S1_at	9,62	syntaxin 19	stx19
Str.6151.1.S1_at	9,50	ATPase, Na+/K+ transporting, beta 2 polypeptide	atp1b2
Str.447.1.S1_at	9,48	ATPase, H+/K+ transporting, nongastric, alpha polypeptide	atp12a
Str.41254.1.S1_s_at	9,47	SRY (sex determining region Y)-box 2	sox2
Str.6141.1.S1_a_at	9,39	glycine amidinotransferase (L-arginine:glycine amidinotransferase)	gatm
Str.7025.2.S2_at	9,36	hypothetical LOC100496454	LOC100496454
StrJgi.4169.1.S1_s_at	9,32	hypothetical protein LOC100488209	LOC100488209
Str.7482.2.S1_a_at	9,31	protocadherin 8, gene 2	pcdh8.2

Str.4932.1.S1_a_at	9,17	hypothetical protein LOC100494704 VENT homeobox 2, gene 1	LOC100494704 ventx2.1
Str.15097.1.S1_a_at	9,15	hypothetical protein hypothetical protein	LOC100497333 LOC100498266
Str.538.2.A2_at	9,14	chordin	chrd
Str.6229.2.S1_at	9,12	ephrin-B2	efnb2
Str.2980.2.A1_a_at	9,05	transcription factor AP-2 alpha (activating enhancer binding protein 2 alpha)	tfap2a
Str.6718.1.S1_at	8,97	hypothetical LOC100494381	LOC100494381
Str.11206.1.S1_a_at	8,93	hypothetical LOC100496939	LOC100496939
Str.20278.2.A1_a_at	8,90	hypothetical protein LOC100489209	LOC100489209
StrJgi.7797.1.S1_s_at	8,84	hyaluronan synthase 2	has2
Str.15369.1.S1_at	8,76	hypothetical protein LOC100127584	LOC100127584
Str.10804.1.S2_s_at	8,76	keratin 5, gene 7	krt5.7
Str.79.2.S1_at	8,75	POU domain, class 5, transcription factor 1.2-like	LOC100498076
Str.114.1.S1_at	8,74	SRY (sex determining region Y)-box 17 alpha	sox17a
Str.1955.1.S1_at	8,73	hypothetical protein LOC100491352	LOC100491352
Str.20147.1.S1_at	8,73	fibroblast growth factor 8 (androgen-induced)	fgf8
Str.42150.1.S1_at	8,64	novel zinc finger protein	LOC733912
Str.10814.1.S1_a_at	8,56	T, brachyury homolog	t
Str.7018.1.S1_at	8,56	frizzled-related protein	frzb
Str.10716.1.S1_at	8,55	forkhead box D4-like 1, gene 1	foxd4l1.1
Str.4900.1.S1_at	8,53	zinc finger protein 470	znf470
Str.51679.2.S3_a_at	8,52	hypothetical protein LOC100498064	LOC100498064
StrJgi.754.1.S1_s_at	8,48	G2/M-phase specific E3 ubiquitin protein ligase	g2e3
Str.51679.2.S1_a_at	8,41	hypothetical protein LOC100498497	LOC100498497
Str.14655.1.S2_at	8,39	LIM homeobox 5	lhx5
Str.7693.2.S1_at	8,37	VENT homeobox 1, gene 1	ventx1.1
Str.52227.2.A1_a_at	8,31	hypothetical LOC100484994 hypothetical LOC100486020 hypothetical LOC100489931 hypothetical LOC100490293 hypothetical LOC100492588 hypothetical LOC100498560	LOC100484994 LOC100486020 LOC100489931 LOC100490293 LOC100492588 LOC100498560

Str.7447.2.A1_at	8,30	Heterogeneous nuclear ribonucleoprotein D-like	hnrpdl
Str.15963.1.S1_at	8,29	tyrosine aminotransferase	tat
Str.7571.1.S1_a_at	8,29	hypothetical LOC100491682	LOC100491682
Str.15754.1.S1_s_at	8,26	fibronectin leucine rich transmembrane protein 3	flrt3
Str.2944.1.S1_at	8,26	cone-rod homeobox	crx
Str.490.1.S2_at	8,20	bone morphogenetic protein 4	bmp4
Str.2572.2.S1_x_at	8,20	hypothetical protein LOC100487243	LOC100487243
Str.14828.1.S1_at	8,18	left-right determination factor	lefty
Str.7571.2.S1_a_at	8,16	hypothetical LOC100491590 hypothetical LOC100491682 hypothetical LOC100493923	LOC100491590 LOC100491682 LOC100493923
Str.31317.1.S1_at	8,14	hypothetical protein LOC100487186	LOC100487186
Str.6731.1.S1_at	8,14	zinc finger protein 750	znf750
Str.51845.1.A1_at	8,00	hypothetical protein MGC69473	MGC69473
Str.1534.1.S2_a_at	7,96	hypothetical protein LOC100495042	LOC100495042
Str.2572.4.A1_a_at	7,94	hypothetical LOC100488588	LOC100488588
Str.10455.1.S1_at	7,86	hypothetical LOC100495538	LOC100495538
Str.7017.1.S1_at	7,86	SRY (sex determining region Y)-box 17 beta, gene 2	sox17b.2
Str.15027.1.S1_at	7,85	wingless-type MMTV integration site family, member 8A	wnt8a
Str.1702.1.S1_at	7,78	secreted frizzled-related protein 2	sfrp2
Str.52227.1.S1_a_at	7,76	hypothetical protein LOC100492588	LOC100492588
Str.17465.2.S1_a_at	7,67	hypothetical LOC100493277	LOC100493277
Str.3072.1.S1_at	7,65	grainyhead-like 3	grhl3
Str.6681.1.S1_a_at	7,60	keratin	krt
Str.6282.1.A1_x_at	7,59	filamin C, gamma	flnc
Str.6185.1.S1_at	7,58	cornifelin homolog	cnfn
Str.7693.2.S1_a_at	7,50	VENT homeobox 1, gene 1 VENT homeobox 1, gene 2	ventx1.1 ventx1.2
Str.740.1.S1_at	7,44	chromosome 3 open reading frame 54	c3orf54
Str.10337.1.S1_at	7,37	dual specificity phosphatase 6	dusp6

Str.27989.2.A1_s_at	7,34	piggyBac transposable element-derived protein 4-like	LOC100494255
Str.21559.2.S1_x_at	7,25	Y box binding protein 2	ybx2
Str.30372.1.S1_x_at	7,15	Nucleolar protein 5A (56kDa with KKE/D repeat)	TEgg001j23.1
Str.27186.1.S1_at	7,15	histone cluster 2, H3c	hist2h3c
Str.36384.1.S1_at	7,15	nodal homolog 2-A-like	LOC100491883
Str.6900.1.S2_s_at	7,14	ER degradation enhancer, mannosidase alpha-like 1 angiopoietin-related protein 1-like	edem1 LOC100491105
Str.10803.1.S1_at	7,13	goosecoid homeobox	gsc
Str.15.1.S1_at	7,13	cell division cycle 25 homolog B	cdc25b
Str.49496.1.S1_s_at	7,11	apelin receptor	aplnr
Str.27467.1.S1_at	7,11	zinc finger protein 350	znf350
Str.10021.1.S1_at	7,11	orthodenticle homeobox 2	otx2
Str.11939.1.S1_at	7,06	l-amino-acid oxidase-like	LOC100496394
Str.30175.1.S1_at	7,04	VENT homeobox 3, gene 2	ventx3.2
Str.6981.1.S1_at	7,04	growth arrest and DNA-damage-inducible, gamma	gadd45g
Str.8142.1.A1_at	7,03	TSC22 domain family, member 3	tsc22d3
Str.23268.1.A1_at	6,99	peptidase M20 domain containing 1	pm20d1
Str.37312.1.S1_x_at	6,95	hypothetical protein LOC100145106	LOC100145106
Str.10236.1.S1_at	6,94	receptor-interacting serine-threonine kinase 4	ripk4
Str.7735.3.S1_a_at	6,91	nodal homolog 3-B-like nodal homolog nodal homolog 3, gene 2	LOC100491713 nodal nodal3.2
Str.25552.1.S2_at	6,90	lysophosphatidic acid receptor 2	lpar2
Str.7693.1.S1_at	6,79	VENT homeobox 1, gene 2	ventx1.2
Str.7073.1.S1_at	6,79	iroquois homeobox 2	irx2
Str.16160.1.S1_at	6,79	forkhead box I4, gene 2	foxi4.2
Str.8390.1.S2_at	6,75	GATA binding protein 4	gata4
Str.16319.2.S1_at	6,68	hypothetical protein LOC100489354	LOC100489354
Str.11968.1.A1_at	6,63	RAS, dexamethasone-induced 1	rasd1
Str.10727.1.S1_at	6,63	deoxyribonuclease gamma-like	LOC100497175

Str.10803.1.S1_s_at	6,62	goosecoid homeobox hypothetical LOC100135186	gsc LOC100135186
Str.12750.1.A1_at	6,62	LIM homeobox 1	lhx1
Str.1716.1.S1_x_at	6,58	purinergic receptor P2Y, G-protein coupled, 2	p2ry2
Str.27405.1.A1_at	6,47	WNT1 inducible signaling pathway protein 3	wisp3
Str.15223.4.S1_a_at	6,42	eukaryotic translation initiation factor 4A2	eif4a2
Str.8895.3.S3_at	6,42	GATA-binding factor 2-like	LOC100487142
StrEns.9366.1.S1_a_at	6,38	oocyte zinc finger protein XlCOF6-like	LOC100495878
Str.36919.1.S1_at	6,37	VENT homeobox 3, gene 1	ventx3.1
Str.1534.1.S2_at	6,35	hypothetical protein hypothetical protein hypothetical protein	LOC100489830 LOC100494885 LOC100495042
Str.15023.1.S1_a_at	6,33	dickkopf 1	dkk1
Str.1273.1.S1_at	6,28	histone H4-like	LOC100496593
Str.52067.1.S1_s_at	6,28	zinc finger protein 568	znf568
Str.51804.1.S1_at	6,27	chemokine (C-X-C motif) receptor 7	cxcr7
Str.27170.2.A1_x_at	6,27	hypothetical protein LOC100145554	LOC100145554
Str.488.1.S1_at	6,26	hypothetical protein MGC76328	MGC76328
Str.16849.2.S1_at	6,25	histidine ammonia-lyase, gene 1	hal.1
Str.27139.1.S1_at	6,22	PR domain containing 1, with ZNF domain	prdm1
Str.27989.1.S1_at	6,21	hypothetical protein LOC100493710	LOC100493710
Str.8101.1.S1_at	6,19	ferritin, heavy polypeptide 1	fth1
Str.6630.1.S2_at	6,18	X-box binding protein 1	xbp1
Str.17625.1.S1_at	6,14	hypothetical LOC100495344	LOC100495344
Str.4744.1.S1_at	6,11	dual specificity phosphatase 5	dusp5
Str.6659.1.S1_at	6,11	nerve growth factor receptor	ngfr
Str.8646.3.S1_a_at	6,11	inhibitor of DNA binding 3, dominant negative helix-loop-helix protein	id3
Str.21522.1.S1_at	6,10	uroplakin 2	upk2
Str.42133.2.A1_at	6,09	hypothetical LOC100486754	LOC100486754
Str.27583.3.S1_at	6,07	MGC89648 protein	MGC89648
Str.266.1.S1_at	6,06	chemokine (C-X-C motif) receptor 4	cxcr4
Str.42133.1.S1_x_at	6,02	zinc finger protein 33A	znf33a

Str.51679.2.S2_at	6,00	hypothetical protein hypothetical protein	LOC100498064 LOC100498497
Str.51828.3.S1_s_at	5,99	hypothetical protein LOC100489130	LOC100489130
Str.3160.2.S1_a_at	5,97	serine/arginine-rich splicing factor 6	srsf6
Str.26882.1.S1_at	5,96	siamois homeodomain 1	sia1
Str.10008.1.S1_at	5,90	hypothetical protein LOC100487199	LOC100487199
Str.12012.1.S1_at	5,88	ankyrin repeat domain 10	ankrd10
Str.27186.1.S1_s_at	5,84	histone H3.2-like	LOC100496129
Str.52193.1.S1_at	5,83	High-mobility group nucleosomal binding domain 2	TEgg003n10.1
StrJgi.8558.1.S1_s_at	5,81	hypothetical protein hypothetical protein hypothetical protein hypothetical protein hypothetical protein	LOC100486020 LOC100488381 LOC100493631 LOC100494089 LOC100498455
Str.43435.1.A1_s_at	5,81	heart and neural crest derivatives expressed 2	hand2
StrEns.11954.1.S1_a_at	5,79	hypothetical protein LOC100494960	LOC100494960
Str.9440.1.S1_at	5,77	activated leukocyte cell adhesion molecule	alcam
Str.37384.1.S1_at	5,69	frizzled homolog 8	fzd8
Str.33.1.S1_at	5,67	protein kinase domain containing, cytoplasmic homolog, gene 1	pkdcc.1
StrEns.171.1.S1_s_at	5,65	phosphatidic acid phosphatase type 2B	ppap2b
Str.50024.1.S1_at	5,64	serine dehydratase	sds
Str.49462.1.S1_at	5,60	T-box 2	tbx2
Str.30427.1.S1_at	5,57	StAR-related lipid transfer (START) domain containing 13	stard13
Str.48764.1.A1_at	5,56	Mdm2 p53 binding protein homolog	mdm2
Str.11235.2.S1_at	5,52	hypothetical protein LOC100145165	LOC100145165
Str.31298.1.S1_at	5,50	iroquois homeobox 1	irx1
Str.10459.1.A1_at	5,49	Ubiquitin-conjugating enzyme E2D 3 (UBC4/5 homolog)	ube2d3
Str.6149.1.S1_at	5,47	glutamine--fructose-6-phosphate transaminase 1	gfpt1
Str.51121.1.S1_at	5,45	Kruppel-like factor 17	klf17

Str.23519.2.S1_a_at	5,44	Death inducer-obliterator 1	dido1
Str.6018.1.S1_at	5,43	hairy and enhancer of split 4	hes4
Str.26907.1.S1_at	5,43	nodal homolog 1	nodal1
Str.6304.1.S2_at	5,42	calponin 1, basic, smooth muscle	cnn1
Str.36162.1.A1_at	5,41	hypothetical protein LOC100498210	LOC100498210
Str.20470.1.S2_at	5,38	cyclin E2	ccne2
StrAffx.22.1.S1_at	5,37	hypothetical protein hypothetical protein	LOC100486038 LOC100487146
Str.21783.1.S1_at	5,36	Sec61 alpha 1 subunit (S. cerevisiae)	sec61a1
Str.41326.1.S1_s_at	5,33	hairy and enhancer of split 6, gene 1	hes6.1
Str.1865.1.S1_at	5,30	cerberus 1, cysteine knot superfamily	cer1
Str.18694.2.S1_x_at	5,29	hypothetical protein LOC100498107	LOC100498107
Str.2177.1.A1_a_at	5,26	sphingosine-1-phosphate receptor 5	s1pr5
Str.20538.3.A1_at	5,24	hypothetical protein LOC100497342	LOC100497342
Str.17388.1.S1_at	5,24	hypothetical LOC100495861	LOC100495861
Str.27013.1.S1_a_at	5,22	uroplakin 3B	upk3b
Str.37201.1.S1_at	5,18	melanopsin-B-like	LOC100495677
Str.27847.1.A1_at	5,16	hypothetical protein LOC100493690	LOC100493690
Str.27924.1.S1_at	5,14	zinc finger protein ZIC 4-like	LOC100493609
Str.48741.1.S1_x_at	5,13	Peptidyl-prolyl isomerase G (cyclophilin G)	ppig
Str.16957.1.S1_at	5,12	fused in sarcoma	fus
Str.11165.7.S1_at	5,10	sarcoplasmic/endoplasmic reticulum calcium ATPase 2-like	LOC100489059
StrJgi.6845.1.S1_x_at	5,08	oocyte zinc finger protein XlCOF7.1-like	LOC100495340
Str.20538.1.S2_a_at	5,07	KH domain containing, RNA binding, signal transduction associated 1	khdrbs1
Str.420.1.S2_a_at	5,07	ABO blood group (transferase A, alpha 1-3-N-acetylgalactosaminyltransferase; transferase B, alpha 1-3-galactosyltransferase)	abo
Str.37703.1.S1_at	5,04	transportin 1	tnpo1
StrEns.4645.1.S1_at	5,04	nodal homolog 4-A-like	LOC100497218

Str.24746.1.S1_at	5,04	solute carrier family 43, member 1	slc43a1
StrEns.8996.1.S1_a_at	5,03	hypothetical protein LOC100496030	LOC100496030
Str.10535.1.S1_at	4,98	hypothetical LOC100495377	LOC100495377
Str.8191.1.S2_at	4,96	phospholipase A2, group XIIB	pla2g12b
StrJgi.784.1.S1_s_at	4,95	retinoblastoma-like 1 (p107)	rbl1
Str.5015.1.A1_at	4,95	neural precursor cell expressed, developmentally down-regulated 9	nedd9
Str.37936.1.A1_at	4,92	fibroblast growth factor 20	fgf20
Str.111.1.S1_at	4,91	hematopoietically expressed homeobox	hhex
Str.16175.1.S1_a_at	4,90	growth differentiation factor 3	gdf3
Str.9391.1.A1_at	4,90	Hypothetical protein LOC549444	LOC549444
Str.50563.1.A1_at	4,90	Hypothetical protein LOC100216216	LOC100216216
Str.6578.1.S2_a_at	4,86	serine/arginine-rich splicing factor 1	srsf1
Str.6723.1.S1_x_at	4,84	pinhead	pnhd
Str.154.1.S1_at	4,84	frizzled homolog 10	fzd10
Str.18694.1.S1_at	4,84	uncharacterized protein ywlC-like	LOC100497798
Str.20533.6.S1_x_at	4,83	hypothetical LOC100486606	LOC100486606
Str.28734.1.A1_at	4,81	hypothetical protein LOC100489967	LOC100489967
Str.40271.2.S1_a_at	4,80	Hypothetical protein LOC550005	LOC550005
Str.16161.1.S1_at	4,80	sizzled	szl
Str.11217.1.S1_at	4,78	MGC89906 protein	MGC89906
Str.10785.1.S1_at	4,77	hypothetical LOC100497479	LOC100497479
Str.1843.1.S1_at	4,76	v-ski sarcoma viral oncogene homolog	ski
Str.10305.2.S1_at	4,74	hypothetical protein LOC100216037	LOC100216037
Str.18775.1.S1_at	4,69	CKLF-like MARVEL transmembrane domain containing 8	cmtm8
Str.3002.1.A1_at	4,67	Hypothetical protein LOC779546	LOC779546
Str.43058.1.S1_at	4,60	zinc finger protein	LOC100337651
Str.1183.1.S1_at	4,56	transmembrane protein 127	tmem127
Str.6139.1.S2_at	4,55	GATA binding protein 6	gata6

Str.7077.1.A1_at	4,55	hormonally up-regulated Neu-associated kinase	hunk
Str.7705.5.S1_at	4,51	odd-skipped related 2	osr2
Str.28286.1.S1_at	4,51	RNA binding motif protein 25	rbm25
Str.15853.1.S1_at	4,49	pleckstrin homology domain-containing family N member 1-like	LOC100491834
Str.6156.1.S1_a_at	4,49	forkhead box C1	foxc1
StrJgi.7085.1.S1_s_at	4,49	PR domain containing 9	prdm9
Str.18694.2.S1_a_at	4,49	uncharacterized protein ywlC-like hypothetical protein	LOC100497798 LOC100498107
Str.15587.1.S1_at	4,48	hypothetical protein LOC100487200	LOC100487200
Str.1567.1.S2_at	4,47	ST6 (alpha-N-acetyl-neuraminyl-2,3-beta-galactosyl-1,3)-N-acetylgalactosaminide alpha-2,6-sialyltransferase 2	st6galnac2
Str.28803.2.S1_a_at	4,47	hypothetical LOC100486098	LOC100486098
Str.37570.1.S1_at	4,45	solute carrier family 7 (cationic amino acid transporter, y+ system), member 3	slc7a3
Str.51825.1.S1_at	4,44	Hypothetical protein LOC733820	LOC733820
Str.10072.1.S2_at	4,43	Solute carrier family 2 (facilitated glucose transporter), member 2	slc2a2
Str.24244.1.S1_at	4,41	SRY (sex determining region Y)-box 21	sox21
Str.31333.1.S1_a_at	4,40	protein kinase domain containing, cytoplasmic homolog, gene 2	pkdcc.2
Str.11402.1.A1_at	4,35	protein phosphatase 1, regulatory (inhibitor) subunit 3C, gene 1	ppp1r3c.1
Str.10016.1.S1_at	4,35	cdc42 effector protein (Rho GTPase binding) 4	cdc42ep4
Str.10174.1.A1_at	4,32	single-strand-selective monofunctional uracil-DNA glycosylase 1	smug1
Str.10713.1.S1_at	4,30	growth arrest-specific 1	gas1
Str.14504.1.S1_at	4,29	rho GTPase-activating protein 39-like	LOC100485974

Str.1093.1.S1_at	4,26	ADP-ribosylation factor-like 4C	arl4c
Str.9958.1.S1_at	4,25	chromosome 7 open reading frame 11	c7orf11
Str.954.1.S1_at	4,24	potassium channel tetramerisation domain containing 15	kctd15
Str.5982.1.S1_a_at	4,22	darmin	darmin
StrEns.1208.1.S1_at	4,18	nodal homolog 2-A-like	LOC100496994
Str.21565.4.S1_at	4,17	RNA binding motif protein, X-linked	rbmx
Str.24254.1.S1_at	4,15	wingless-type MMTV integration site family, member 5B	wnt5b
Str.5804.3.S1_a_at	4,12	hypothetical LOC100487483 hypothetical LOC100490010 hypothetical LOC100490596 hypothetical LOC100491185 hypothetical LOC100492994 hypothetical LOC100493564	LOC100487483 LOC100490010 LOC100490596 LOC100491185 LOC100492994 LOC100493564
Str.26607.1.S1_at	4,11	protein unc-80 homolog	LOC100492079
Str.6167.1.S1_at	4,09	phosphorylase, glycogen, muscle	pygm
Str.26626.1.S1_at	4,06	growth arrest and DNA-damage-inducible, alpha	gadd45a
Str.7519.1.S1_at	4,01	ras homolog gene family, member B	rhob
Str.916.1.S1_at	4,00	lin-28 homolog A (C. elegans)	lin28a
Str.51815.1.S1_at	3,98	notochord homeobox	not
Str.1180.1.S2_at	3,98	forkhead box A1	foxa1
Str.15005.1.S1_at	3,98	hairy and enhancer of split 3, gene 1	hes3.1
Str.27547.1.S3_at	3,96	hypothetical protein LOC550042	LOC550042
Str.4965.1.S1_at	3,96	minichromosome maintenance complex component 6	mcm6.2
Str.3344.1.S1_at	3,94	novel protein similar to hatching enzymes	LOC594901
Str.993.1.S1_a_at	3,91	mex-3 homolog C	mex3c
Str.11106.1.S1_at	3,90	hypothetical protein LOC100488554	LOC100488554
Str.35184.1.A1_s_at	3,88	capping protein (actin filament) muscle Z-line, alpha 1	capza1
Str.643.1.S1_a_at	3,88	hypothetical LOC100486597	LOC100486597

Str.5849.2.A1_s_at	3,87	zinc finger E-box binding homeobox 2	zeb2
Str.16322.1.S1_at	3,86	Sp9 transcription factor homolog	sp9
Str.514.1.S1_at	3,83	pim-1 oncogene	pim1
Str.28107.1.S1_at	3,83	snail homolog 1	snai1
Str.51836.1.S1_at	3,80	angiopoietin 4	angpt4
Str.15072.2.A1_a_at	3,77	delta-like 1	dll1
Str.24583.1.S1_at	3,75	leucine-rich repeats and immunoglobulin-like domains 3	lrig3
Str.15996.4.S1_at	3,74	hypothetical LOC100490120	LOC100490120
Str.13766.1.S1_at	3,73	zinc finger protein 608	znf608
Str.27389.1.S1_at	3,69	transmembrane protein 150B	tmem150b
Str.7002.1.S1_at	3,69	hypothetical LOC100497373	LOC100497373
Str.21604.1.S1_at	3,69	5'-nucleotidase, cytosolic III	nt5c3
StrJgi.5287.1.S1_s_at	3,68	kin of IRRE like 2	kirrel2
StrJgi.6058.1.S1_at	3,67	LIM/homeobox protein Lhx3-like	LOC100496651
Str.3082.1.S1_at	3,62	wnt11 protein	wnt11
Str.5394.1.S1_at	3,61	carboxylesterase 2	ces2
Str.11087.1.S1_at	3,60	distal-less homeobox 5	dlx5
Str.20011.1.S1_at	3,59	receptor tyrosine kinase-like orphan receptor 2	ror2
Str.49050.1.S1_at	3,58	Fast skeletal myosin light chain 2	TNeu107a14.1
Str.10659.1.S1_at	3,57	transcription factor AP-2 epsilon (activating enhancer binding protein 2 epsilon)	tfap2e
Str.24871.1.S1_x_at	3,56	zinc finger protein 33B	znf33b
Str.6103.1.S1_at	3,55	MID1 interacting protein 1 (gastrulation specific G12 homolog)	mid1ip1
Str.10076.1.S1_at	3,52	angiomotin like 2	amotl2
Str.42133.3.A1_x_at	3,52	zinc finger protein 502-like gastrula zinc finger protein XlCGF57.1-like zinc finger protein 613-like MGC146893 zinc finger protein 3 zinc finger protein 33A zinc finger protein 33B zinc finger protein 665	LOC100485089 LOC100489449 LOC100493688 MGC146893 znf3 znf33a znf33b znf665
Str.24842.3.S1_at	3,51	ropporin 1-like	ropn1l
Str.11288.1.S1_at	3,51	hypothetical LOC100486074	LOC100486074

Str.13147.1.A1_at	3,50	zinc finger protein 219-like	LOC100495520
Str.21950.2.S1_a_at	3,49	hypothetical LOC100488570	LOC100488570
Str.16343.1.A1_at	3,48	Hypothetical protein LOC100145152	LOC100145152
Str.10208.1.S1_at	3,47	solute carrier family 12 (sodium/chloride transporters), member 3, gene 2	slc12a3.2
Str.9193.1.A1_a_at	3,46	UPF0632 protein C2orf89-like	LOC100491951
Str.6363.1.S2_at	3,45	acidic (leucine-rich) nuclear phosphoprotein 32 family, member C	anp32c
Str.49171.3.S1_at	3,45	hypothetical LOC100488154	LOC100488154
Str.38997.1.A1_at	3,42	proprotein convertase subtilisin/kexin type 9-like	LOC100484989
Str.10900.1.S1_at	3,41	serum/glucocorticoid regulated kinase 1	sgk1
Str.6695.1.S2_at	3,40	zinc finger, MIZ-type containing 2	zmiz2
Str.39816.2.S1_at	3,28	hypothetical LOC100488648	LOC100488648
Str.21565.6.A1_at	3,28	hypothetical LOC100485563	LOC100485563
Str.7820.2.S1_a_at	3,24	immediate early response gene 2 protein-like	LOC100491464
Str.29569.1.S1_at	3,23	Meningioma (disrupted in balanced translocation) 1, gene 1	mn1.1
Str.2514.1.S1_a_at	3,22	NIMA (never in mitosis gene a)-related kinase 2	nek2
Str.22063.1.S1_at	3,20	hypothetical LOC100489698	LOC100489698
Str.51755.2.A1_a_at	3,19	hypothetical protein LOC100491437	LOC100491437
Str.10330.1.S2_at	3,16	sprouty homolog 1, antagonist of FGF signaling	spry1
Str.2247.1.S1_at	3,15	RAB34, member RAS oncogene family	rab34
Str.51988.1.S1_at	3,14	serine/arginine-rich splicing factor 11	srsf11
Str.33742.1.A1_a_at	3,13	hypothetical protein LOC100494123	LOC100494123
Str.51680.1.A1_at	3,12	zinc finger protein 721	znf721
Str.15643.1.A1_at	3,10	hypothetical protein LOC100145695	LOC100145695
Str.1973.2.A1_a_at	3,05	huntingtin-associated protein 1	hap1

Str.10123.1.S1_at	3,02	glucose-fructose oxidoreductase domain containing 1	gfod1
Str.16252.1.S1_at	3,02	SRY (sex determining region Y)-box 1	sox1
Str.10371.1.S1_at	3,00	chromosome 8 open reading frame 4	c8orf4
Str.51787.1.S1_at	3,00	histone cluster 1, H2ah	hist1h2ah
Str.40984.1.S1_at	2,98	hypothetical protein LOC100494082	LOC100494082
Str.27184.1.S1_a_at	2,98	matrix metallopeptidase 1 (interstitial collagenase)	mmp1
Str.51982.1.A1_s_at	2,96	iroquois homeobox 3	irx3
Str.11815.1.S1_at	2,95	protein phosphatase 1, regulatory (inhibitor) subunit 15B	ppp1r15b
Str.40960.1.S1_at	2,95	zinc finger, SWIM-type containing 5	zswim5
Str.2514.4.A1_a_at	2,94	NIMA (never in mitosis gene a)-related kinase 2	nek2
Str.30747.1.A1_at	2,94	regulator of G-protein signaling 16	rgs16
Str.4877.1.S1_at	2,94	caudal type homeobox 4	cdx4
StrJgi.6297.1.S1_at	2,92	homeobox protein siamois-like	LOC100489935
Str.15740.1.A1_at	2,92	MAP kinase interacting serine/threonine kinase 2	mknk2
Str.50722.6.S1_at	2,90	transient receptor potential cation channel subfamily M member 4-like	LOC100491327
Str.49514.1.S1_at	2,89	T-box 3	tbx3
Str.49437.1.S1_at	2,82	Hypothetical protein LOC100144964	LOC100144964
Str.30700.3.A1_s_at	2,82	solute carrier family 41, member 2	slc41a2
Str.169.2.S1_a_at	2,81	sal-like 1	sall1
Str.23452.1.A1_at	2,79	empty spiracles homeobox 1	emx1
Str.40558.2.A1_at	2,79	Hypothetical protein LOC100158524	LOC100158524
Str.246.1.S1_at	2,79	mab-21-like 2	mab21l2
Str.8107.1.S1_at	2,77	forkhead box A2	foxa2
Str.27386.1.S1_at	2,74	RasGEF domain family, member 1B	rasgef1b
Str.10824.1.S1_at	2,74	KIT ligand	kitlg
Str.6084.1.S2_at	2,73	lymphocyte antigen 6 complex, similar to G6C	ly6g6c

Str.27109.1.S1_at	2,72	oligodendrocyte transcription factor 3	olig3
Str.2696.1.S1_at	2,71	forkhead box C2 (MFH-1, mesenchyme forkhead 1)	foxc2
Str.5969.1.S1_at	2,70	CDGSH iron sulfur domain 1	cisd1
Str.28780.1.S1_at	2,65	RAS-like, family 11, member B	rasl11b
Str.15404.1.S1_at	2,64	carbohydrate (N-acetylglucosamine-6-O) sulfotransferase 2	chst2
StrJgi.8558.1.S1_x_at	2,63	hypothetical protein LOC100494089	LOC100494089
Str.10666.1.S1_at	2,63	follistatin	fst
Str.19278.2.S1_at	2,61	hypothetical protein LOC100491368	LOC100491368
Str.2504.2.S1_at	2,59	RNA binding motif protein 6	rbm6
Str.5989.1.S1_at	2,59	retinoblastoma binding protein 6	rbbp6
Str.10221.1.S2_at	2,58	hypothetical LOC100495650	LOC100495650
Str.11224.1.S1_at	2,57	zinc finger protein 238.2-like	LOC100489646
StrEns.4639.1.S1_s_at	2,56	arachidonate 5-lipoxygenase-activating protein	alox5ap
Str.20309.1.A1_at	2,54	cyclin-dependent kinase 6	cdk6
Str.24871.1.S2_s_at	2,54	zinc finger protein 613-like	LOC100493688
Str.11302.1.S1_at	2,54	forkhead box D3	foxd3
Str.8068.3.S1_at	2,53	Solute carrier family 5 (iodide transporter), member 8	slc5a8
Str.303.1.S1_at	2,50	G protein-coupled receptor, family C, group 5, member C	gprc5c

Listed are all genes, downregulated ≥ 5.65 fold change and with an adjusted *p*-value ≤ 0.05.

Set-probe number	fold change [log2]	gene name	symbol
Str.49500.1.S2_at	-3,71	stearoyl-CoA desaturase (delta-9-desaturase)	scd
Str.27228.1.S1_at	-2,84	cyclin B5	LOC394448
Str.27519.1.S1_at	-2,83	TATA box binding protein like 2	tbpl2
Str.26929.1.S1_at	-2,78	novel trypsin family protein	LOC733551
Str.38389.1.S1_at	-2,74	hypothetical LOC100327245	LOC100327245
Str.51968.1.S1_at	-2,70	ribonuclease H1	rnaseh1
Str.52195.1.S1_s_at	-2,67	ankyrin repeat domain 37	ankrd37
Str.27358.1.S1_at	-2,55	transmembrane protease, serine 11F	tmprss11f
Str.17786.1.S1_at	-2,52	adaptor-related protein complex 4, sigma 1 subunit	ap4s1

BMO1/MBT microarray

Listed are all genes, which are upregulated ≥ 5.65 fold at the MBT and show transcriptional changes upon BMO1 injections.

fold change [log2]	gene name	symbol
3,196	Hypothetical protein LOC550005	LOC550005
2,167	histone cluster 1, H2ah	hist1h2ah
1,482	histone H4-like	LOC100496593
1,129	hypothetical protein LOC100496030	LOC100496030
0,907	mesendoderm nuclear factor, gene 1	menf.1
0,756	RNA binding motif protein 6	rbm6
0,625	histone H3.2-like	LOC100496129
0,592	transportin 1	tnpo1
0,523	hypothetical protein LOC100145106	LOC100145106
-0,343	hypothetical protein LOC100216037	LOC100216037
-0,383	hypothetical protein LOC100494704 VENT homeobox 2, gene 1	LOC100494704 ventx2.1
-0,397	MGC89648 protein	MGC89648
-0,519	growth arrest and DNA-damage-inducible, alpha	gadd45a
-0,536	hypothetical protein LOC100495042	LOC100495042
-0,537	cdc42 effector protein (Rho GTPase binding) 4	cdc42ep4
-0,556	leucine-rich repeats and immunoglobulin-like domains 3	lrig3
-0,578	hypothetical protein hypothetical protein hypothetical protein	LOC100489830 LOC100494885 LOC100495042
-0,604	growth arrest and DNA-damage-inducible, gamma	gadd45g
-0,623	RAS, dexamethasone-induced 1	rasd1
-0,629	cyclin-dependent kinase 6	cdk6
-0,641	cone-rod homeobox	crx

-0,642	glucose-fructose oxidoreductase domain containing 1	gfod1
-0,646	hypothetical LOC100496454	LOC100496454
-0,653	VENT homeobox 3, gene 1	ventx3.1
-0,660	NIMA (never in mitosis gene a)-related kinase 2	nek2
-0,686	transcription factor AP-2 alpha (activating enhancer binding protein 2 alpha)	tfap2a
-0,696	filamin C, gamma	flnc
-0,713	hypothetical protein LOC100493690	LOC100493690
-0,732	single-strand-selective monofunctional uracil-DNA glycosylase 1	smug1
-0,736	forkhead box I4, gene 2	foxi4.2
-0,756	carbohydrate (N-acetylglucosamine-6-O) sulfotransferase 2	chst2
-0,777	mab-21-like 2	mab21l2
-0,777	hairy and enhancer of split 4	hes4
-0,781	dual specificity phosphatase 5	dusp5
-0,787	hypothetical protein MGC76328	MGC76328
-0,792	phosphatidic acid phosphatase type 2B	ppap2b
-0,811	hypothetical protein LOC550042	LOC550042
-0,814	minichromosome maintenance complex component 6	mcm6.2
-0,840	sal-like 1	sall1
-0,843	hairy and enhancer of split 6, gene 1	hes6.1
-0,889	hypothetical LOC100496939	LOC100496939
-0,896	phosphorylase, glycogen, muscle	pygm
-0,900	lysophosphatidic acid receptor 6	lpar6
-0,901	huntingtin-associated protein 1	hap1
-0,902	T, brachyury homolog	t
-0,907	hypothetical protein hypothetical protein	LOC100486038 LOC100487146

-0,923	solute carrier family 7 (cationic amino acid transporter, y+ system), member 3	slc7a3
-0,924	Hypothetical protein LOC779546	LOC779546
-0,926	G2/M-phase specific E3 ubiquitin protein ligase	g2e3
-0,932	PR domain containing 1, with ZNF domain	prdm1
-0,967	zinc finger protein 608	znf608
-0,969	hypothetical LOC100497373	LOC100497373
-0,986	VENT homeobox 1, gene 1 VENT homeobox 1, gene 2	ventx1.1 ventx1.2
-0,993	Nucleolar protein 5A (56kDa with KKE/D repeat)	TEgg001j23.1
-0,997	kin of IRRE like 2	kirrel2
-0,999	POU domain, class 5, transcription factor 1.2-like	LOC100498076
-1,005	hypothetical LOC100484994 hypothetical protein hypothetical protein hypothetical protein hypothetical protein hypothetical LOC100498560	LOC100484994 LOC100486020 LOC100489931 LOC100490293 LOC100492588 LOC100498560
-1,007	hypothetical protein LOC100487199	LOC100487199
-1,017	serine/arginine-rich splicing factor 1	srsf1
-1,021	receptor-interacting serine-threonine kinase 4	ripk4
-1,033	hypothetical LOC100486098	LOC100486098
-1,053	MAP kinase interacting serine/threonine kinase 2	mknk2
-1,060	retinoblastoma-like 1 (p107)	rbl1
-1,080	LIM homeobox 1	lhx1
-1,098	arachidonate 5-lipoxygenase-activating protein	alox5ap
-1,100	novel zinc finger protein	LOC733912
-1,102	potassium channel, subfamily K, member 6	kcnk6
-1,115	wingless-type MMTV integration site family, member 5B	wnt5b
-1,125	hypothetical LOC100486074	LOC100486074
-1,129	VENT homeobox 1, gene 1	ventx1.1

-1,132	hypothetical protein LOC100489354	LOC100489354
-1,141	High-mobility group nucleosomal binding domain 2	TEgg003n10.1
-1,148	hypothetical LOC100495377	LOC100495377
-1,152	hypothetical LOC100495538	LOC100495538
-1,156	nerve growth factor receptor	ngfr
-1,158	zinc finger protein 568	znf568
-1,172	transmembrane protein 127	tmem127
-1,205	lin-28 homolog A (C. elegans)	lin28a
-1,213	TSC22 domain family, member 3	tsc22d3
-1,227	Heterogeneous nuclear ribonucleoprotein D-like	hnrpdl
-1,232	serine/arginine-rich splicing factor 6	srsf6
-1,278	rho GTPase-activating protein 39-like	LOC100485974
-1,280	Death inducer-obliterator 1	dido1
-1,303	hypothetical protein MGC69473	MGC69473
-1,312	uncharacterized protein ywlC-like	LOC100497798
-1,312	regulator of G-protein signaling 16	rgs16
-1,319	uncharacterized protein ywlC-like hypothetical protein	LOC100497798 LOC100498107
-1,339	forkhead box D4-like 1, gene 1	foxd4l1.1
-1,351	SRY (sex determining region Y)-box 1	sox1
-1,352	immediate early response gene 2 protein-like	LOC100491464
-1,352	ER degradation enhancer, mannosidase alpha-like 1 angiopoietin-related protein 1-like	edem1 LOC100491105
-1,353	Meningioma (disrupted in balanced translocation) 1, gene 1	mn1.1
-1,360	forkhead box C1	foxc1
-1,363	SRY (sex determining region Y)-box 21	sox21
-1,383	T-box 3	tbx3

-1,431	ankyrin repeat domain 10	ankrd10
-1,451	uroplakin 2	upk2
-1,457	cornifelin homolog	cnfn
-1,470	eukaryotic translation initiation factor 4A2	eif4a2
-1,506	LIM homeobox 5	lhx5
-1,510	zinc finger protein 750	znf750
-1,517	serine/arginine-rich splicing factor 11	srsf11
-1,524	hypothetical protein LOC100498107	LOC100498107
-1,536	angiopoietin 4	angpt4
-1,542	Fast skeletal myosin light chain 2	TNeu107a14.1
-1,552	angiomotin like 2	amotl2
-1,555	GATA binding protein 4	gata4
-1,557	potassium channel tetramerisation domain containing 15	kctd15
-1,561	hypothetical protein LOC100487200	LOC100487200
-1,580	novel protein similar to hatching enzymes	LOC594901
-1,593	transcription factor AP-2 epsilon (activating enhancer binding protein 2 epsilon)	tfap2e
-1,595	deoxyribonuclease gamma-like	LOC100497175
-1,603	cyclin E2	ccne2
-1,629	iroquois homeobox 2	irx2
-1,631	zinc finger protein ZIC 4-like	LOC100493609
-1,648	forkhead box D3	foxd3
-1,713	lymphocyte antigen 6 complex, similar to G6C	ly6g6c
-1,719	X-box binding protein 1	xbp1
-1,731	transcription factor HES-1-like	LOC100496131
-1,738	hypothetical LOC100486597	LOC100486597
-1,761	ADP-ribosylation factor-like 4C	arl4c
-1,764	Solute carrier family 2 (facilitated glucose transporter), member 2	slc2a2
-1,771	ATPase, Na+/K+ transporting, beta 2 polypeptide	atp1b2
-1,889	homeobox C8	hoxc8

-1,902	zinc finger E-box binding homeobox 2	zeb2
-1,930	cell division cycle 25 homolog B	cdc25b
-1,964	delta-like 1	dll1
-2,016	distal-less homeobox 5	dlx5
-2,038	hypothetical LOC100495344	LOC100495344
-2,044	neural precursor cell expressed, developmentally down-regulated 9	nedd9
-2,078	phospholipase A2, group XIIB	pla2g12b
-2,083	keratin	krt
-2,107	Sp9 transcription factor homolog	sp9
-2,112	sphingosine-1-phosphate receptor 5	s1pr5
-2,126	calponin 1, basic, smooth muscle	cnn1
-2,155	chromosome 7 open reading frame 11	c7orf11
-2,180	UPF0632 protein C2orf89-like	LOC100491951
-2,190	hypothetical LOC100494381	LOC100494381
-2,311	hypothetical protein LOC100491368	LOC100491368
-2,366	gastrula-specific protein 17	gs17
-2,414	zinc finger protein 219-like	LOC100495520
-2,598	sarcoplasmic/endoplasmic reticulum calcium ATPase 2-like	LOC100489059
-2,706	uroplakin 3B	upk3b
-3,857	purinergic receptor P2Y, G-protein coupled, 2	p2ry2

BMO2/MBT microarray

Listed are all genes, which are upregulated ≥ 5.65 at the MBT and show transcriptional changes upon BMO2 injections.

fold change [log2]	gene name	symbol
2,113	5'-nucleotidase, cytosolic III	nt5c3
1,747	protein phosphatase 1, regulatory (inhibitor) subunit 3C, gene 1	ppp1r3c.1
1,105	hypothetical LOC100486074	LOC100486074
1,071	fused in sarcoma	fus
1,045	hairy and enhancer of split 5, gene 1	hes5.1
0,955	histone H3.2-like	LOC100496129
0,782	histone cluster 1, H2ah	hist1h2ah
0,758	ferritin, heavy polypeptide 1	fth1
0,717	ER degradation enhancer, mannosidase alpha-like 1 angiopoietin-related protein 1-like	edem1 LOC100491105
0,674	Hypothetical protein LOC550005	LOC550005
0,660	fibroblast growth factor 20	fgf20
-0,372	Hypothetical protein LOC733820	LOC733820
-0,445	MGC89648 protein	MGC89648
-0,447	solute carrier family 7 (cationic amino acid transporter, y+ system), member 3	slc7a3
-0,462	hypothetical LOC100491682	LOC100491682
-0,477	Fast skeletal myosin light chain 2	TNeu107a14.1
-0,514	single-strand-selective monofunctional uracil-DNA glycosylase 1	smug1
-0,531	carbohydrate (N-acetylglucosamine-6-O) sulfotransferase 2	chst2
-0,536	hypothetical protein LOC100487199	LOC100487199
-0,549	retinoblastoma-like 1 (p107)	rbl1
-0,559	frizzled homolog 10	fzd10

-0,603	hypothetical LOC100486098	LOC100486098
-0,638	neural precursor cell expressed, developmentally down-regulated 9	nedd9
-0,661	cdc42 effector protein (Rho GTPase binding) 4	cdc42ep4
-0,705	Calponin 2	cnn2
-0,771	serine/arginine-rich splicing factor 11	srsf11
-0,792	hypothetical LOC100486597	LOC100486597
-0,820	nerve growth factor receptor	ngfr
-0,841	hypothetical LOC100495377	LOC100495377
-0,868	Y box binding protein 2	ybx2
-0,894	ankyrin repeat domain 10	ankrd10
-0,899	hypothetical protein LOC100493690	LOC100493690
-0,952	immediate early response gene 2 protein-like	LOC100491464
-1,008	ABO blood group (transferase A, alpha 1-3-N-acetylgalactosaminyltransferase; transferase B, alpha 1-3-galactosyltransferase)	abo
-1,021	hypothetical LOC100488570	LOC100488570
-1,078	hypothetical LOC100495861	LOC100495861
-1,110	transcription factor AP-2 epsilon (activating enhancer binding protein 2 epsilon)	tfap2e
-1,206	sarcoplasmic/endoplasmic reticulum calcium ATPase 2-like	LOC100489059
-1,230	hypothetical protein LOC100487200	LOC100487200
-1,303	l-amino-acid oxidase-like	LOC100496394
-1,344	SRY (sex determining region Y)-box 21	sox21

Acknowledgement/ Danksagung

Mein größter Dank gilt Prof. Ralph Rupp, der mir nicht nur ermöglichte an diesem spannenden Projekt zu arbeiten, sondern mich all die Jahre wissenschaftlich und persönlich förderte. Du hast mir beigebracht kritisch zu hinterfragen, wissenschaftlich gute Arbeit abzuliefern und bist in vielen Belangen ein Vorbild. Danke Ralph, für den gemeinsamen Weg.

Ein weiterer Dank gilt Prof. Peter Becker. Zum Einen dafür, dass Du Dich bereit erklärt hast, mein Erstgutachter zu sein und zum Anderen, dass Du Dein Institut mit Hingabe und Geduld leitest und stets ein offenes Ohr und eine helfende Hand für Deine Mitarbeiter hast.

Vielen Dank auch an mein *Thesis Advisory Committee*: Prof. André Brändli und Dr. Tobias Straub. Ihr Beiden wart mir in unsicheren Zeiten eine große Hilfe. Prof. Brändli, vielen Dank für Ihre grandiosen Ideen. Tobias, tausend Dank für die geduldigen Treffen, in denen Du versucht hast mir die Bioinformatik näher zu bringen und meine Daten in eine mir verständliche Form gebracht hast.

A huge *THANK YOU* goes to all past and present lab members, who constantly made me laugh, cheered me up and supported me. Thank you, Dario, Edith, Barbara, Max, Steffi, Ohnmar, Daniil, Alessandro, Adrian, Julian and Hildegard for an incredible time. Additional, I want to thank Edith and Barbara for the great support- not only scientifically. A special thank goes to Dario. I think over the years we really grew as a "two-people-frog-PhD-Rupp-group" and besides your homemade pizza, from time to time, I even miss you singing Depeche Mode in the lab!

Eine ganze Schüssel voll von DANK geht an die Salat-Club-Mitglieder Edith, Miriam und Simone. Erstens dafür, dass wir aus dem Salat-Club einen Nudel-Club gemacht haben. Zweitens dafür, dass ich mich auch kulinarisch weiterbilden konnte (Ja, Wasserkastanien schmecken!). Drittens dafür, dass wir in dieser Zeit ausschließlich die wichtigen Themen dieser Welt besprochen haben. Viertens für die seelsorgerischen Einheiten, die man ab und an mal nötig hat. DANKE. DANKE. DANKE.

Miriam, danke auch für die viele frische Luft, gesund-haltenden Vitamine und das Korrekturlesen.

Nicht zu vergessen der wichtigste Dank gilt meiner Familie. Danke dafür, dass ihr mich bei all meinen Entscheidungen unterstützt, mir Halt gebt und ich mich, egal was auch passiert, voll und ganz auf Euch verlassen kann.

Dominik, Dir möchte ich ganz besonders danken. Danke, für deine Geduld, Verständnis und Begleitung, wenn ich abends mal wieder Kappen absammeln musste oder das halbe Wochenende im Labor verbracht habe. Danke, dass Du mich bei allem unterstützt und mir immer das Gefühl gibst, jemand ganz besonderes zu sein.